



Inclusive Jet Production at DØ

Fermilab Joint Experimental-Theoretical Seminar
February 15, 2008

Mikko Voutilainen

University of Nebraska-Lincoln

Helsinki Institute of Physics

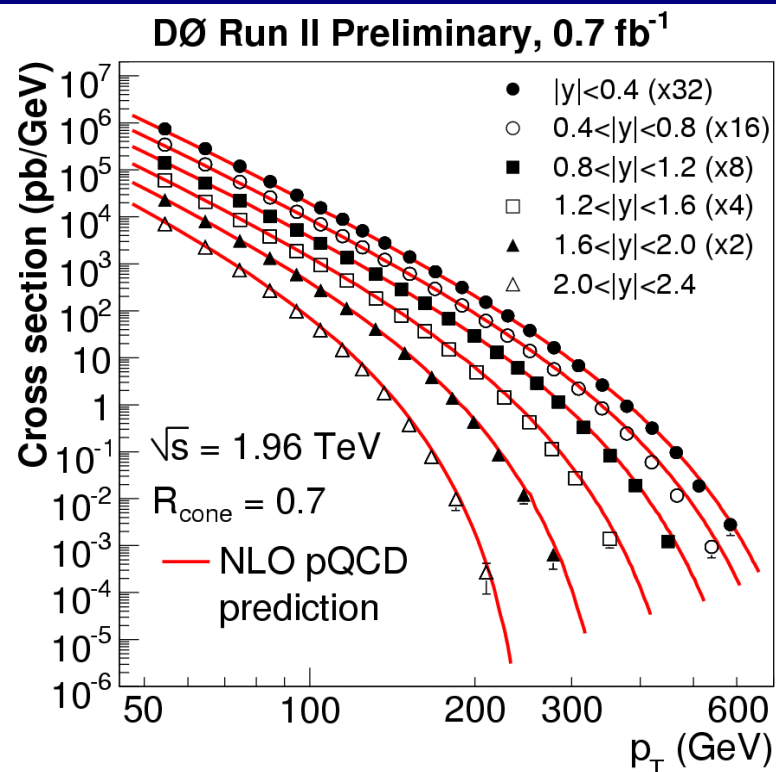
CEA / Saclay

for the DØ collaboration

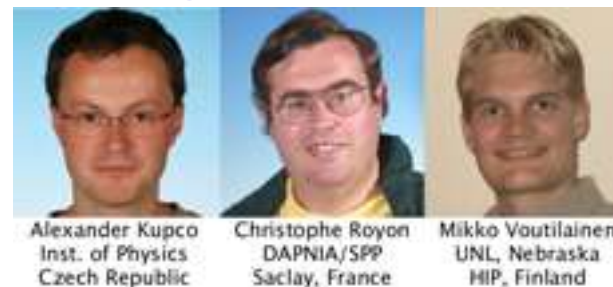


Outline

- **Introduction and motivation**
 - internal structure of the proton
 - structure of quarks
- **Events selection**
 - cuts and efficiencies
- **Jet energy scale (JES)**
 - sample dependence
 - four-momentum calibration
- **Measurement**
 - unfolding
 - understanding the uncertainties
- **Summary and outlook**
 - constraints of proton structure
 - new physics searches at the LHC



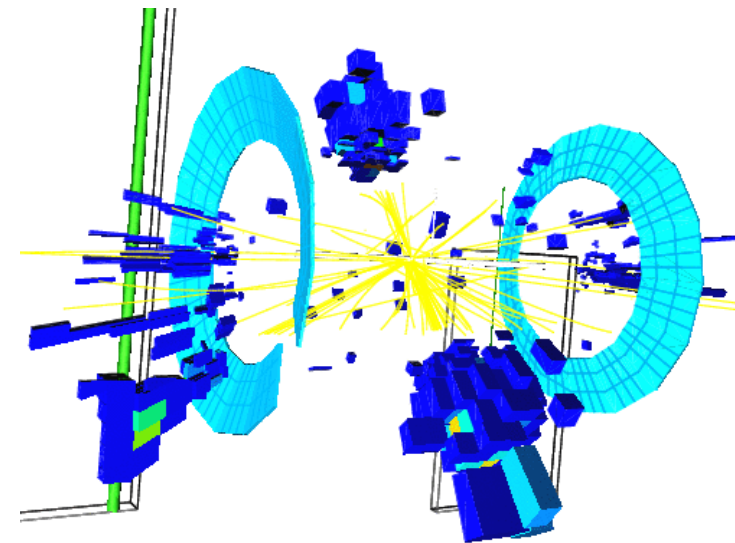
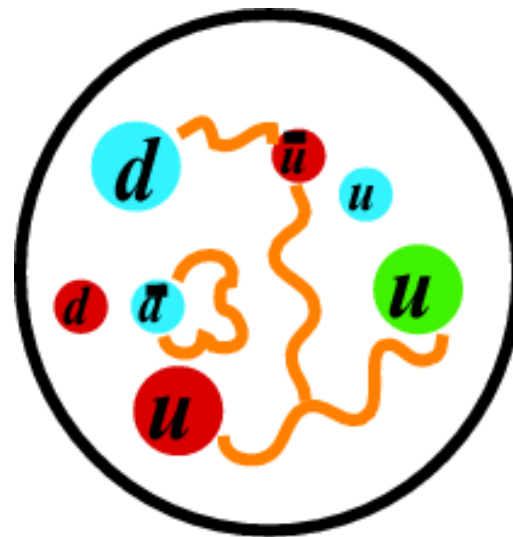
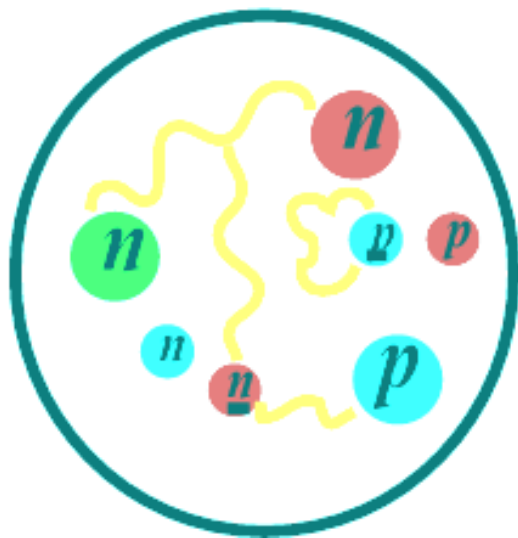
Fermilab Today result of the week on January 24th:
www.fnal.gov/today/08-01-24





Proton structure

- Proton consist of three valence quarks, up-up-down (**uud**) and antiproton of three antiquarks (**$\bar{u}\bar{u}\bar{d}$**) bound together by a sea of gluons (**g**) and virtual quark-antiquark pairs (**$u\bar{u}$** , **$d\bar{d}$** , **$s\bar{s}$** etc.)



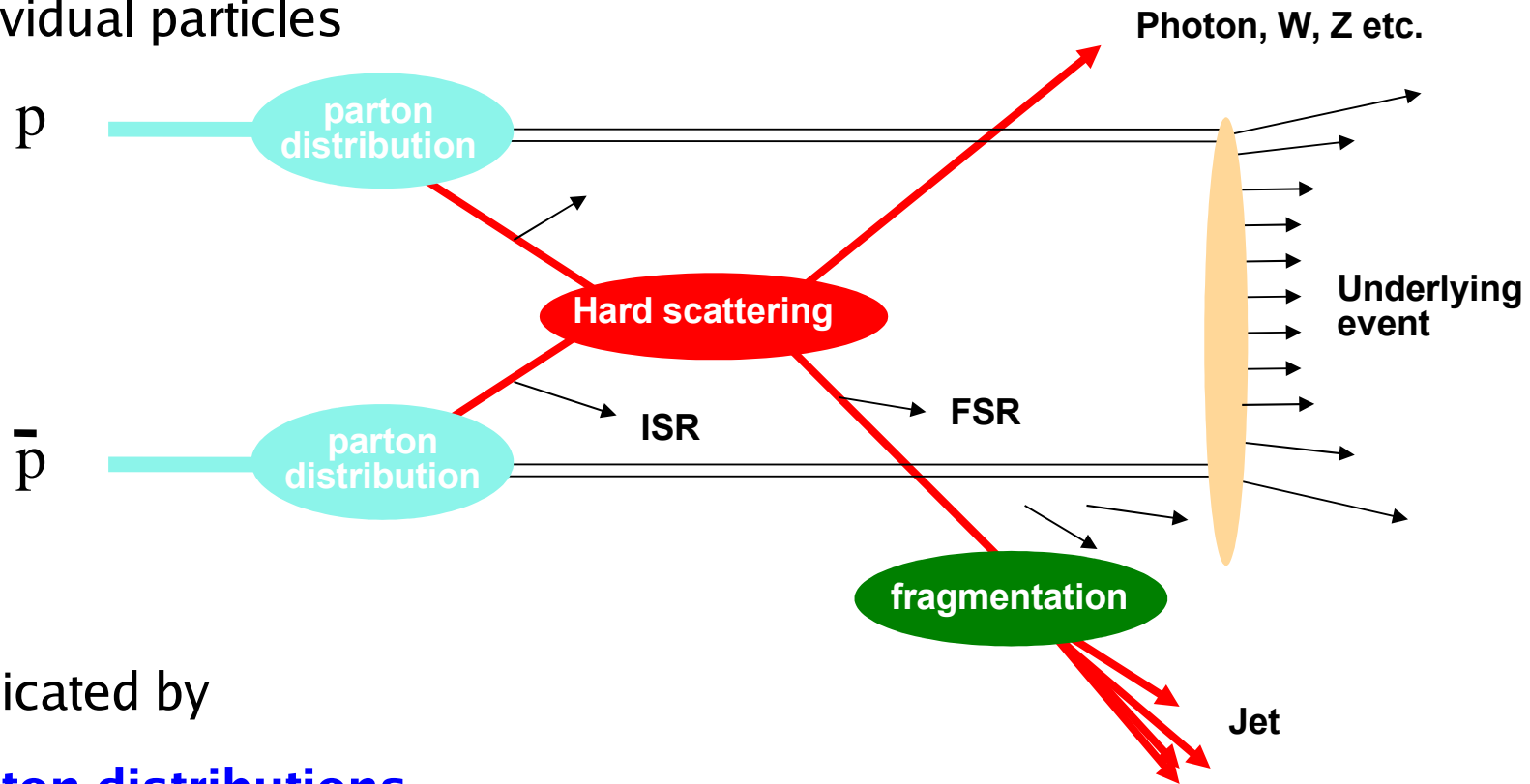
- Higher energies resolve finer detail, and Tevatron's energies are currently the highest available (1.96 TeV)
- Different final states give access to different aspects; inclusive jets look at big picture and can search beyond standard model



Event schematic

Jet is a spray of particles coming from **hard interaction**

- Jets are formed by collisions of partons (quarks and gluons) from individual particles



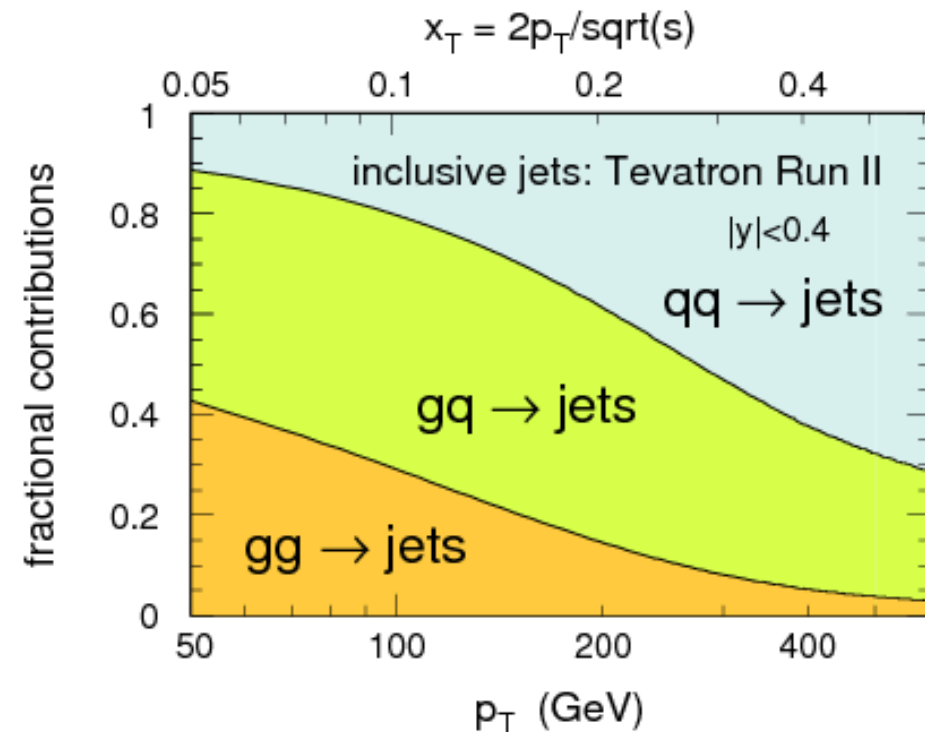
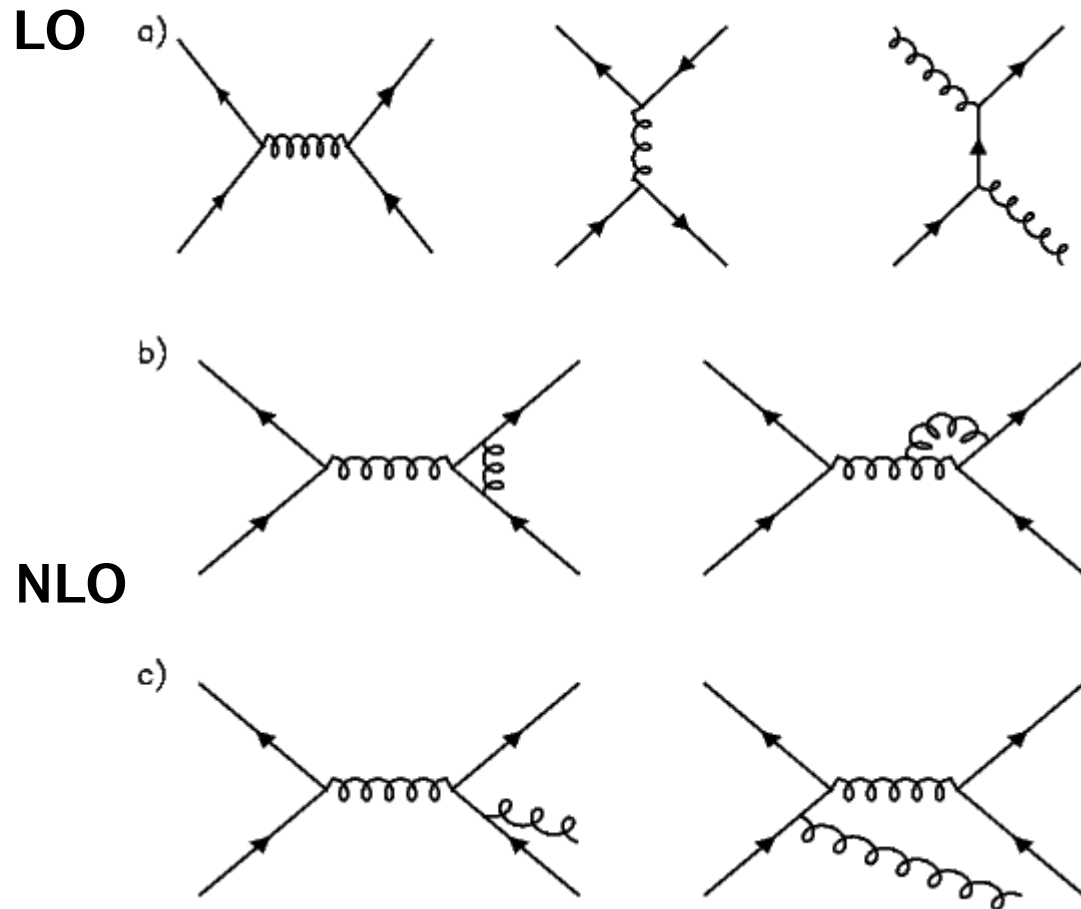
Complicated by

- **Parton distributions**
 - hadron collider is really a broad-band quark and gluon collider
 - both the initial and final states can be colored and radiated gluons
- **Underlying event** from proton remnants



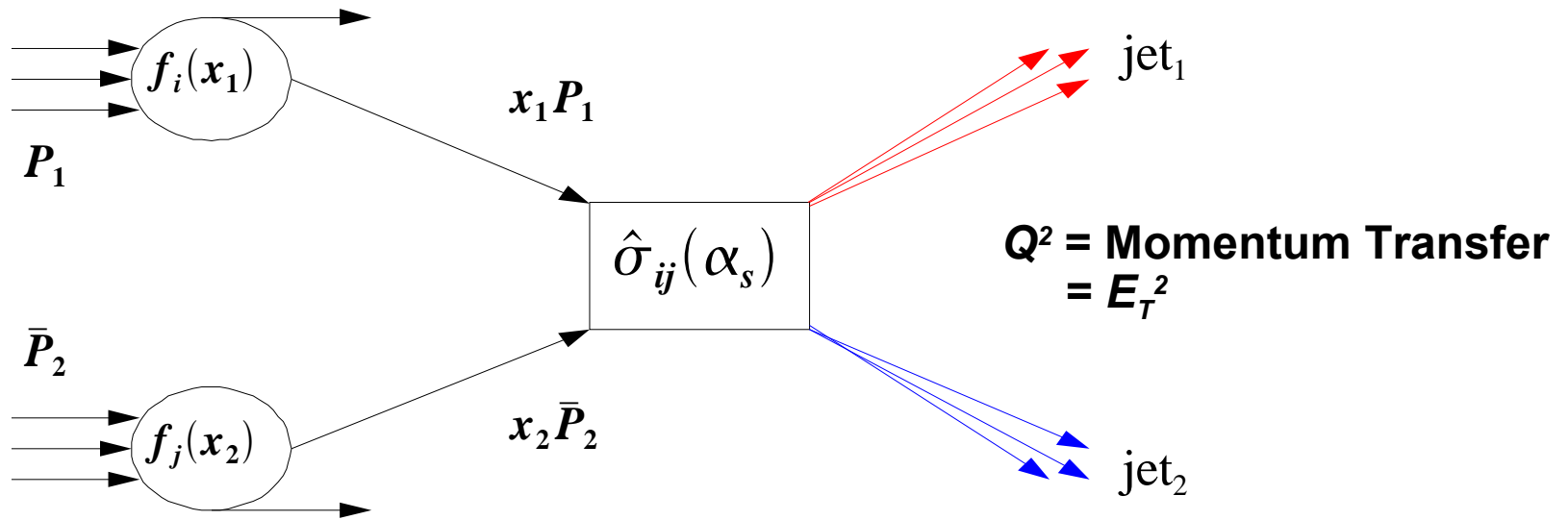
Quantum chromodynamics

- Quantum chromodynamics is calculable using perturbation theory (Feynman diagrams) at high $p_T \Rightarrow$ **hard scatter**
- Standard is next-to-leading-order (NLO), higher orders being calculated

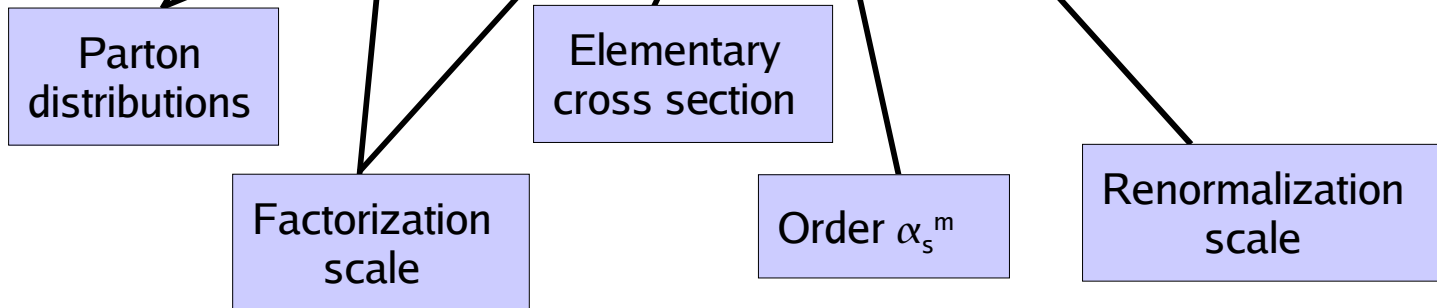




Theory calculation



$$\sigma = \sum_{ij} \int dx_1 dx_2 f_i(x_1, \mu_F^2) f_j(x_2, \mu_F^2) \hat{\sigma}_{ij}(\alpha_s^m(\mu_R^2), \text{elementary process})$$

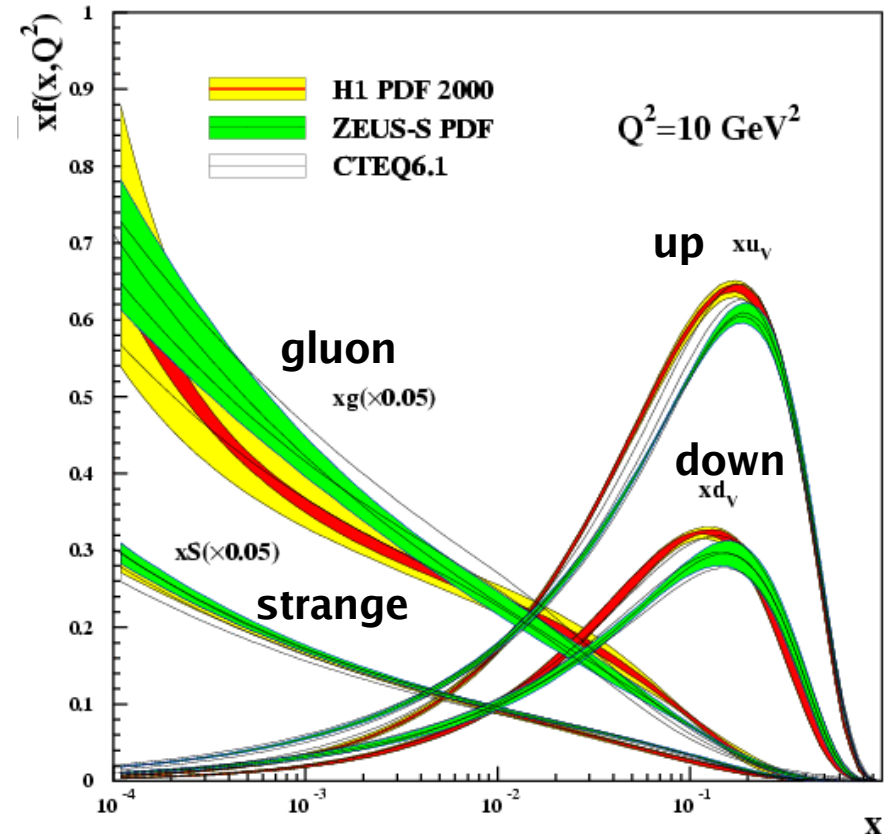




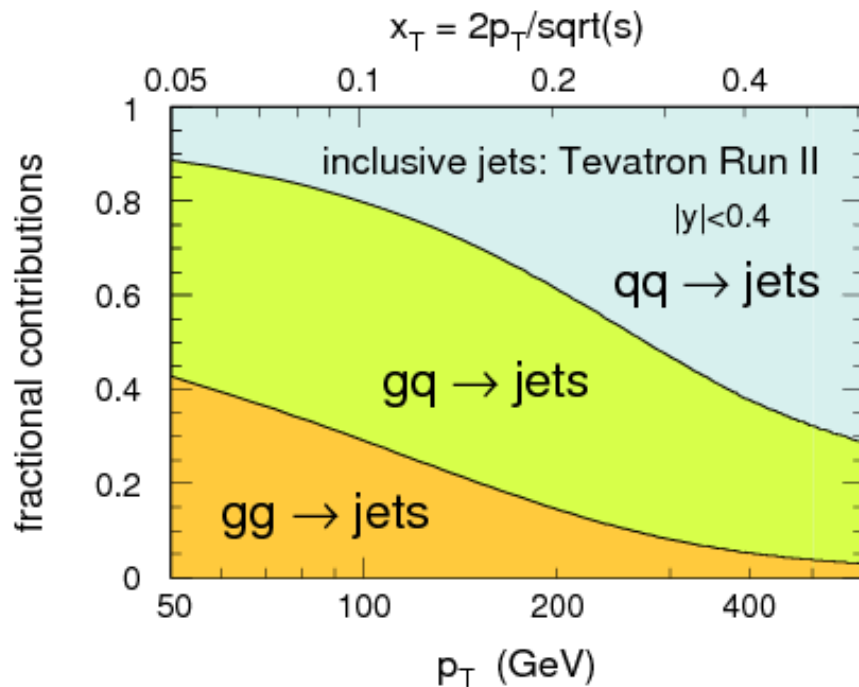
Parton distributions

- Inclusive jet cross section can constrain parton distribution functions (PDFs), especially the **gluon PDF at high x**
- PDFs are needed *e.g.* to reliably calculate backgrounds at the LHC

Proton parton distribution functions

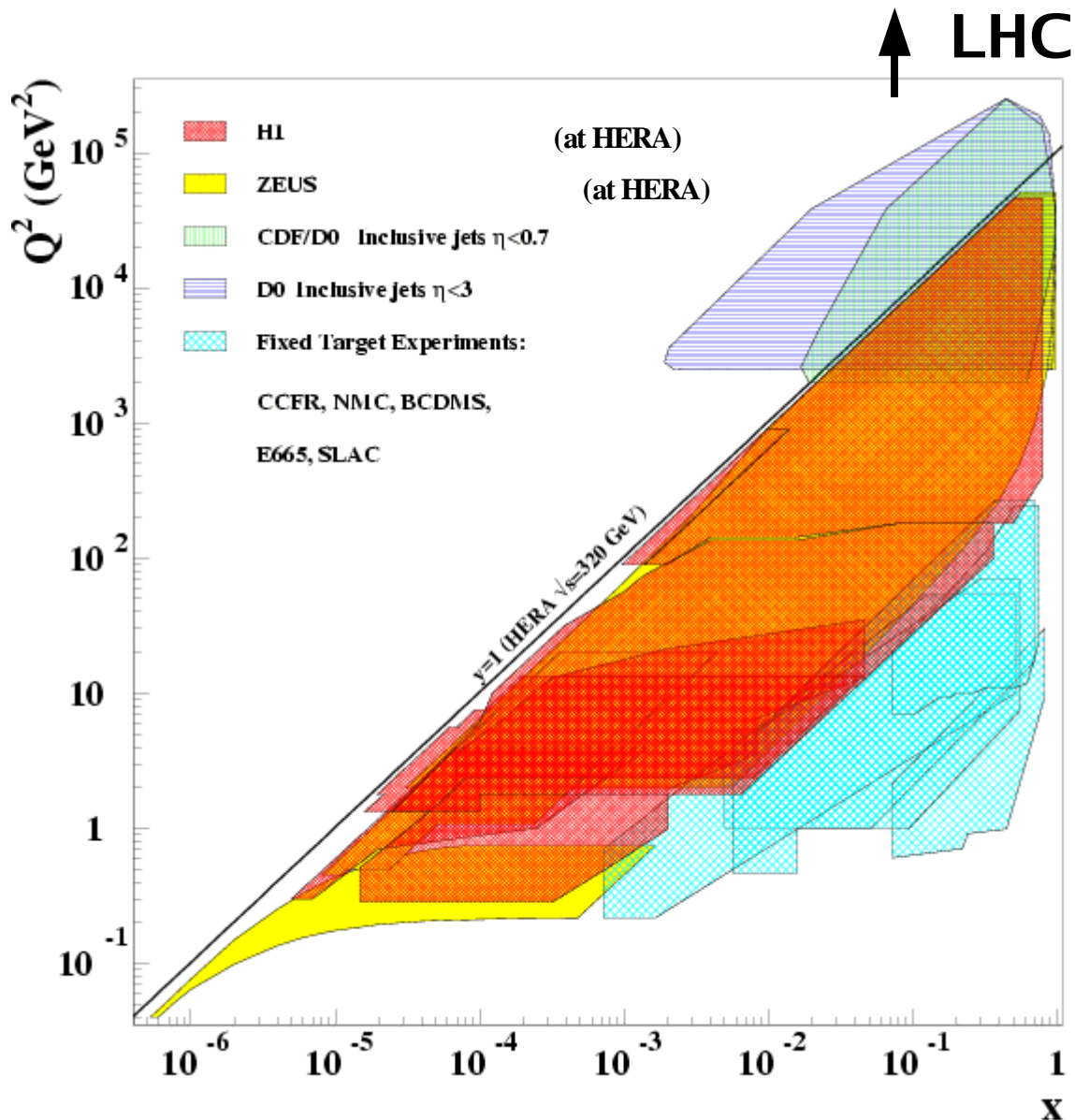


x : momentum fraction carried by individual parton
 $f(x, Q^2)$: probability of finding parton with momentum fraction x in interval dx





DØ kinematic range



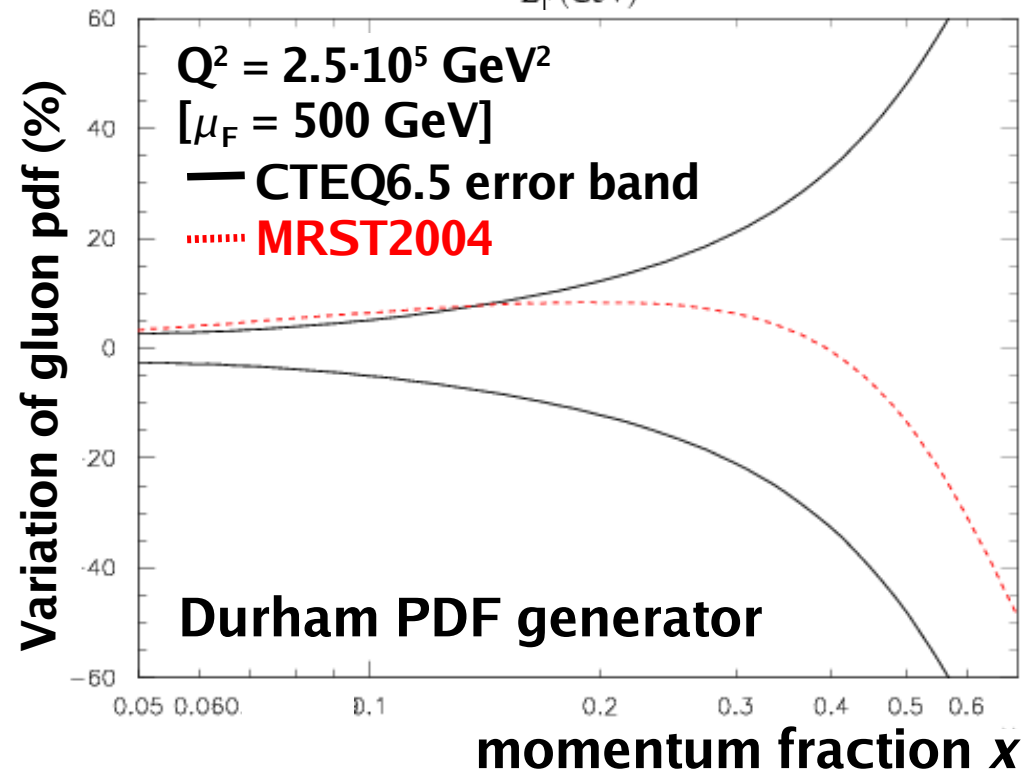
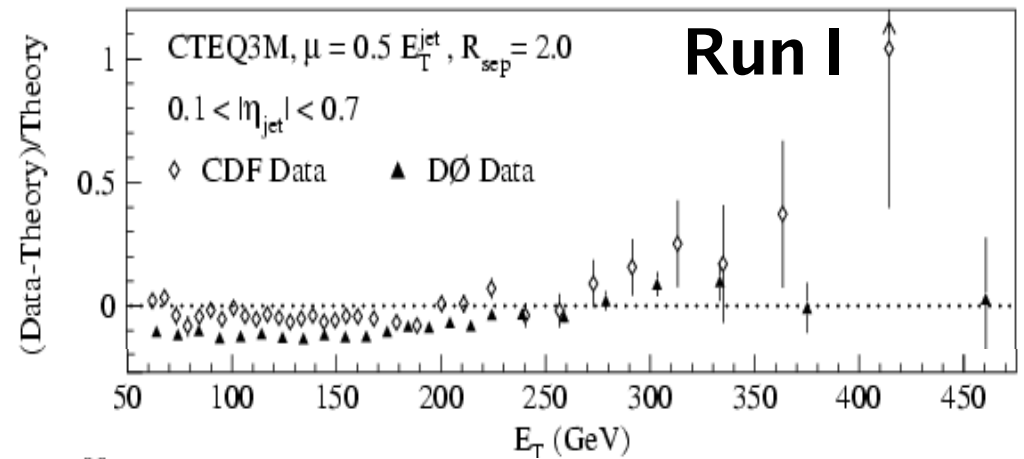
HERA is an electron-proton collider in DESY research center in Hamburg, Germany

- We are complementary to HERA and fixed target experiments



Quark substructure

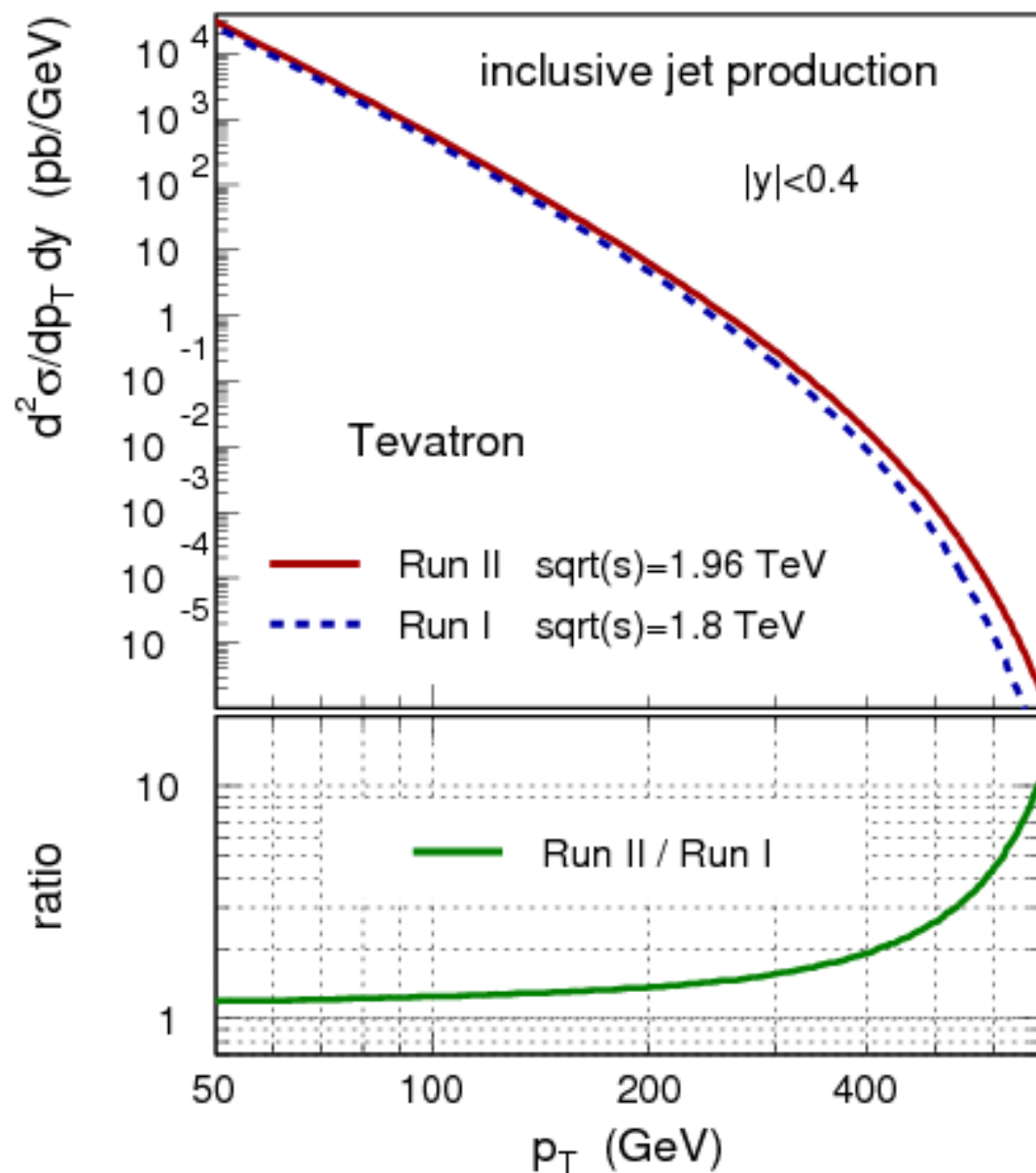
- Run I measurements have left significant freedom for the high x gluon PDF
- Once the high x gluon PDF is nailed down we can search for **quark substructure**
- Important measurement to be performed
 - 1) at low rapidities: sensitive to PDF/quark substructure
 - 2) in wide range of rapidity: at high y , sensitive to PDF
- One single measurement is sensitive to both effects





Run II advantage

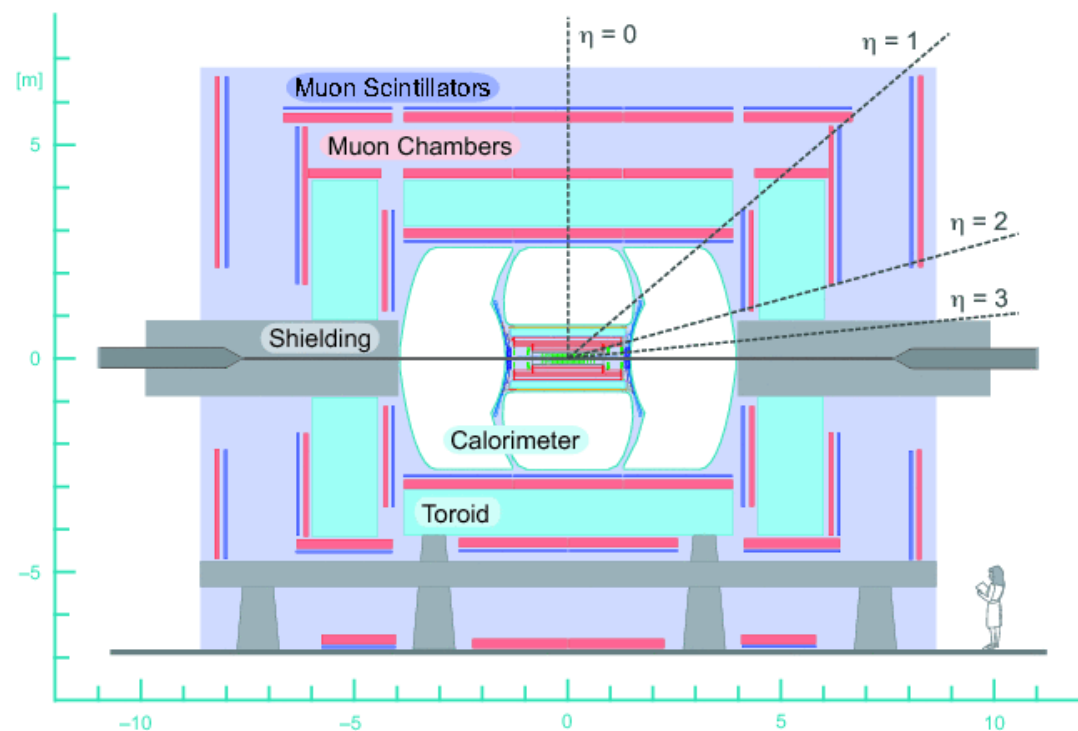
- Luminosity now ten times that of Run I $\Rightarrow \times 3$ gluon PDF sensitivity
- Center-of-mass energy also 10% higher \Rightarrow three times higher cross section at $p_T = 550$ GeV
- Luminosity + cross section increase $\Rightarrow \times 5$ quark substructure sensitivity





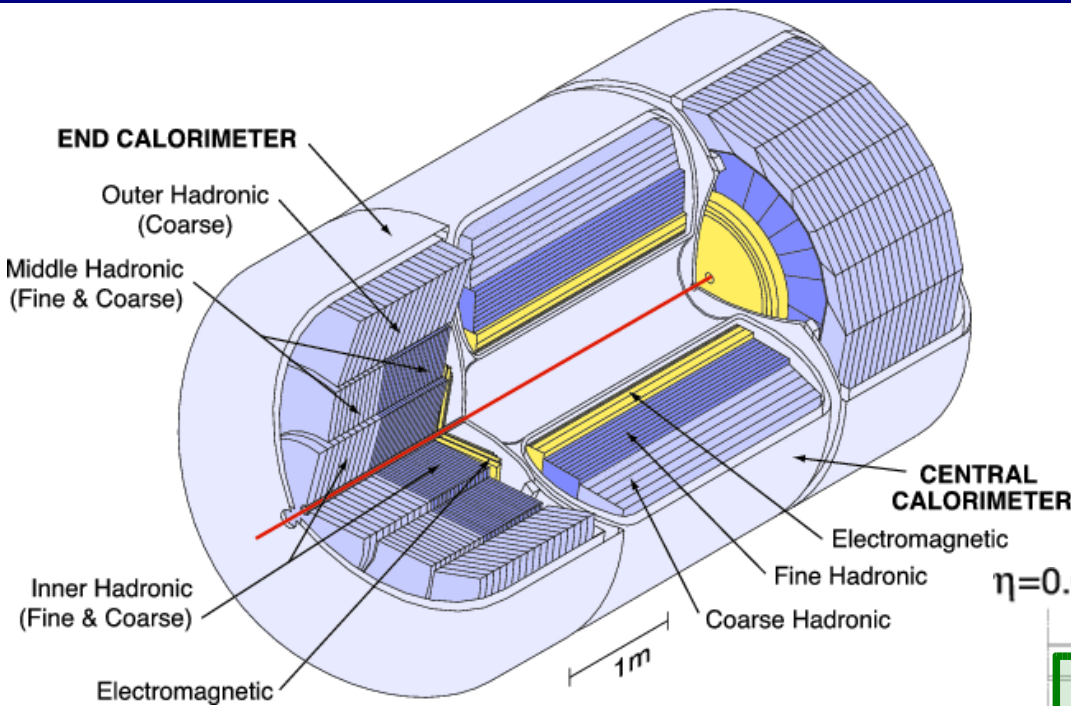
DØ experiment

- Three main systems:
 - Tracker (silicon and scintillating fibre)
 - Calorimeter (lAr/U, some scintillator)
 - Muon chambers and scintillators
- First two used in this measurement



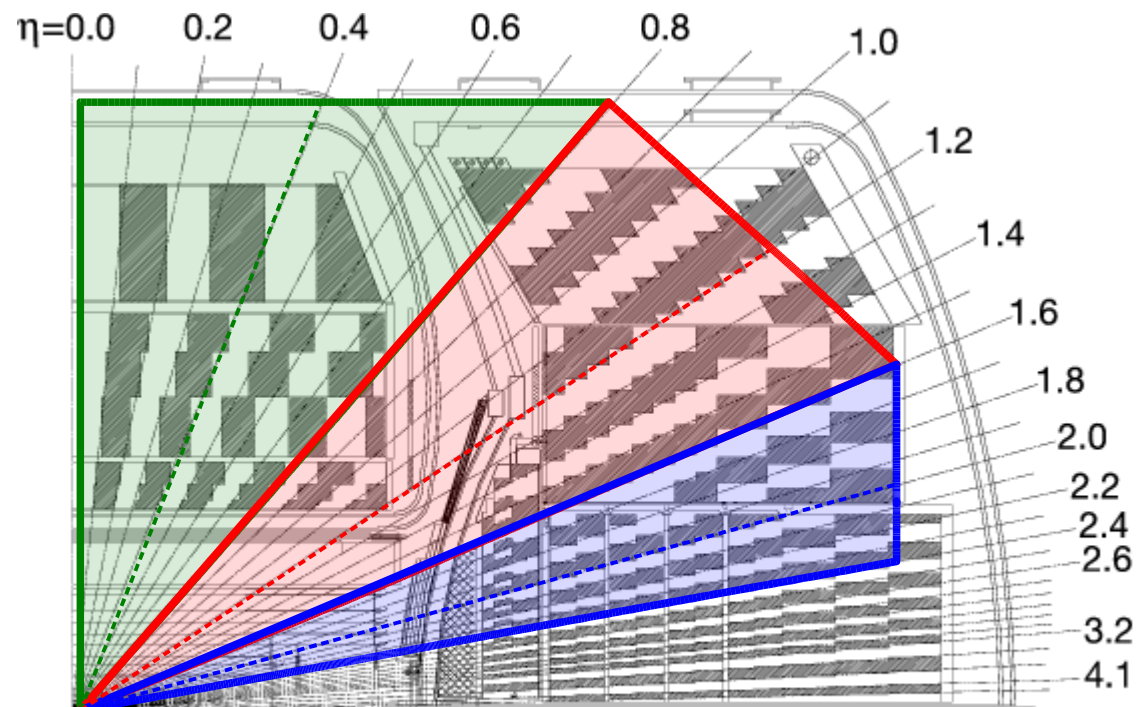


DØ calorimeter



- Calorimeter structure divides the measurement in three regions:
 - **Central calorimeter** (easiest)
 - **Intercryostat region** (challenging)
 - **End caps** (fine segmentation)

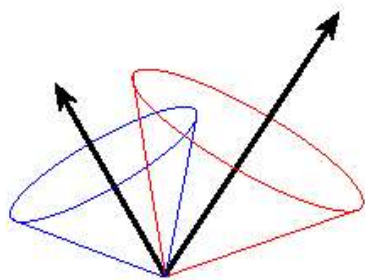
- Calorimeter is the most important detector for jet measurements
- Liquid-Argon/Uranium calorimeter:
 - Stable response, good resolution
 - Partially compensating ($e/\pi \sim 1$)
- Gaps covered with scintillator tiles





Jet algorithm

- Detailed comparison to theory needs a precise definition of jet algorithm
- This measurement uses Run II Midpoint Cone with $R_{\text{cone}} = 0.7$



Run I Legacy Cone:

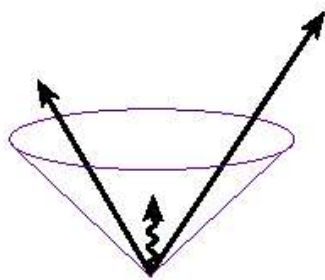
Draw a cone of fixed size in $\eta-\phi$ space around a seed

Compute jet axis from E_T -weighted mean and jet E_T from $\sum E_T$'s

Draw a new cone around the new jet axis and recalculate axis and new E_T

Iterate until stable

Algorithm is **sensitive to soft radiation**



Run II Midpoint Cone:

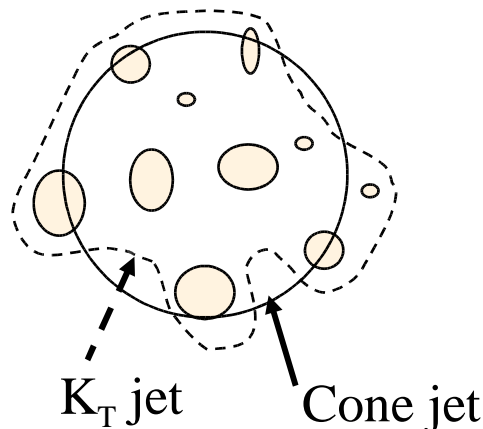
Use 4-vectors instead of E_T

Add additional midpoint seeds between pairs of close jets

Split/merge after stable protojets found
Improved infrared safety at NLO

(DØ Run II/CDF MIDPOINT)

We characterize jets in terms of p_T and y

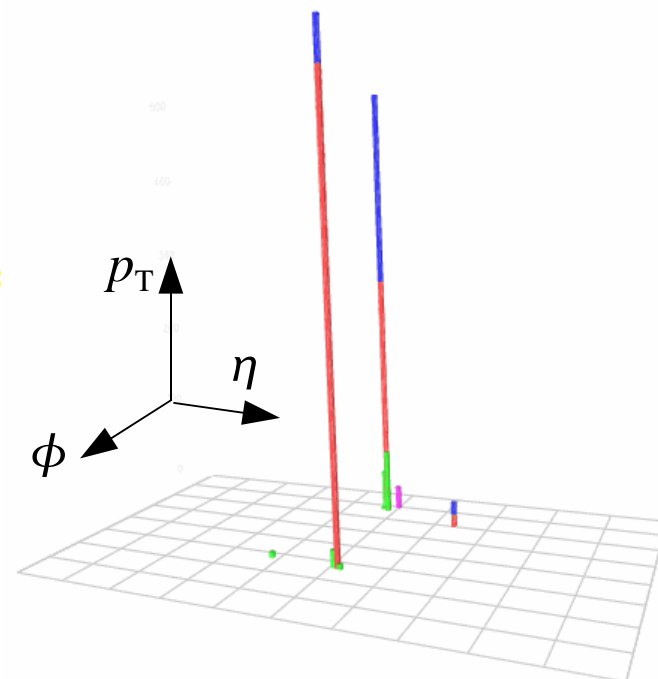
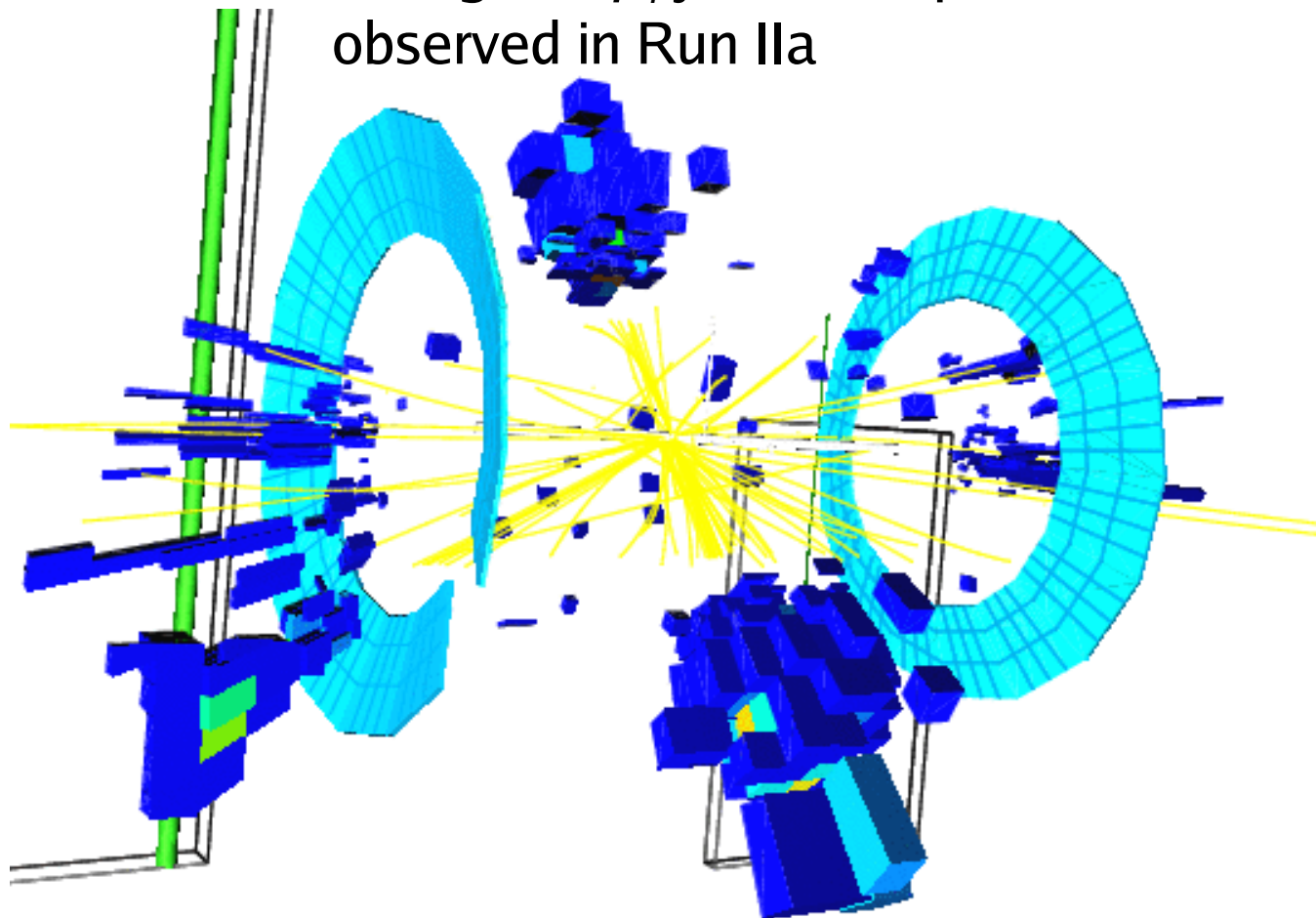




High p_T jets

- The interesting part of the measurement is observing the highest p_T jets ever produced in a collider
- Here's the highest p_T jet and its pair(s) observed in Run IIa

first jet	second jet
$p_T = 624$ GeV	$p_T = 594$ GeV
$y_{\text{jet}} = 0.14$	$y_{\text{jet}} = -0.17$
$\phi_{\text{jet}} = 2.10$	$\phi_{\text{jet}} = 5.27$
$M_{jj} = 1.22$ TeV !	





Counting experiment

This is basically a counting experiment:

Double differential cross section

Number of jets

Jet Energy Scale!

$$\frac{d^2 \sigma}{dp_T dy} = \frac{N}{\epsilon \cdot L \cdot \Delta p_T \Delta y} \cdot C_{smear} \text{ versus } p_T$$

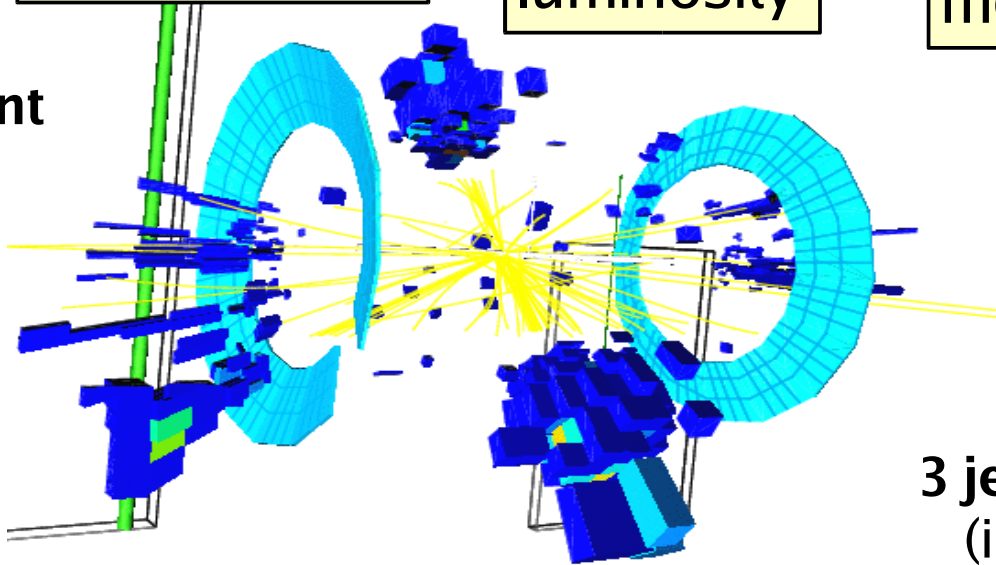
Jet and event efficiency

Integrated luminosity

Bins of transverse momentum and rapidity

Events can move in and out of p_T bins due to calorimeter energy resolution

1 event

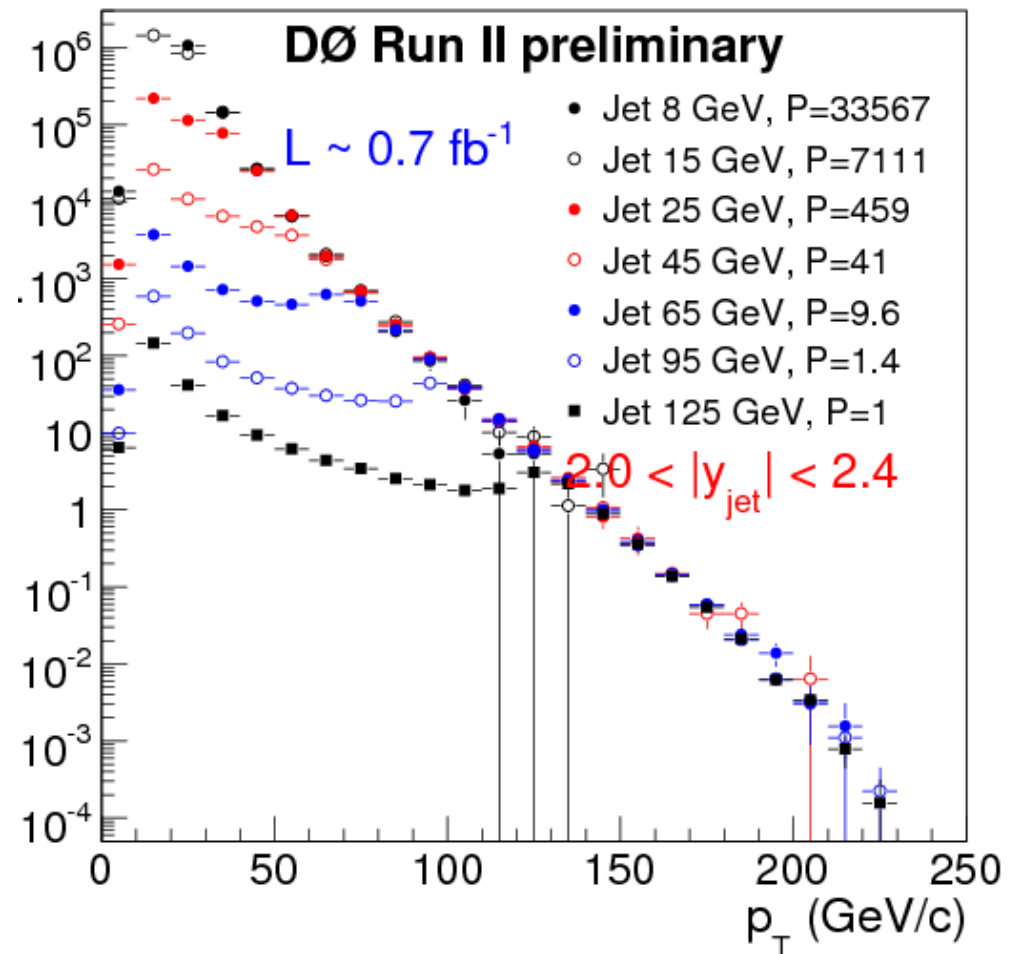
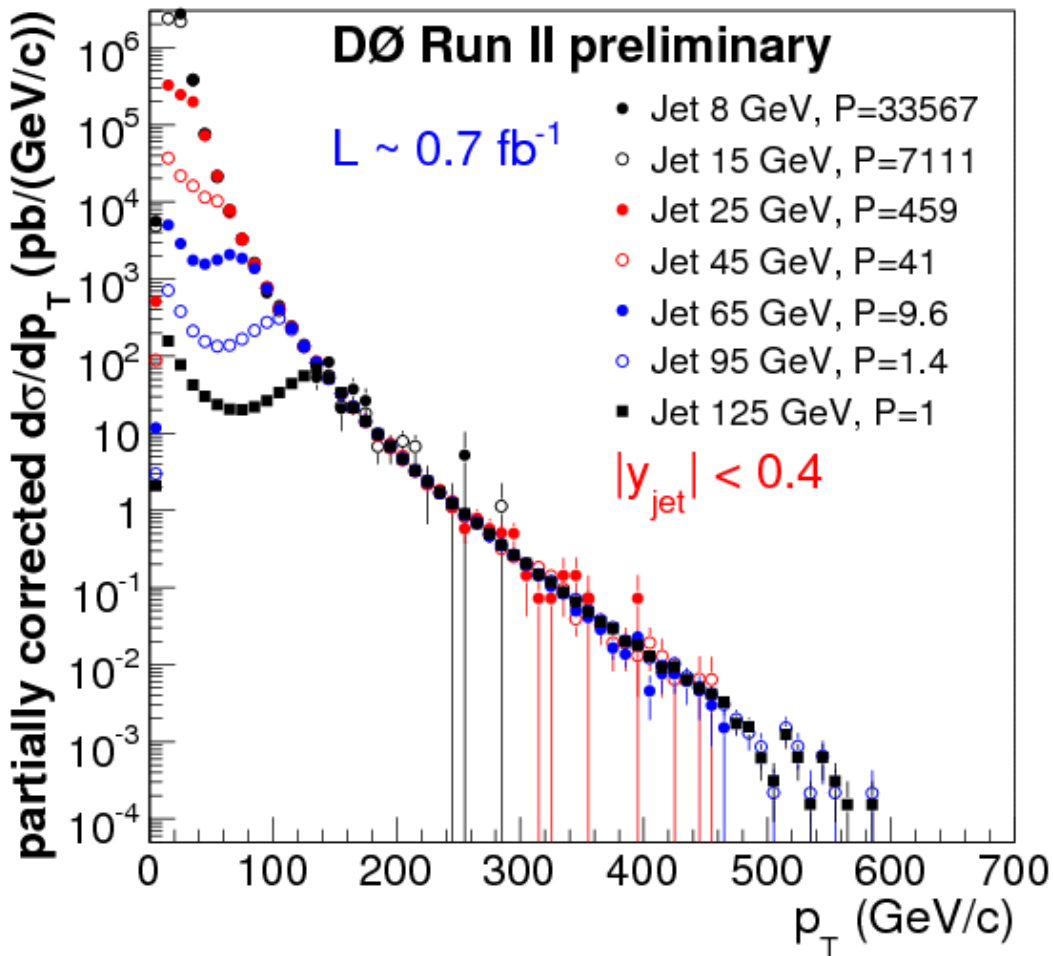


3 jets
(in different bins)



Triggers

- Triggers fire on single jets above p_T threshold
- The measurement spans eight orders of magnitude in six rapidity regions
- Full p_T spectrum combined from seven different triggers





Cuts and efficiencies

$$\frac{d^2 \sigma}{dp_T dy} = \frac{N}{\epsilon \cdot L \cdot \Delta p_T \Delta y} \cdot C_{smear} \quad \text{versus } p_T$$

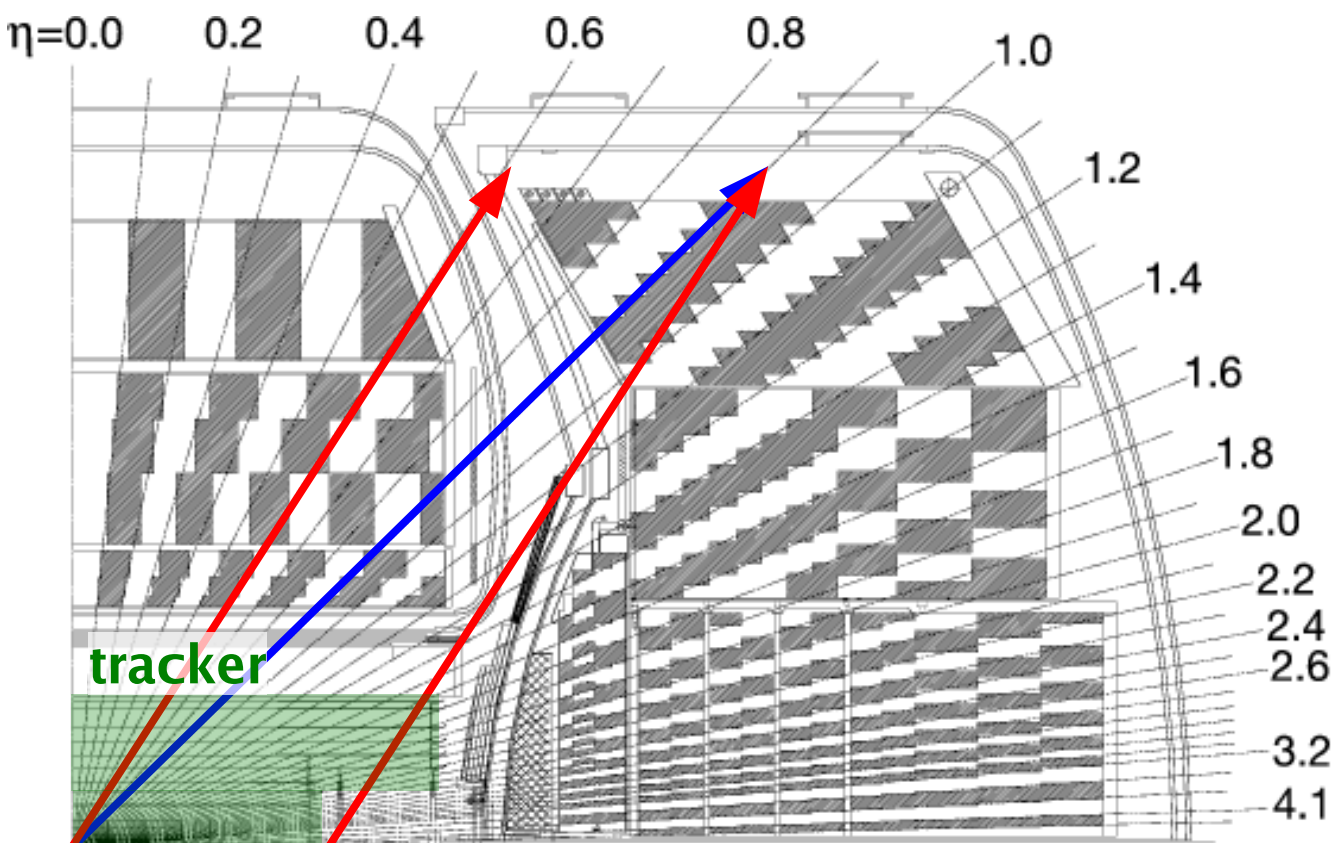
Jet and event efficiency

- Good vertex within central tracking acceptance for reliable p_T reconstruction
- Cut on missing- E_T to avoid cosmic events (over 50% of triggered jets at $p_T > 400$ GeV!)
- JetID to avoid noise jets and electron/photon overlap



Vertex cut

- Interaction vertex position is required to be within $|z_{\text{vtx}}| < 50$ cm of the calorimeter to improve jet p_T resolution
- Jets at large z_{vtx} can hit the calorimeter at a weird angle and at worse miss most of the calorimeter

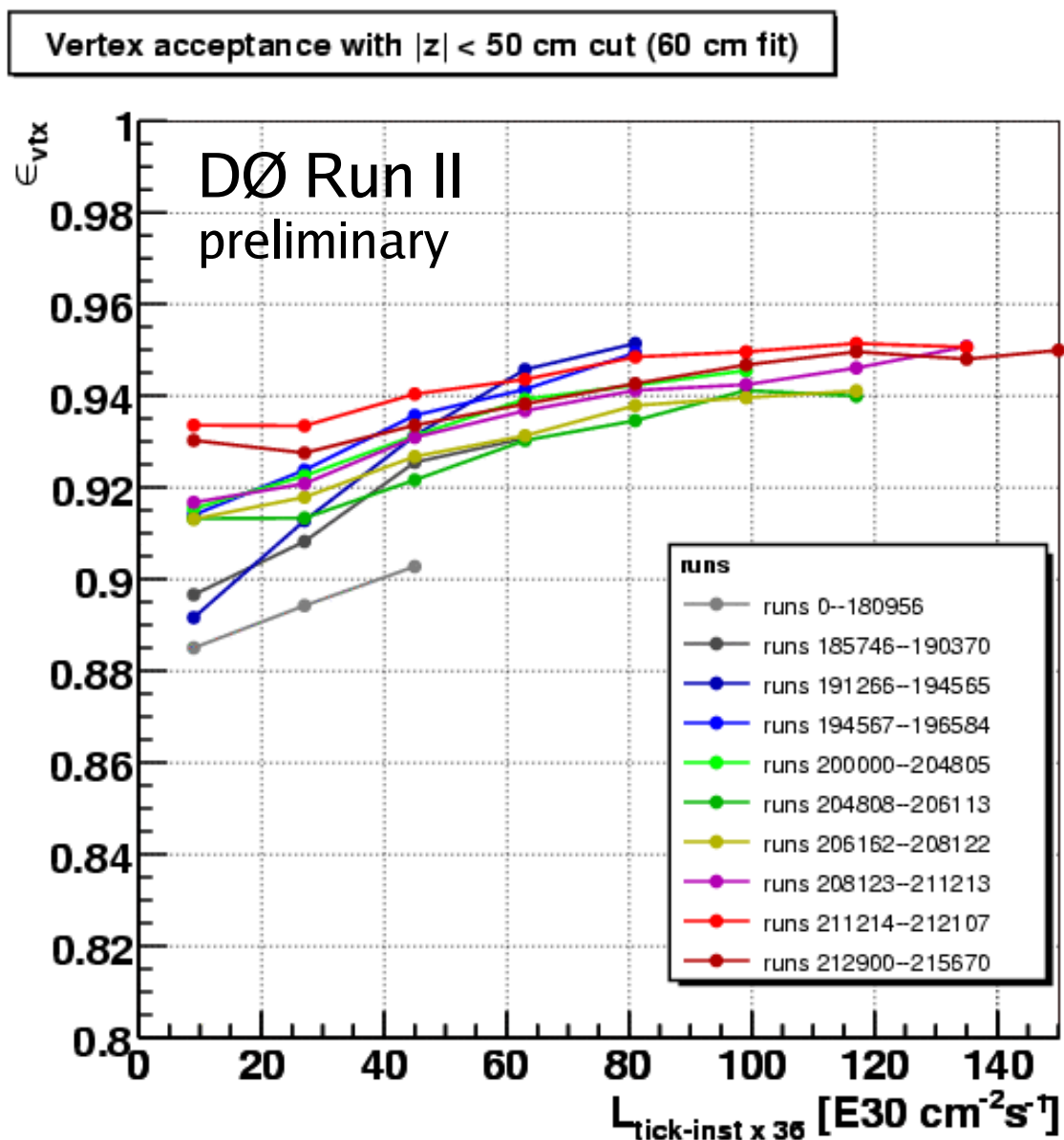


- Vertex is needed for p_T reconstruction (E from the calorimeter, p_T with the vertex)
- Tracking efficiency quickly degrades beyond $|z_{\text{vtx}}|=40\text{--}50$ cm



Vertex efficiency

- Vertex cut efficiency is calculated from the longitudinal beam shape
- Time and luminosity dependence:
 - Beam parameters (β^*) changing in epochs
 - Beam heating with time in store (luminosity $\sim 1 / \text{time}$)
- Average inefficiency $7.0 \pm 0.5\%$
- Leading inefficiency, others much smaller

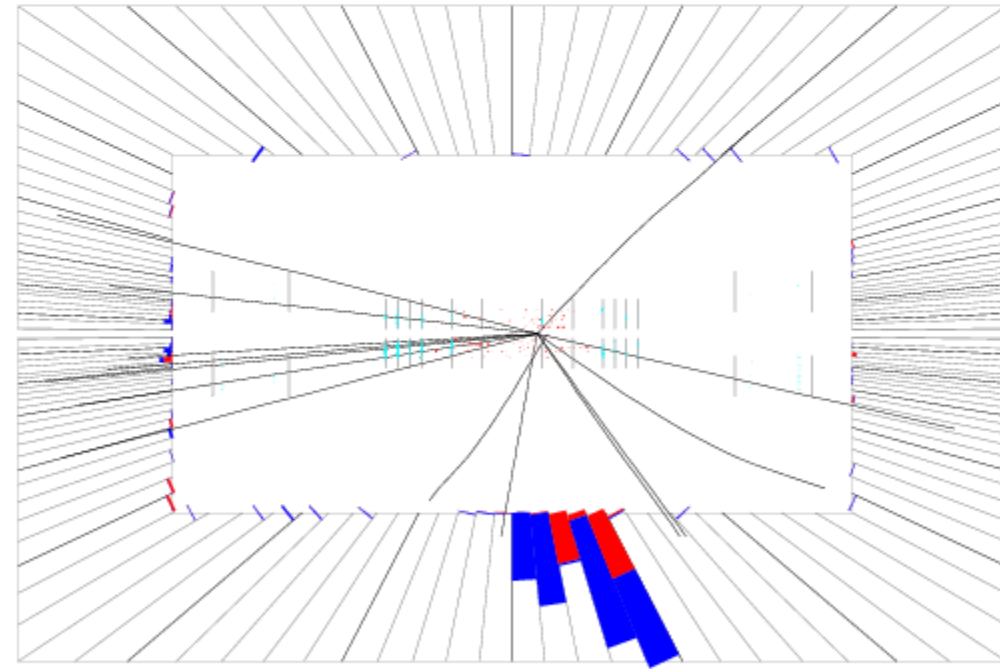




Cosmic background

- Inclusive jet production has little backgrounds except cosmics for high p_T jets
- “Cosmic jets” produced by muon bremsstrahlung
- Photon usually hit the calorimeter from the outside and often pass JetID cuts (EM fraction)
- Energy deposited only on one side \Rightarrow large missing- E_T
- Jet p_T spectrum falls as $\sim p_T^{-7}$, cosmic spectrum only as $\sim p_T^{-3}$

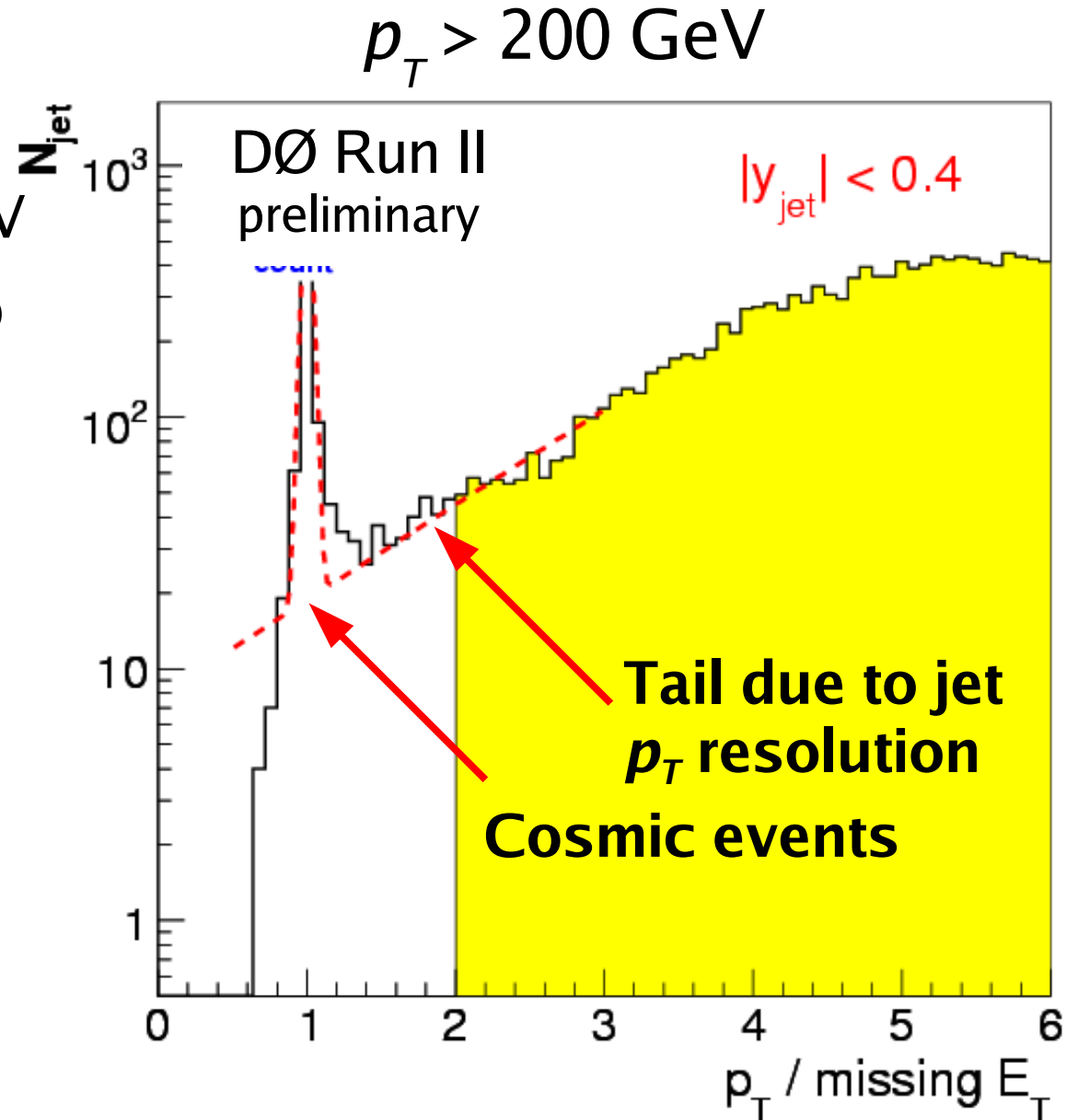
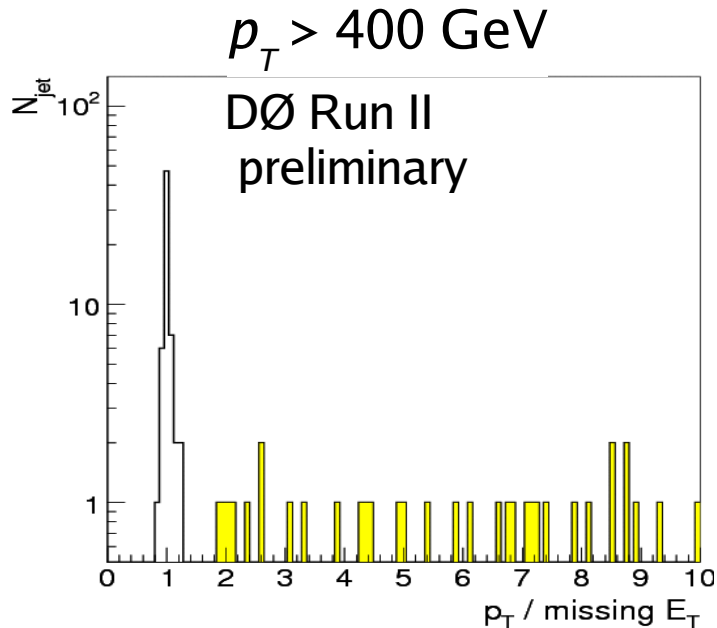
DØ Run II preliminary





Cosmic background

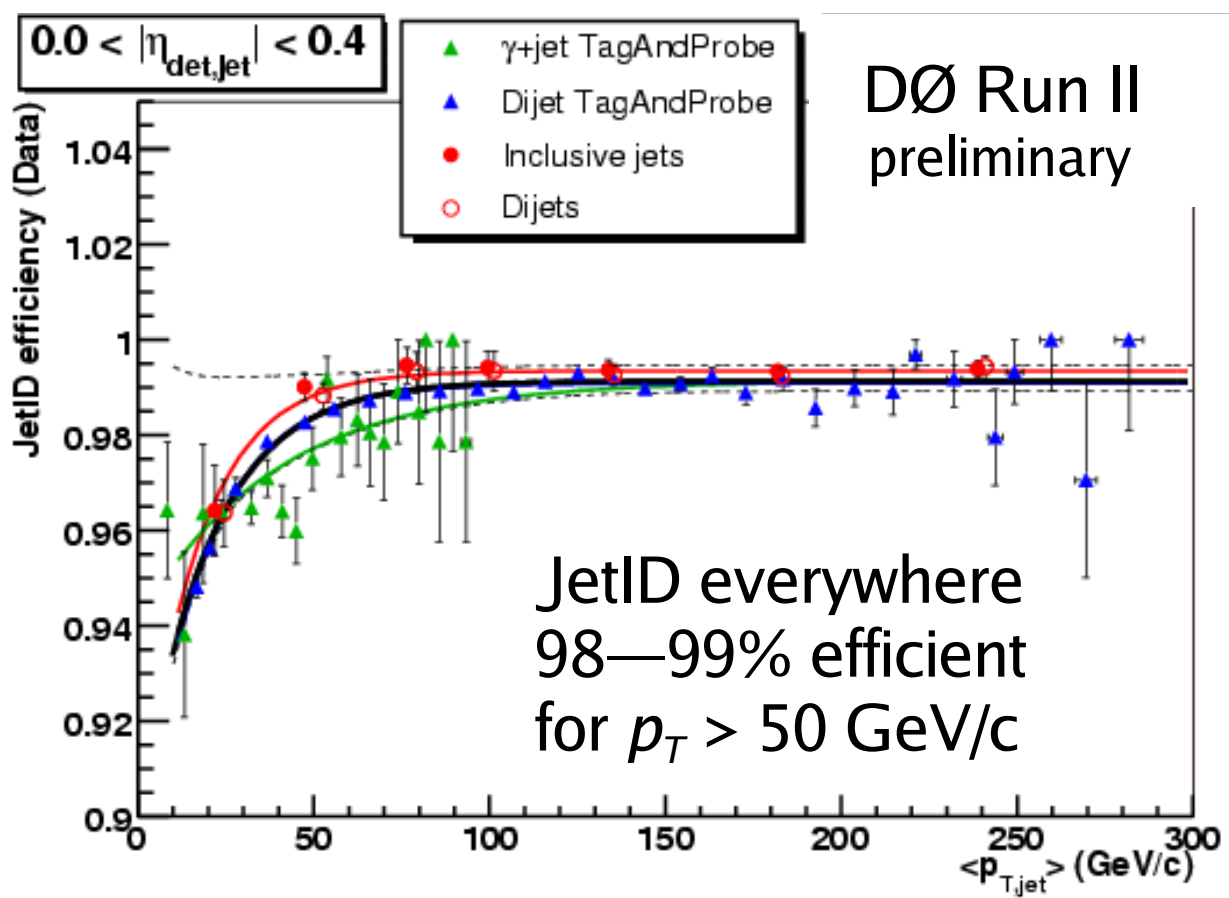
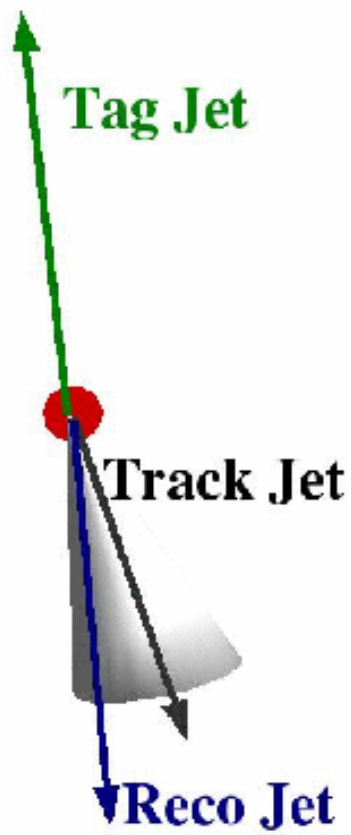
- Cosmic peak at $p_T / \text{MET} \sim 1$ comparable to inclusive jet cross section at $p_T > 400 \text{ GeV}$
- Missing- E_T cut is important to remove cosmic background:
 - high rejection (100%)
 - low inefficiency (<0.5%)





JetID inefficiency

- JetID efficiency determined with the tag-and-probe method:
 - Tag is a good jet (or a photon) and an opposite track jet \Rightarrow good event
 - Probe is a reconstructed jet close to the track jet
- Cross checks with different samples and direct cut fraction

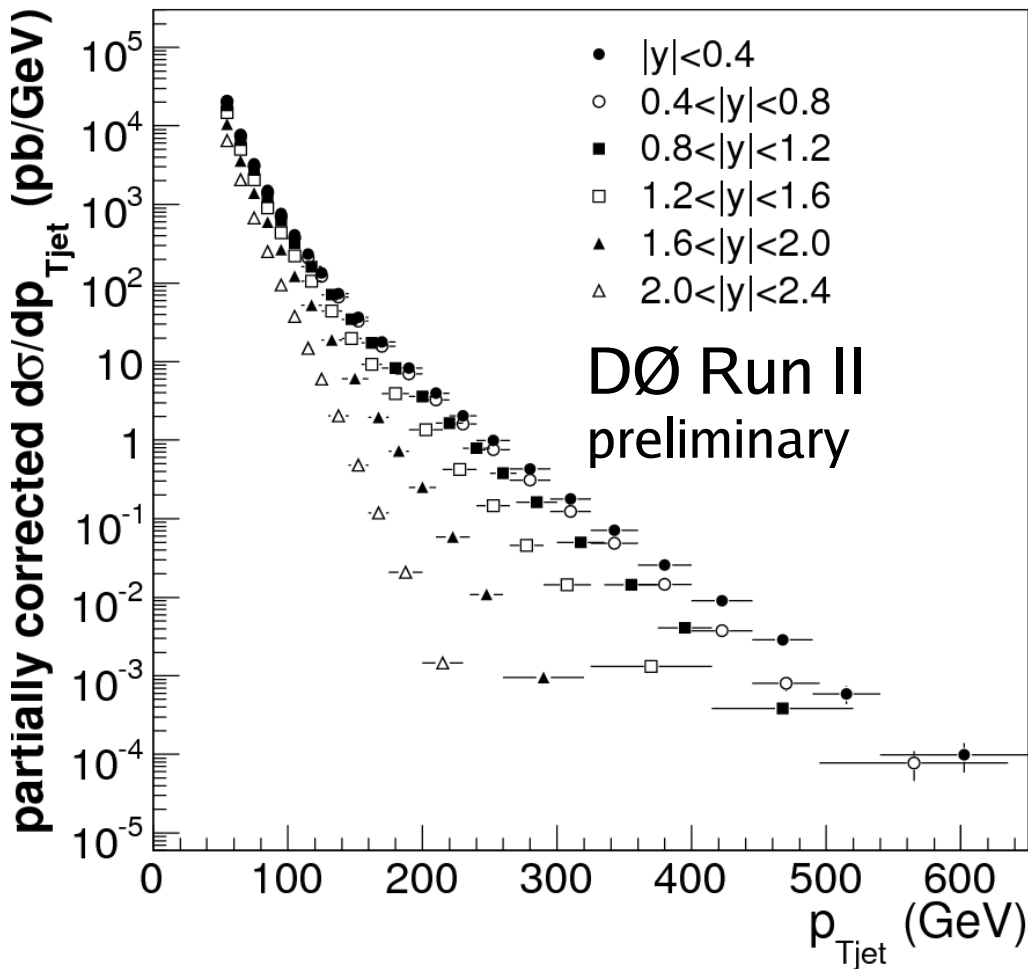




Jet energy scale (JES)

$$\frac{d^2 \sigma}{dp_T dy} = \frac{N}{\epsilon \cdot L \cdot \Delta p_T \Delta y} \cdot C_{smear} \text{ versus } p_T$$

Jet Energy Scale!!



- Cross section proportional to $p_T^{-\alpha}$
 - power $\alpha = 6 \rightarrow 14+$ in CC
 - power $\alpha = 8 \rightarrow 20+$ in EC
- Uncertainty $\delta\sigma$ proportional to $\alpha \times \delta\text{JES} \Rightarrow$ small JES uncertainty needed!

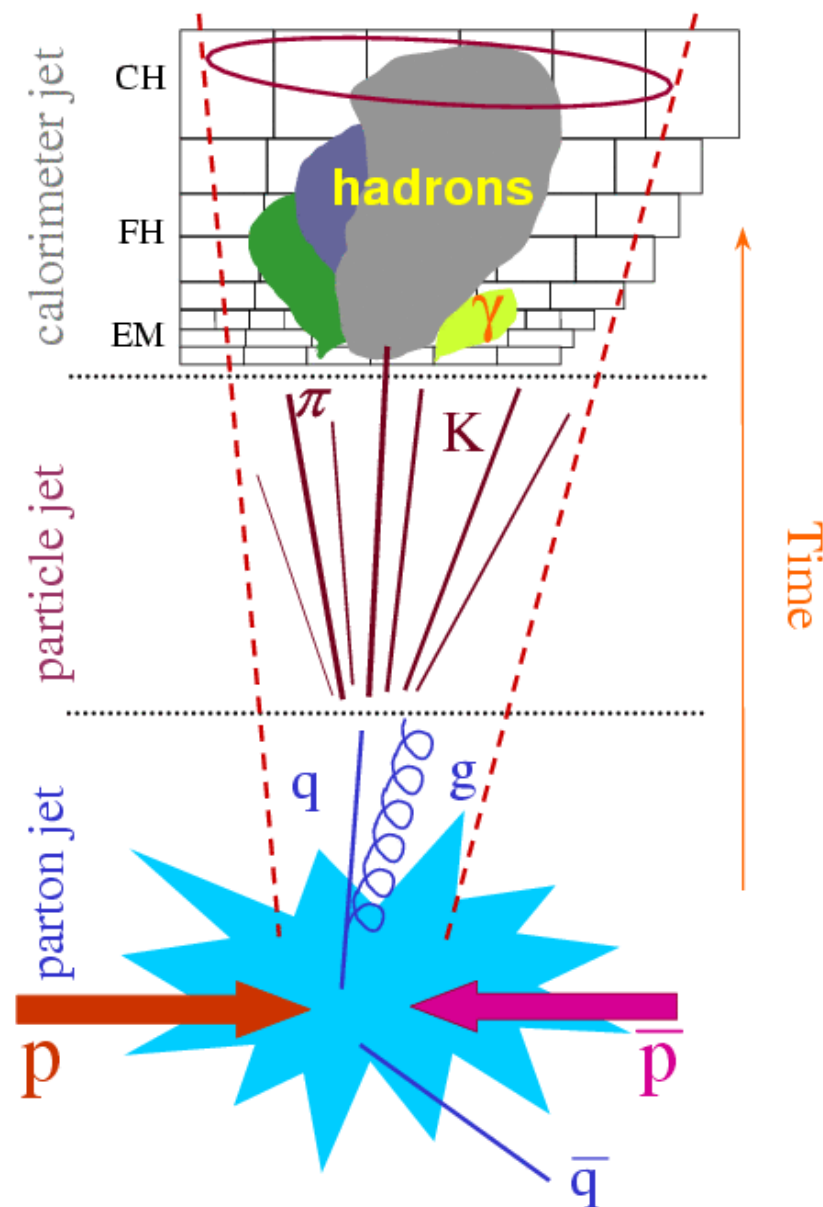


Jet energy scale

- Jet Energy Scale returns the measured calorimeter jet **energy** to the **particle level**

$$E_{ptcl} = \frac{E_{cal} - \text{Offset}}{(F_{\eta} \cdot R) \cdot S} \cdot k_{bias}$$

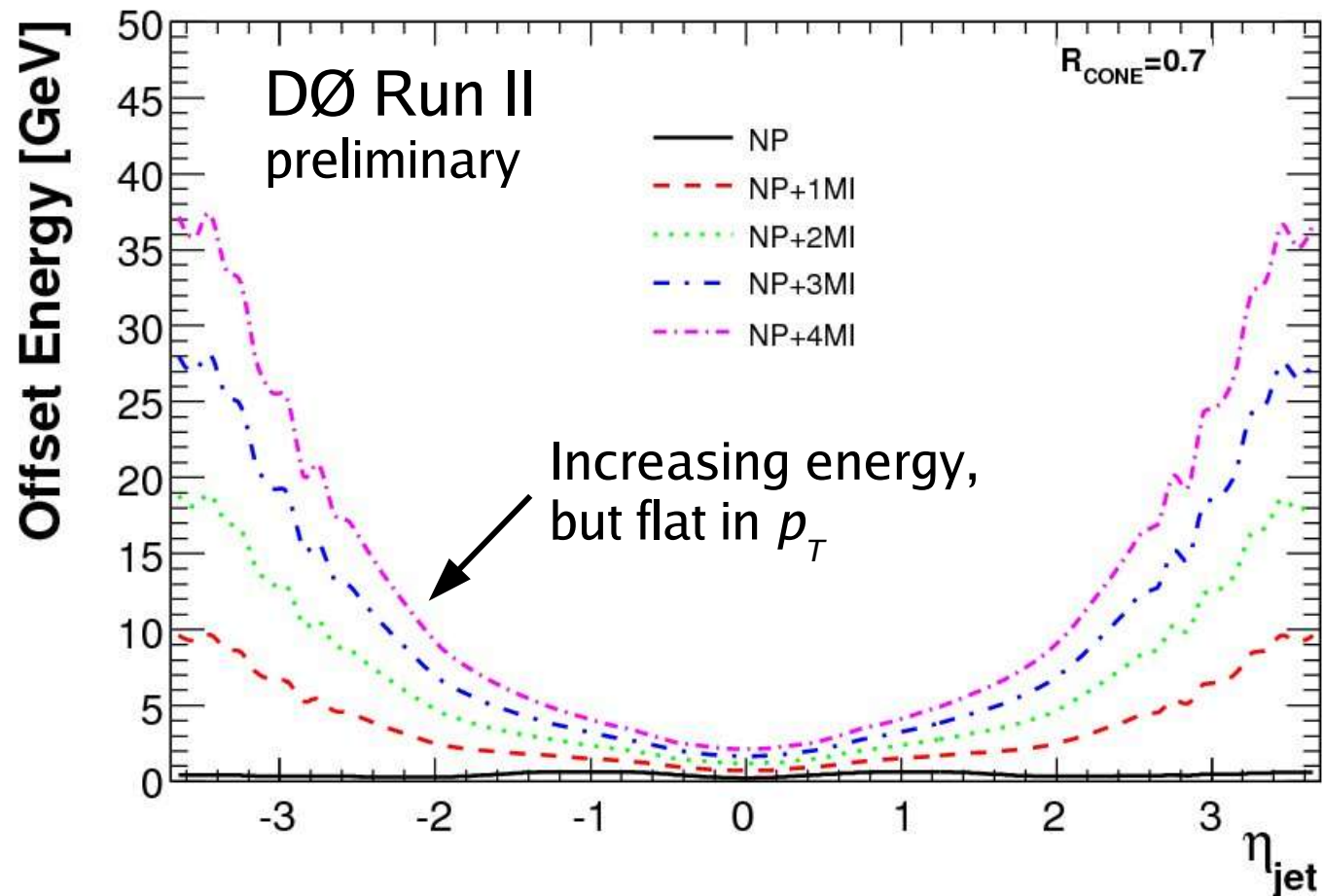
- Offset is energy not associated to the hard scatter: noise, pile-up, **multiple interactions**
- Response is the fraction of particle jet energy deposited in the calorimeter by the particles
- Detector showering accounts for **energy flow** in and out of the calorimeter jet due to detector effects (finite calorimeter tower and hadron shower size, magnetic field)
- Method biases corrected using tuned MC





JES: Offset

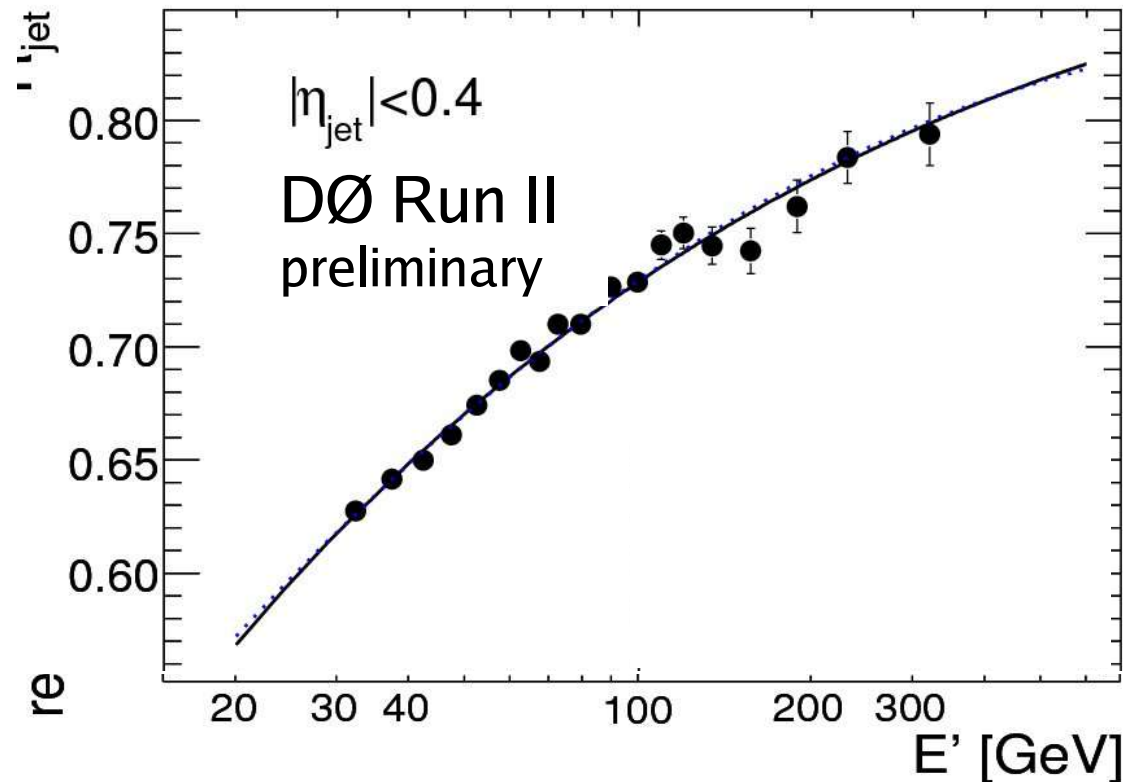
- Offset energy density from the region outside jets in data:
 - Zero Bias events with luminosity and vertex veto (noise and pile-up, NP)
 - Minimum Bias events (multiple interactions, MI)
- Primary contribution from multiple interactions
- Average offset without underlying event 0.5—1.0 GeV/c in p_T
- Less than 1—3% correction at $p_T > 50$ GeV/c





JES: Response

- Response calibration performed in three steps:
 - **Photon energy scale** is calibrated using $Z \rightarrow e^+e^-$ and tuned MC for e/γ energy scale difference
 - **Response in CC** is calibrated with γ +jet events (R_{cc})
 - **Equalization of calorimeter** with dijet (γ +jet) events where one jet (photon) central (F_η)



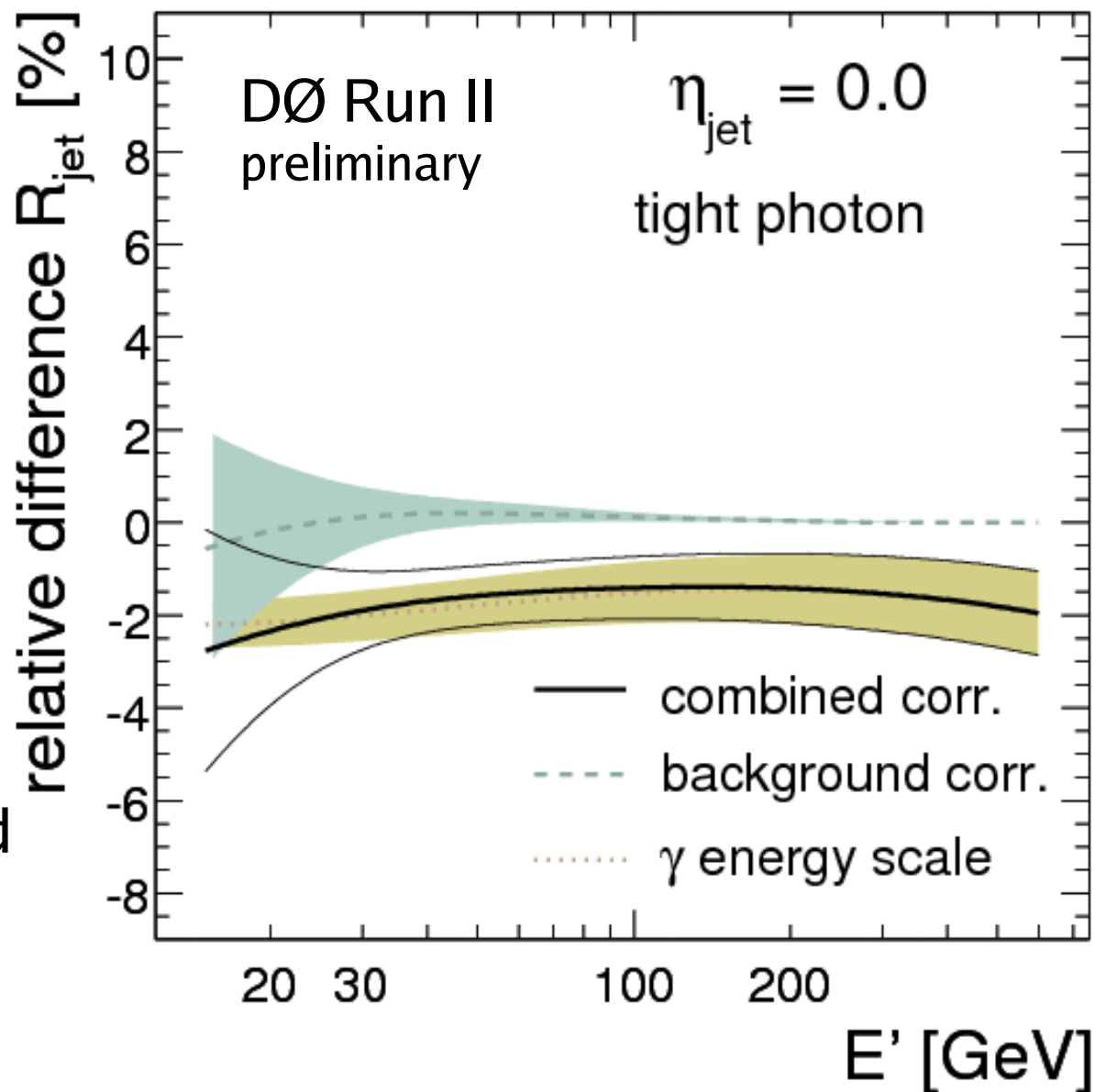
- Hadronic showers (pions) deposit less energy than electrons/photons $\Rightarrow R_{\text{jet}} < 1$
- At each “step” of showering, 1/3 of hadronic shower goes to $\pi^0 \rightarrow \gamma\gamma$ and continues to shower electromagnetically
- At higher energy more “steps” so $R_{\text{jet}} \rightarrow 1$ roughly as powerlaw $R = 1 - a p_T^m$



JES: Photon calibration

- MC tuned for electron response in W/Z group \Rightarrow good simulation of γ/e response differences
- Leading uncertainty material budget
- Background from EM-jets (dijets with one jet misidentified as photon) at low p_T
- Measurement vs E' to avoid jet resolution effects:

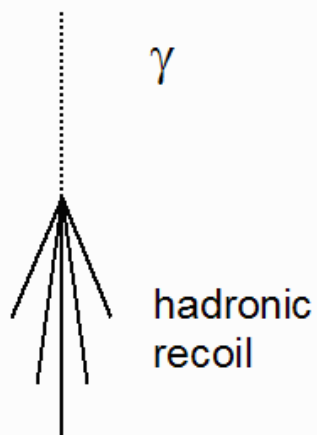
$$E' = p_T^\gamma \cosh(\eta_{\text{jet}})$$





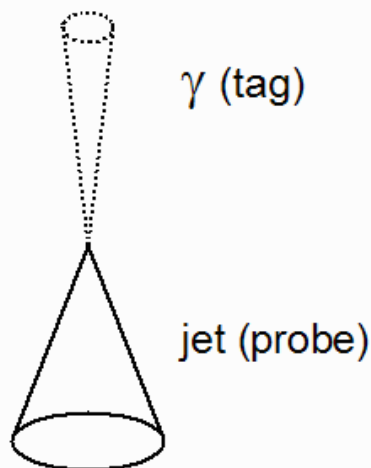
JES: Response calibration

Particle Level



$$\vec{p}_{T,\gamma} + \vec{p}_{T,had} = \vec{0}$$

Detector Level



$$\vec{p}_{T,\gamma} + R_{had}\vec{p}_{T,had} = -\vec{E}_T$$

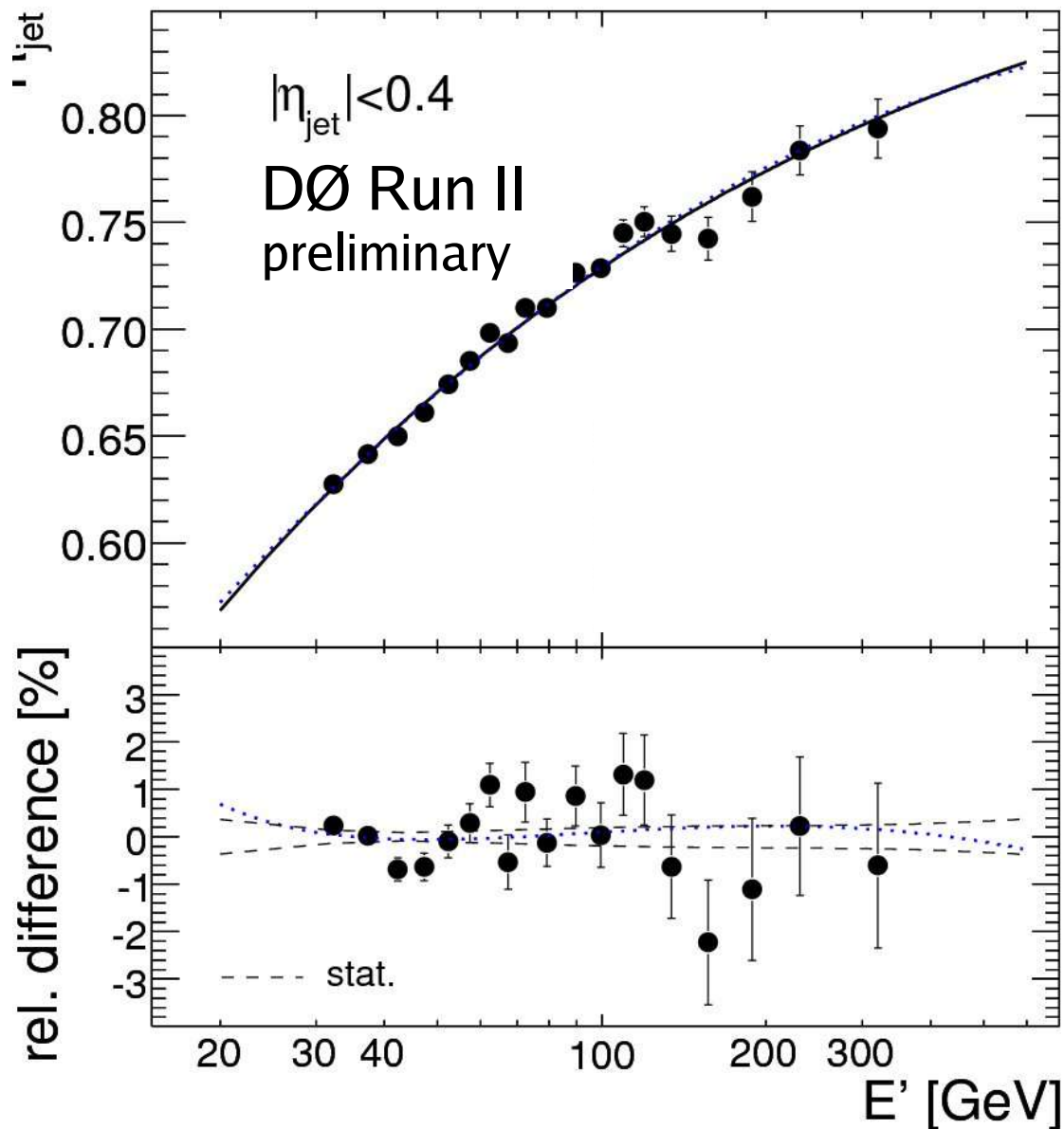
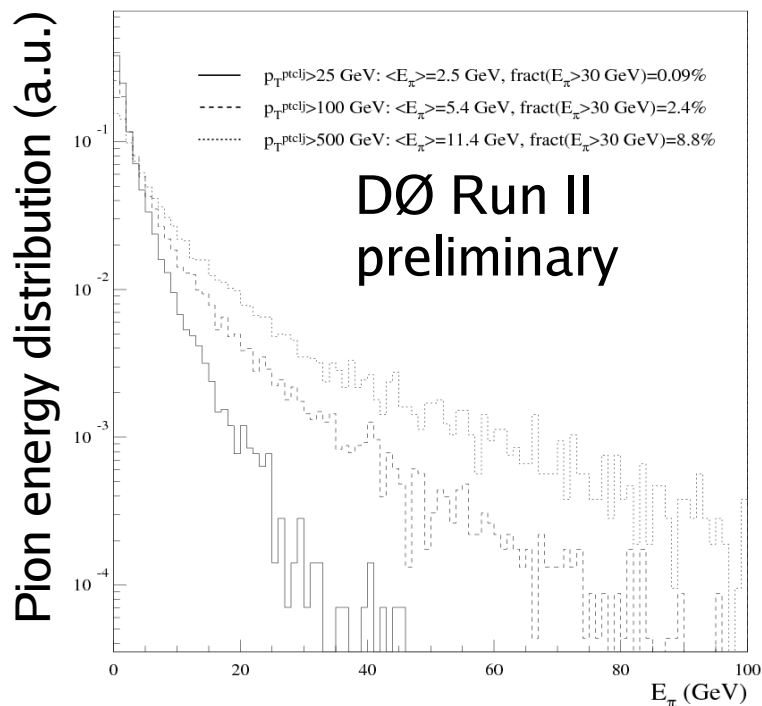
- Response calibration based on transverse momentum conservation
- Photon/central jet and recoil balanced in p_T at parton/particle level

- Calibration through missing- E_T insensitive to the jet cone and showering effects
- Dijet events improve statistics and reach in energy; important for sample dependence



JES: CC response fit

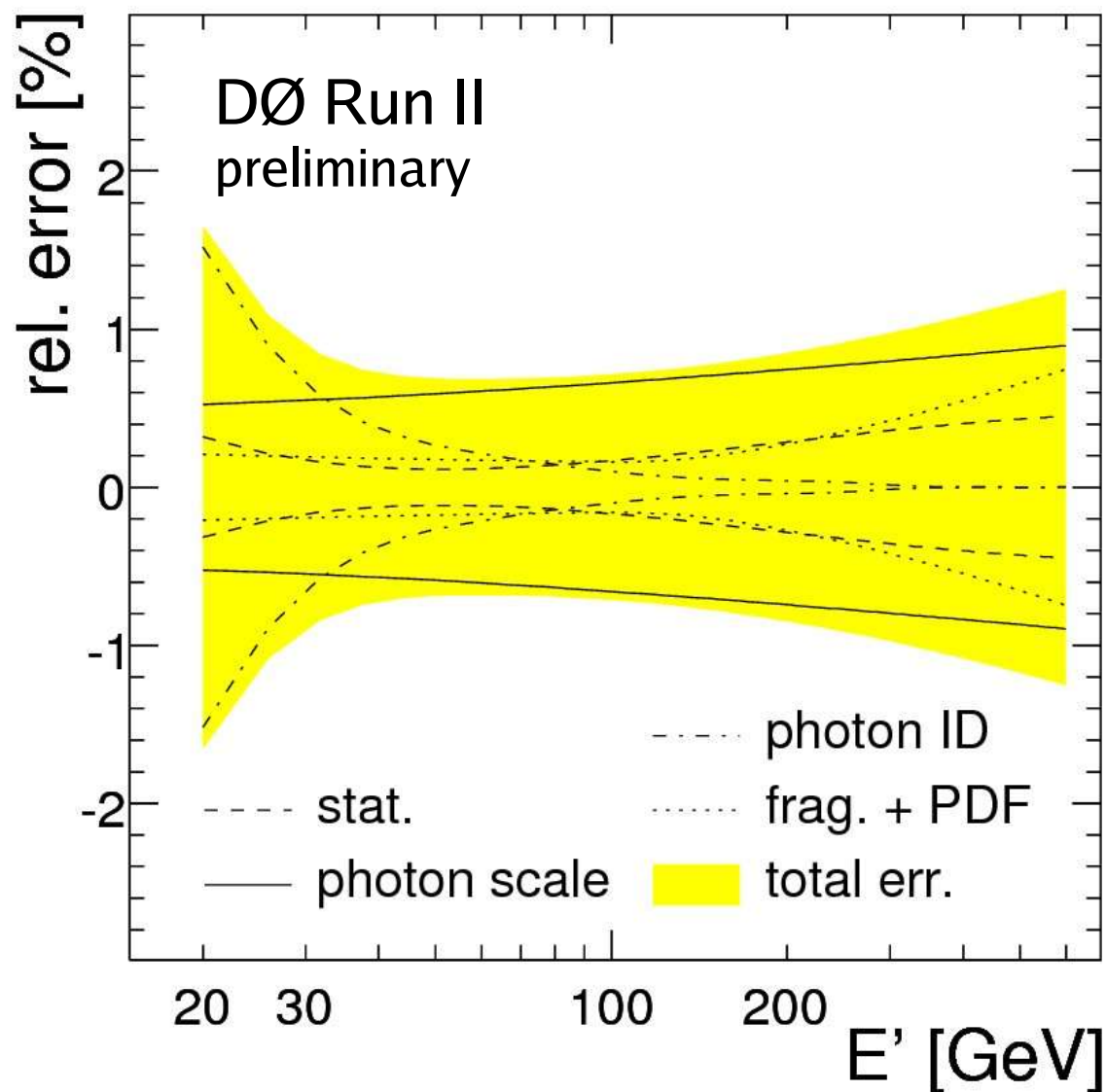
- Over 2% extrapolation uncertainty reduced by scaling single pion response in MC to γ +jet data
- Predict high p_T jet response by fitting low p_T pion response
- Agreement with isolated track data





JES: CC response uncertainty

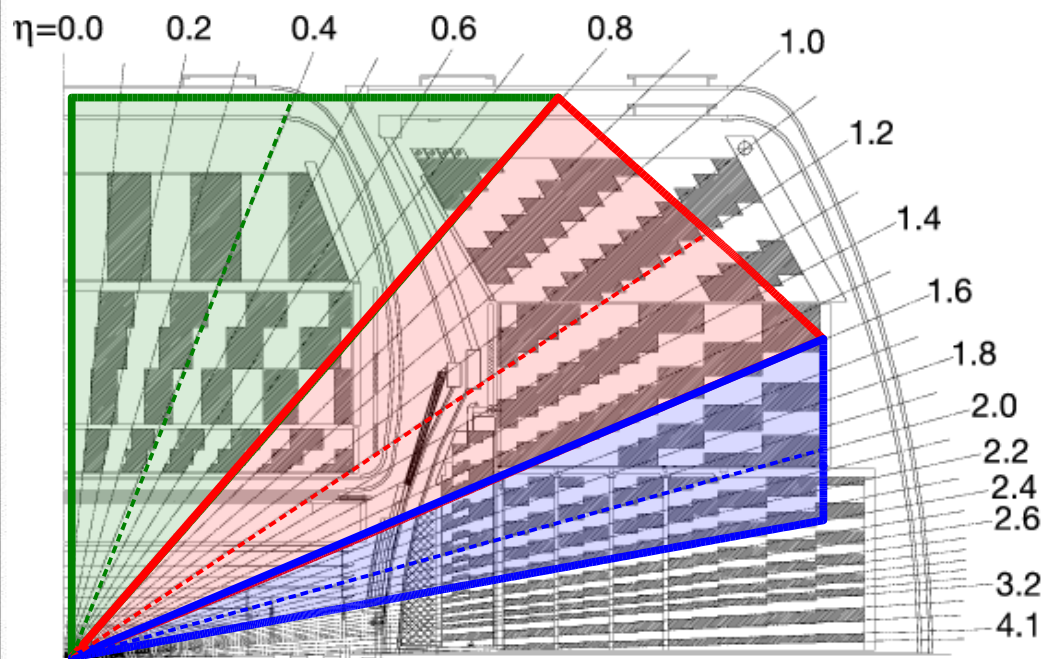
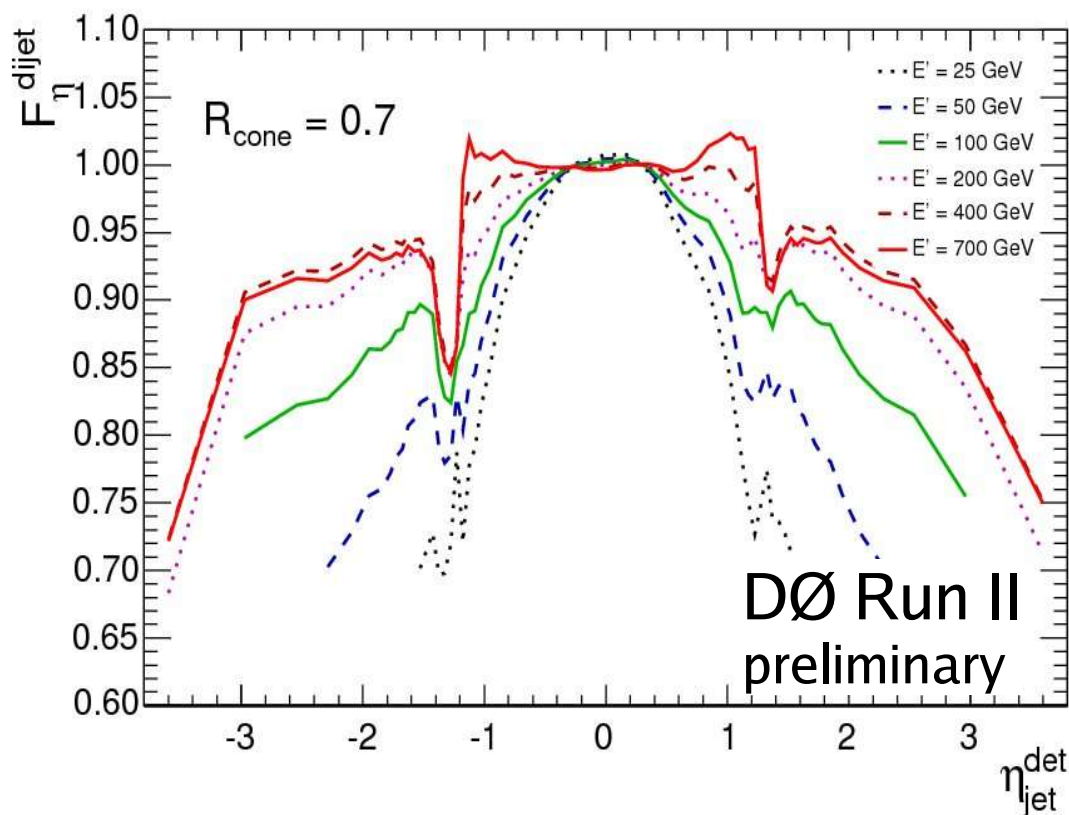
- Uncertainty for CC response dominated by photon scale: EM-scale (0.5%) and material effects (0.5%)
- Fragmentation (Pythia versus Herwig) and PDF uncertainty also contribute a little at high p_T





JES: η -dependence

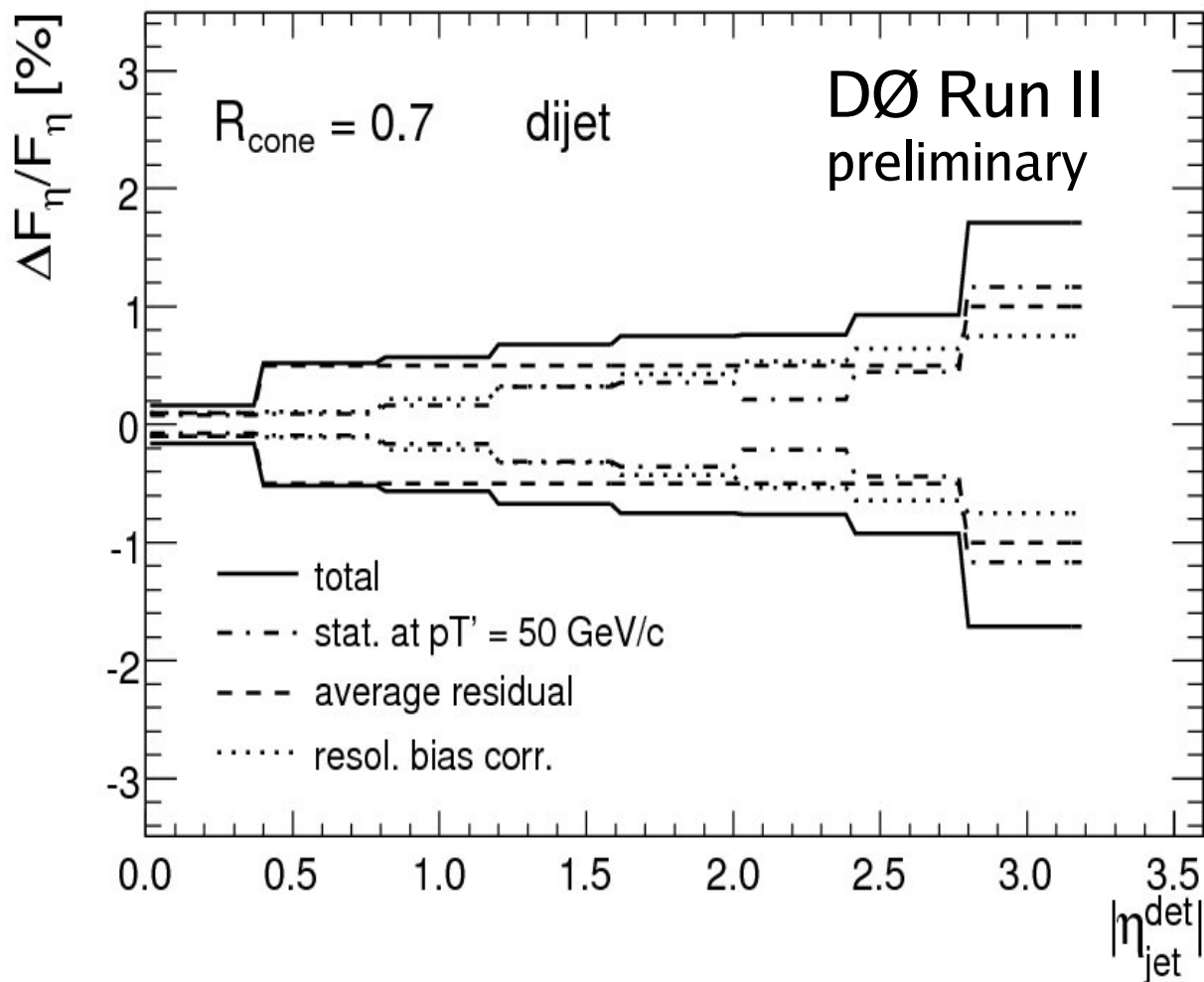
- Response depends on calorimeter region (central, intercryostat, end cap)
- Low residual energy dependence at high E
- Simultaneous fit to dijet and γ +jet samples taking into account sample differences





JES: η -dependence

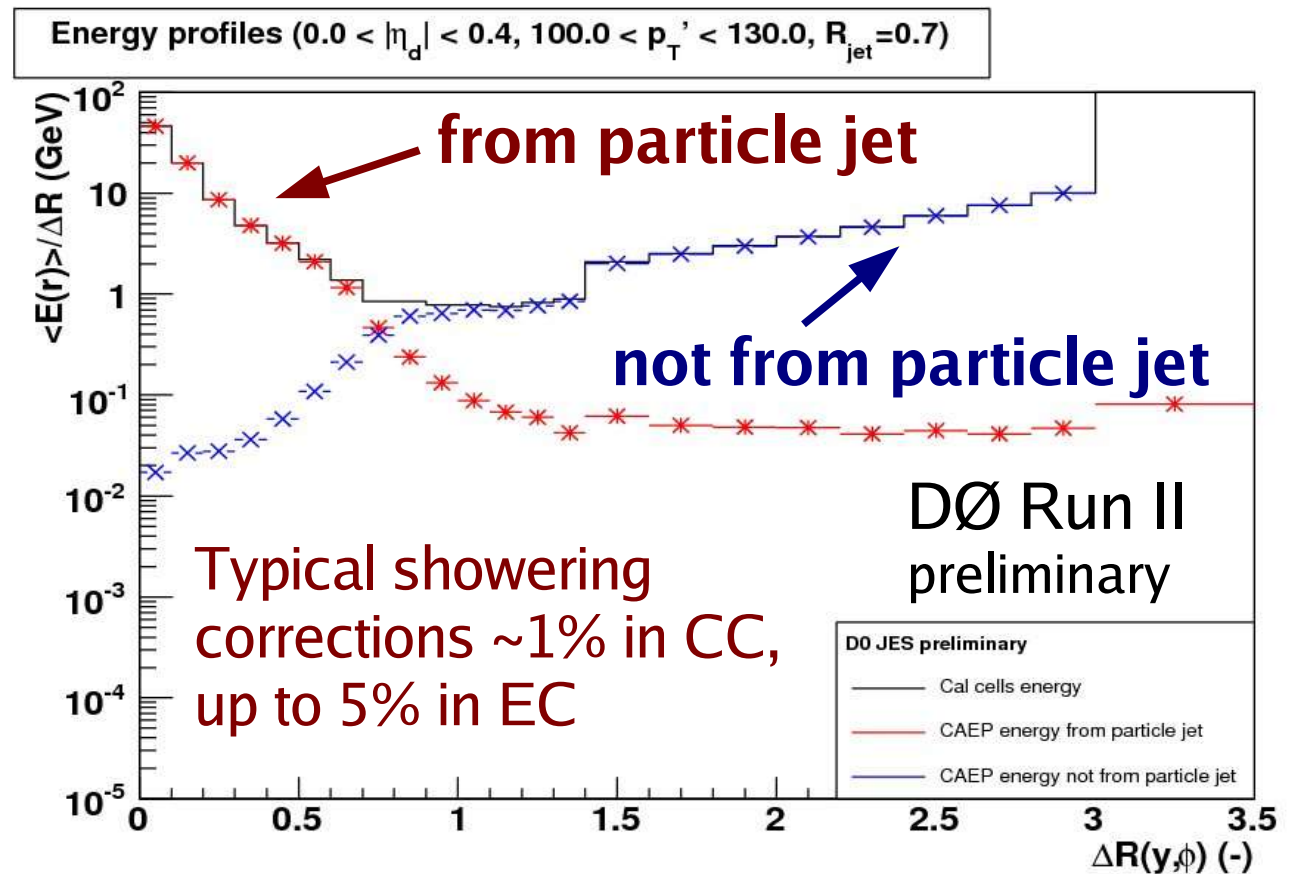
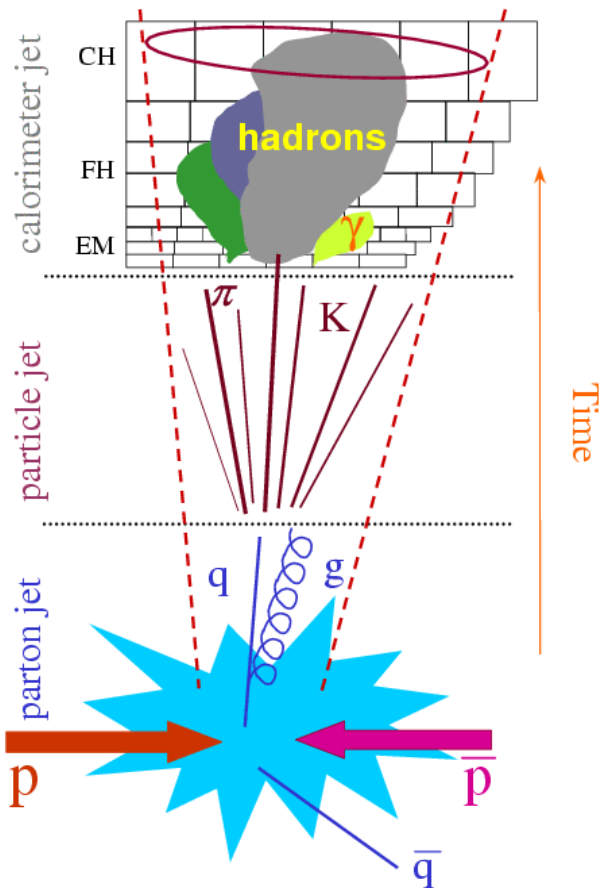
- Largest uncertainty is average residual of 0.5%, total below 1% at $|\eta| < 2.8$
- Resolution bias correction (from dijet) also contributes in EC





JES: Showering

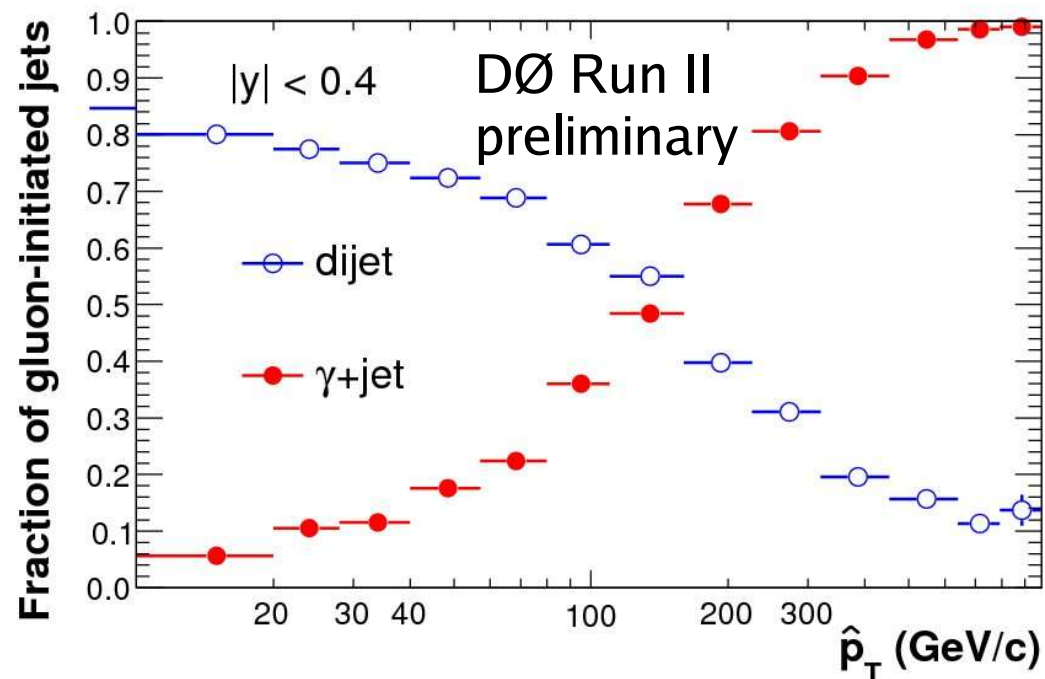
- Showering correction accounts for the net energy flow in and out of jet cone
- Ratio of the calorimeter jet energy to energy deposited by the particle jet
- Data-based method uses energy profiles around jet center



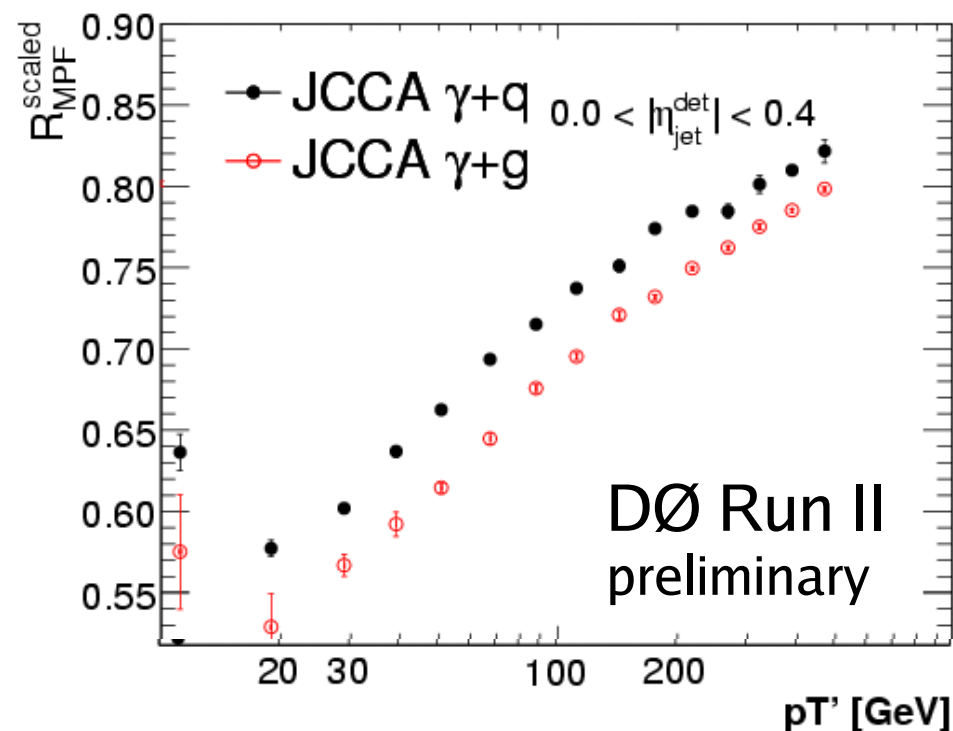


JES: Sample dependence

- Final Run IIa JES precise enough that cannot hide **quark and gluon jet response differences** and the **difference between E and p_T** calibrations under the systematics rug anymore; γ +jet and dijet samples have completely different jet composition



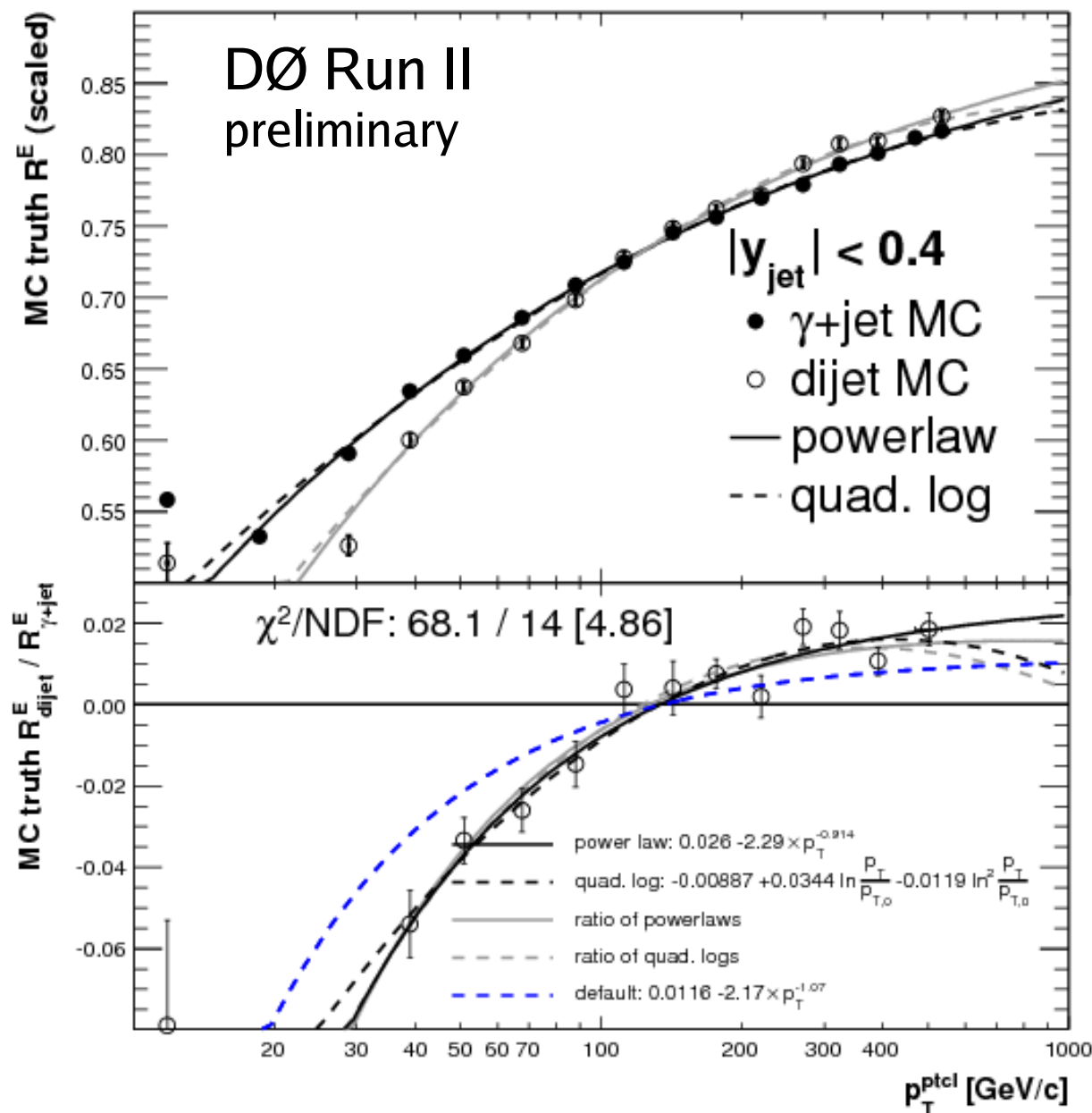
- Knowledge of single pion response is essential to predict the quark and gluon response differences
- Single pion response tuned using γ +jet data





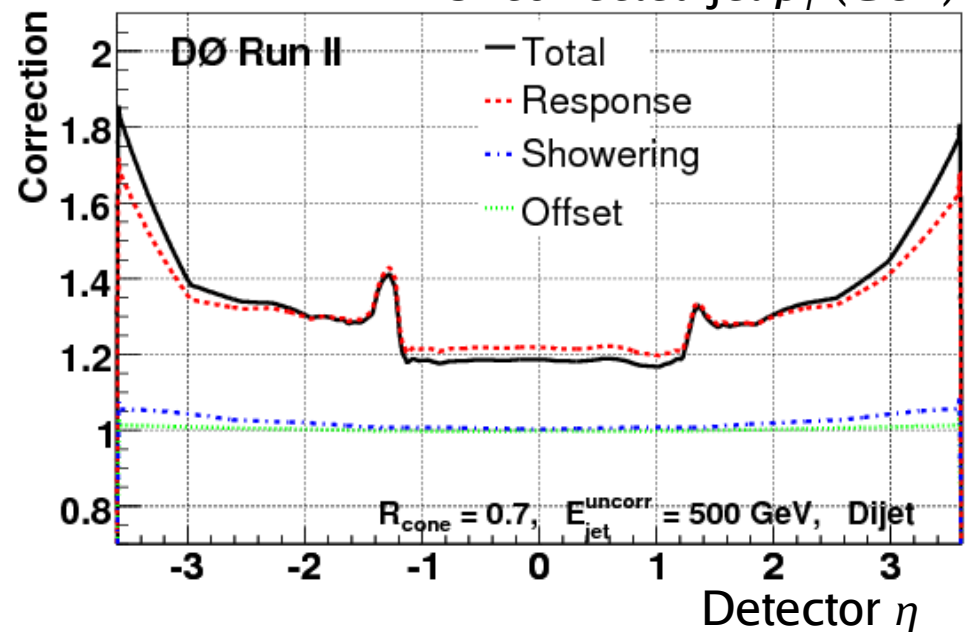
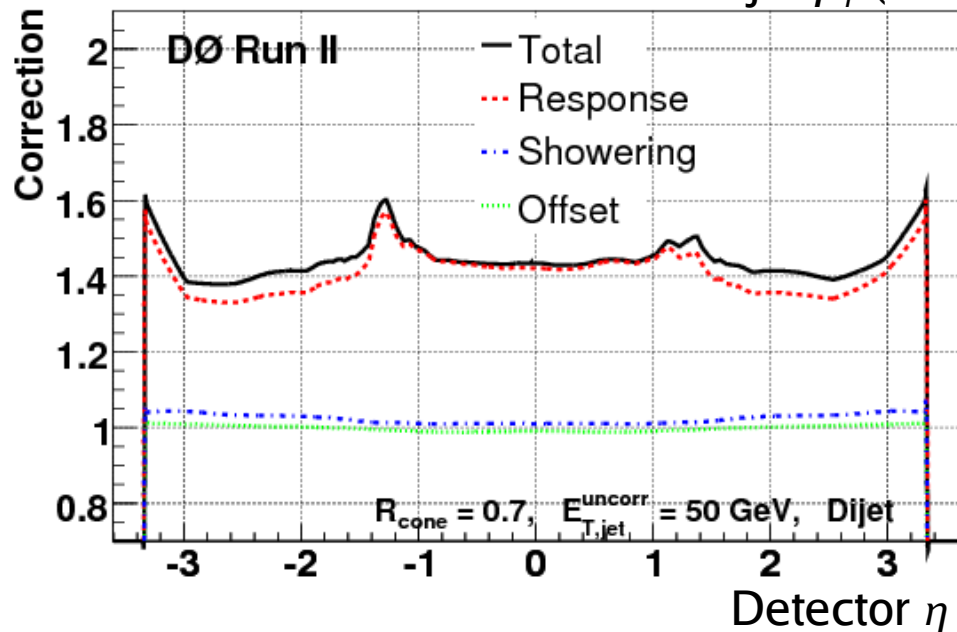
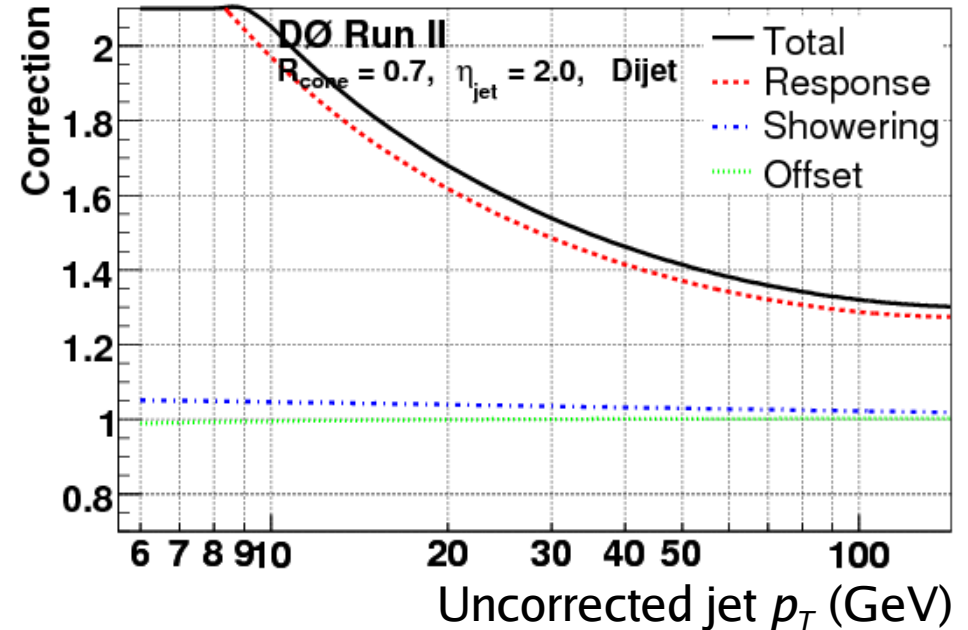
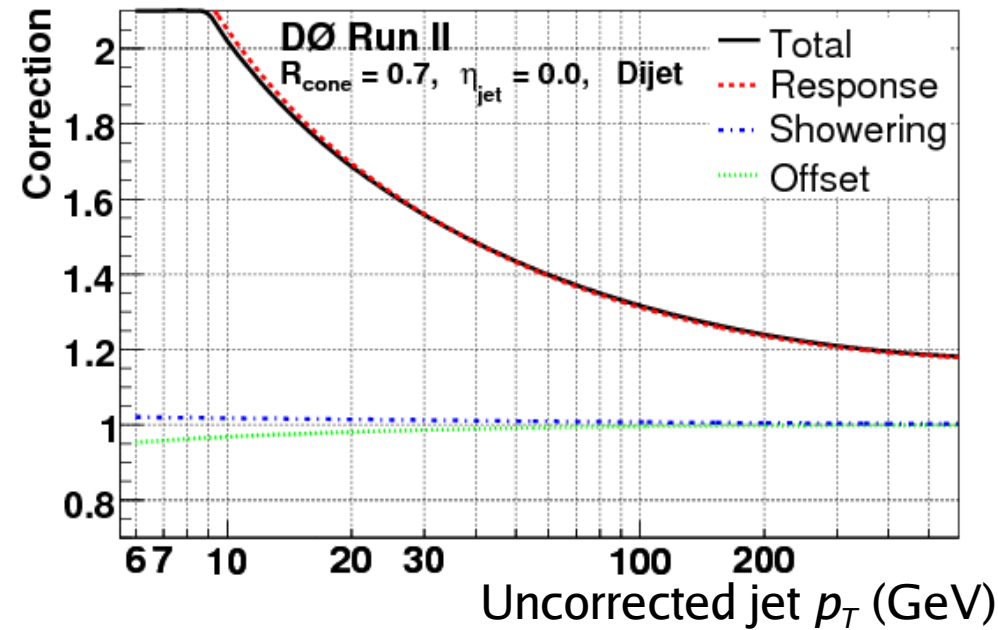
JES: Dijet corrections

- MC with **single pion response scaled to data** is used to derive the ratio of dijet and γ +jet responses in CC (-4% at 50 GeV, +2% at 400 GeV)
- Showering and bias corrections also rederived for dijets using tuned MC
- η -intercalibration for dijets directly from data
- Additional corrections for E / p_T difference and rapidity bias \Rightarrow four-momentum calibration



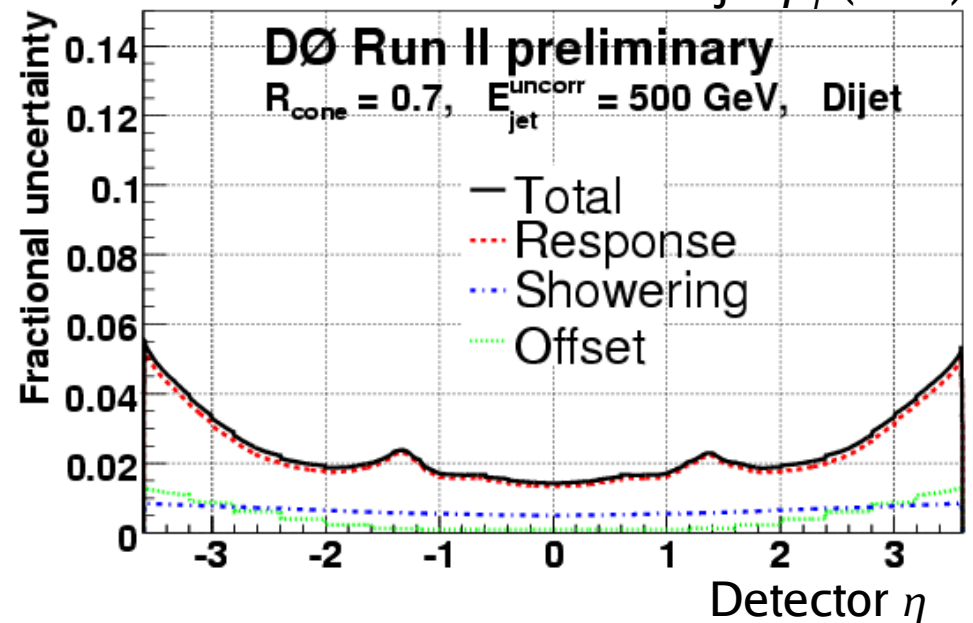
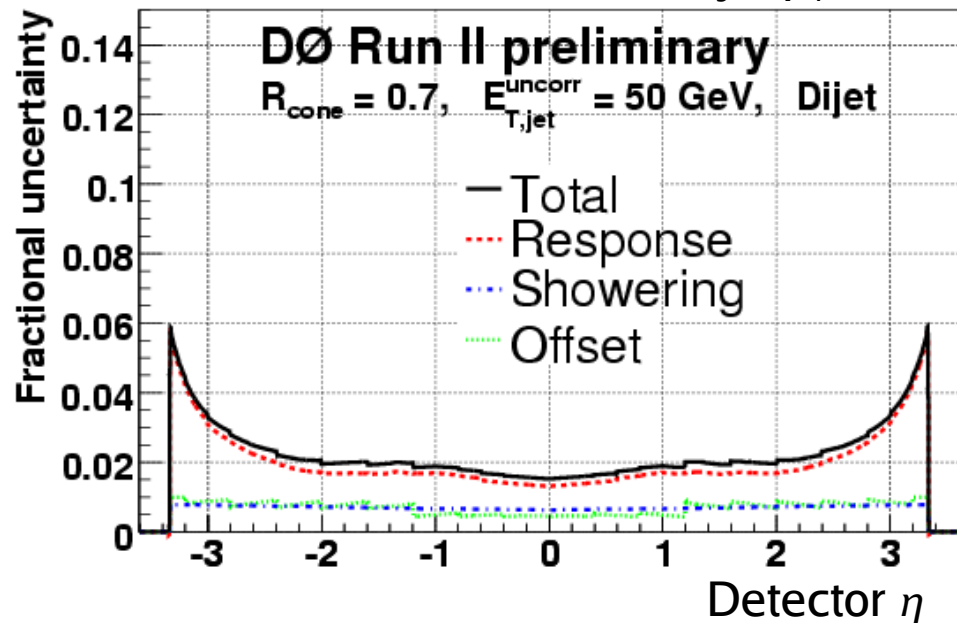
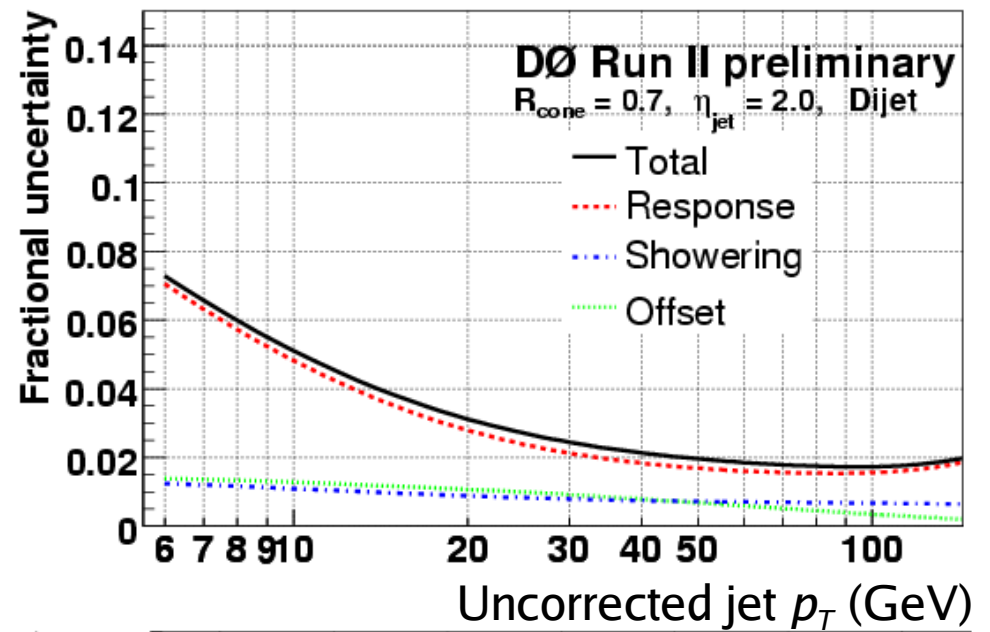
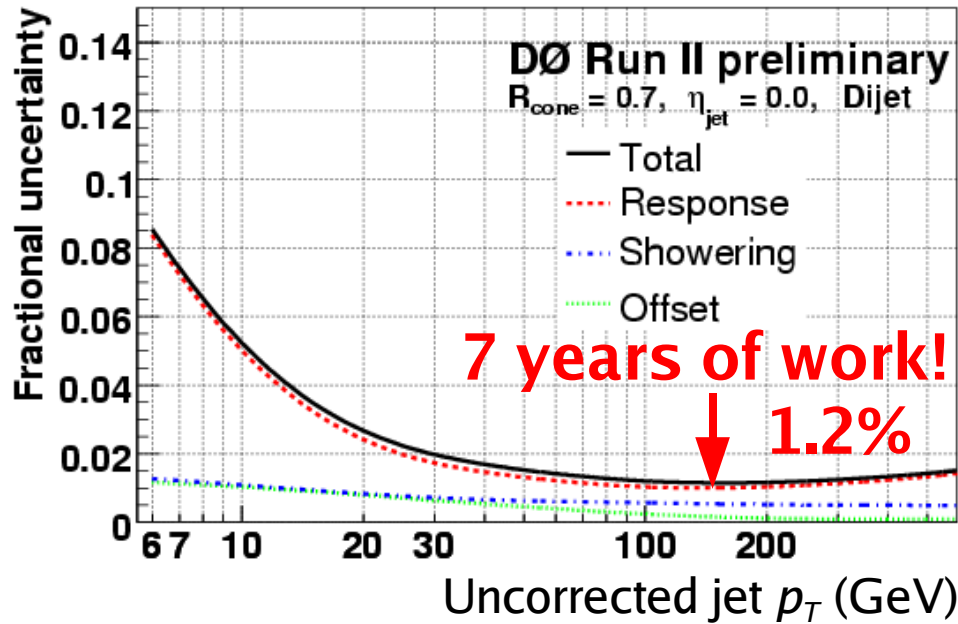


Dijet JES corrections





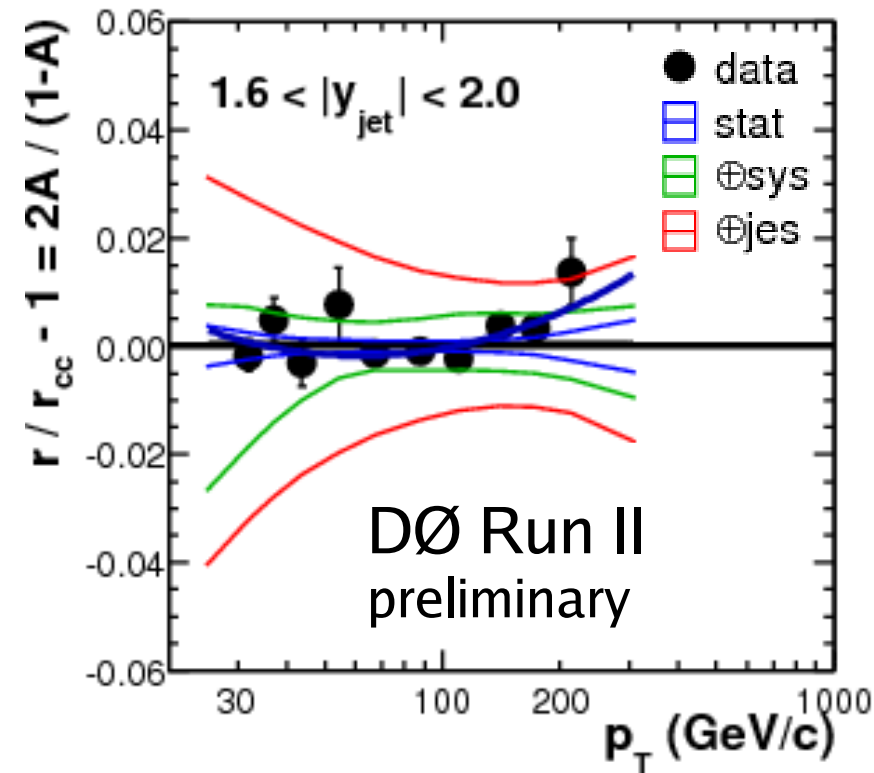
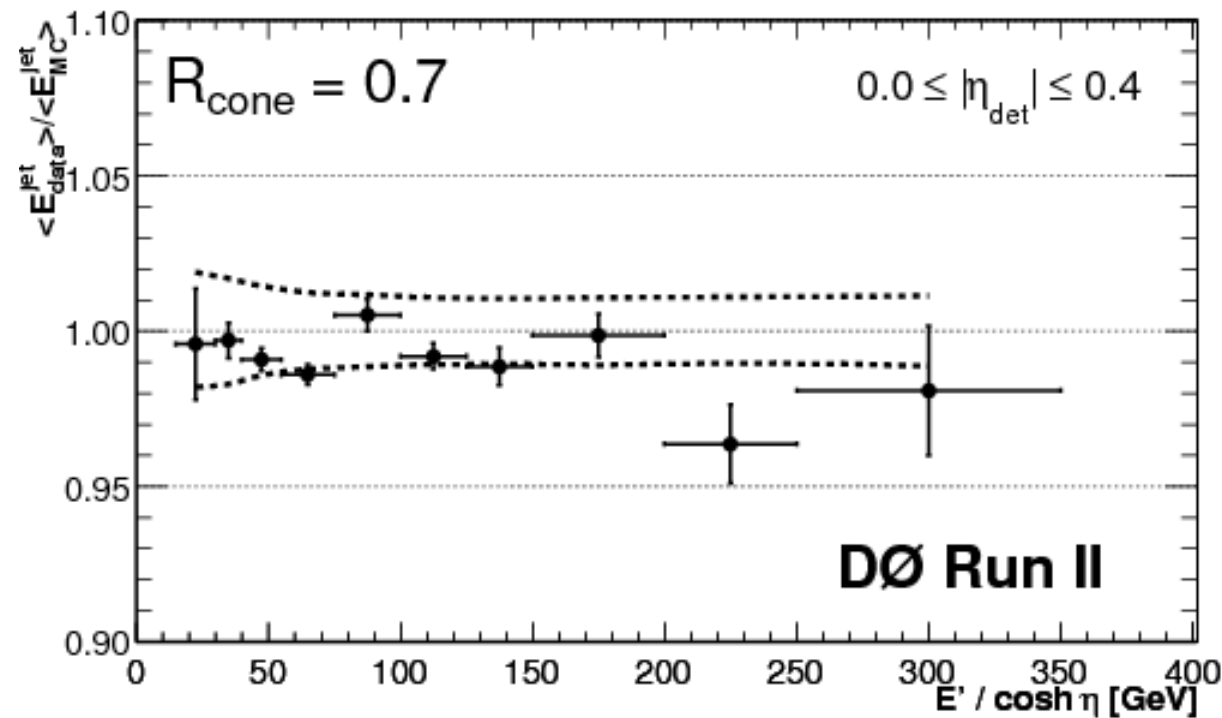
Dijet JES uncertainty





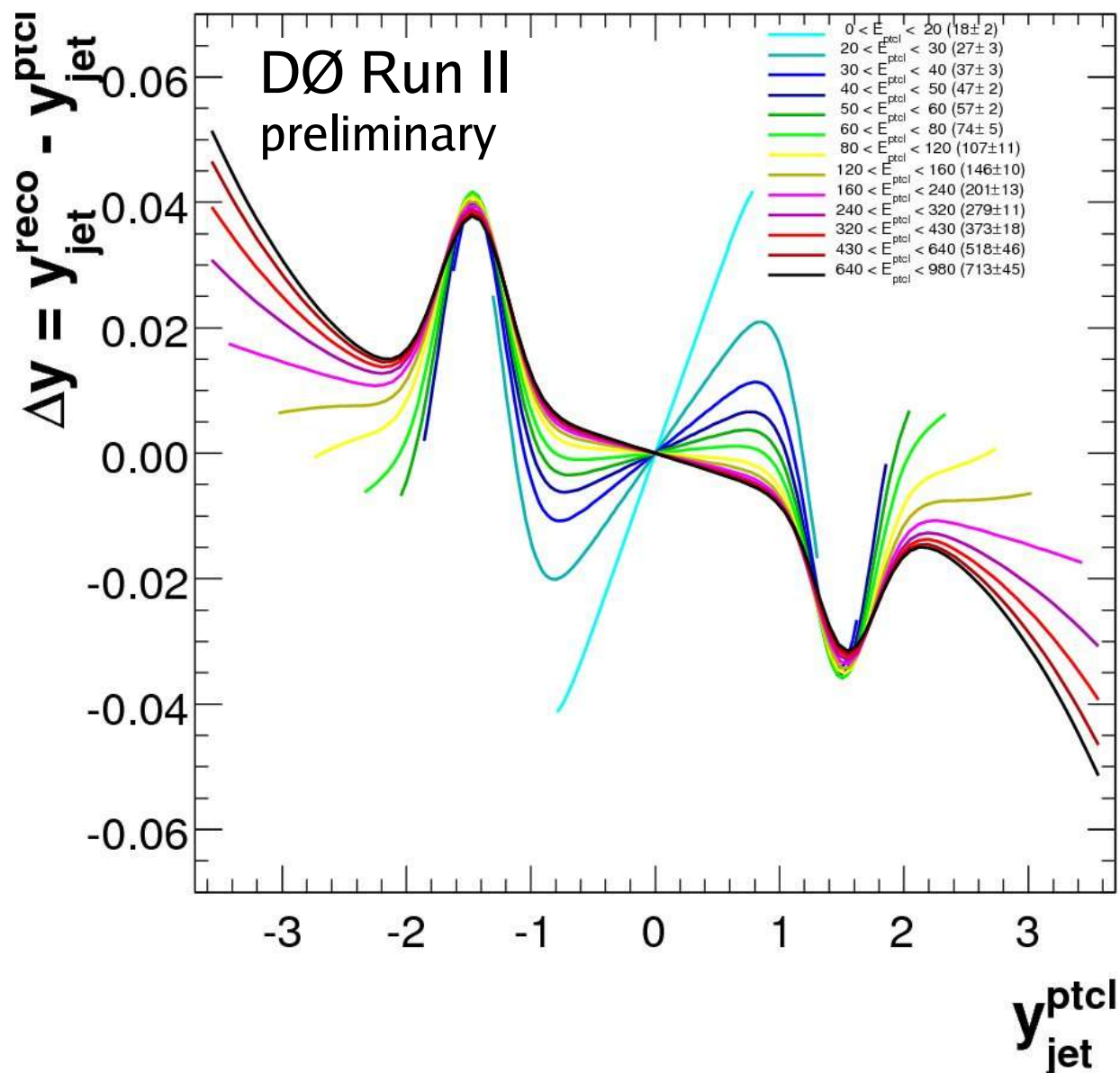
JES: Closure tests

- γ +jet closure tests consistency of JES corrections for absolute scale in CC
- Dijet closure tests the consistency of forward JES relative to CC
- Closure calculated from dijet asymmetry $A = (p_{T,fwd} - p_{T,cc}) / (p_{T,fwd} + p_{T,cc})$
- Explicit correction for residual resolution bias





JES: Rapidity bias

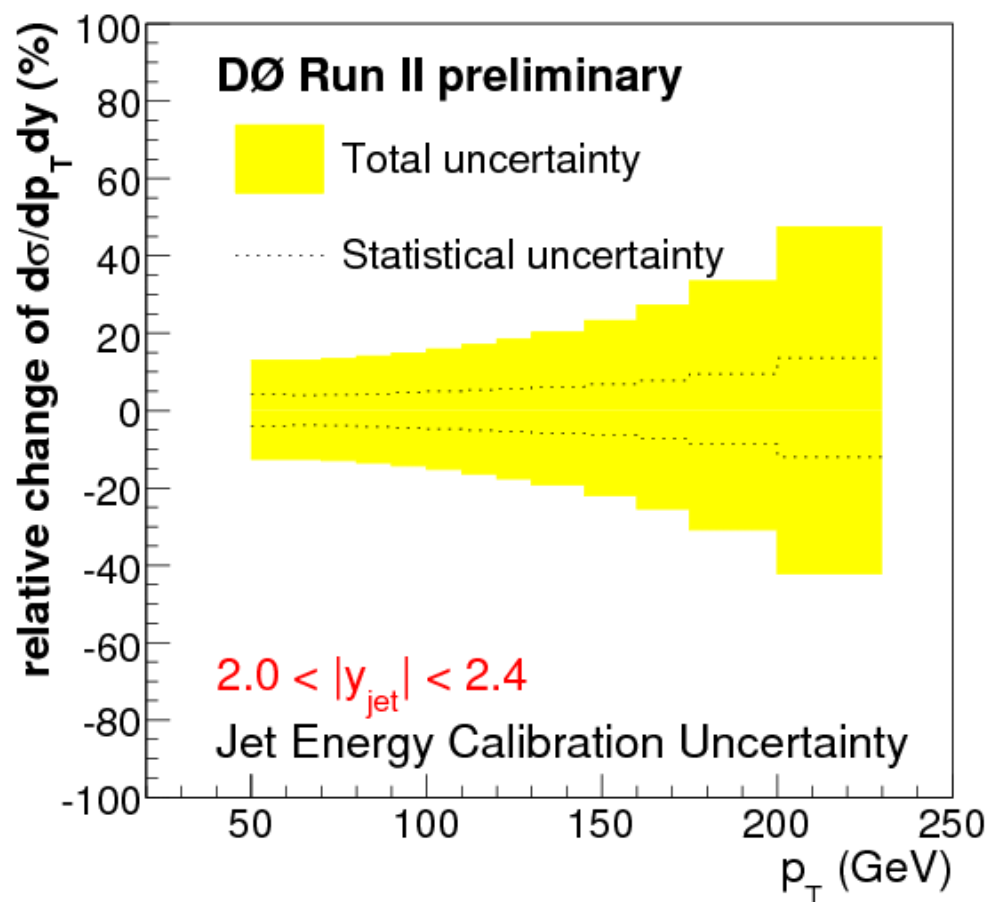
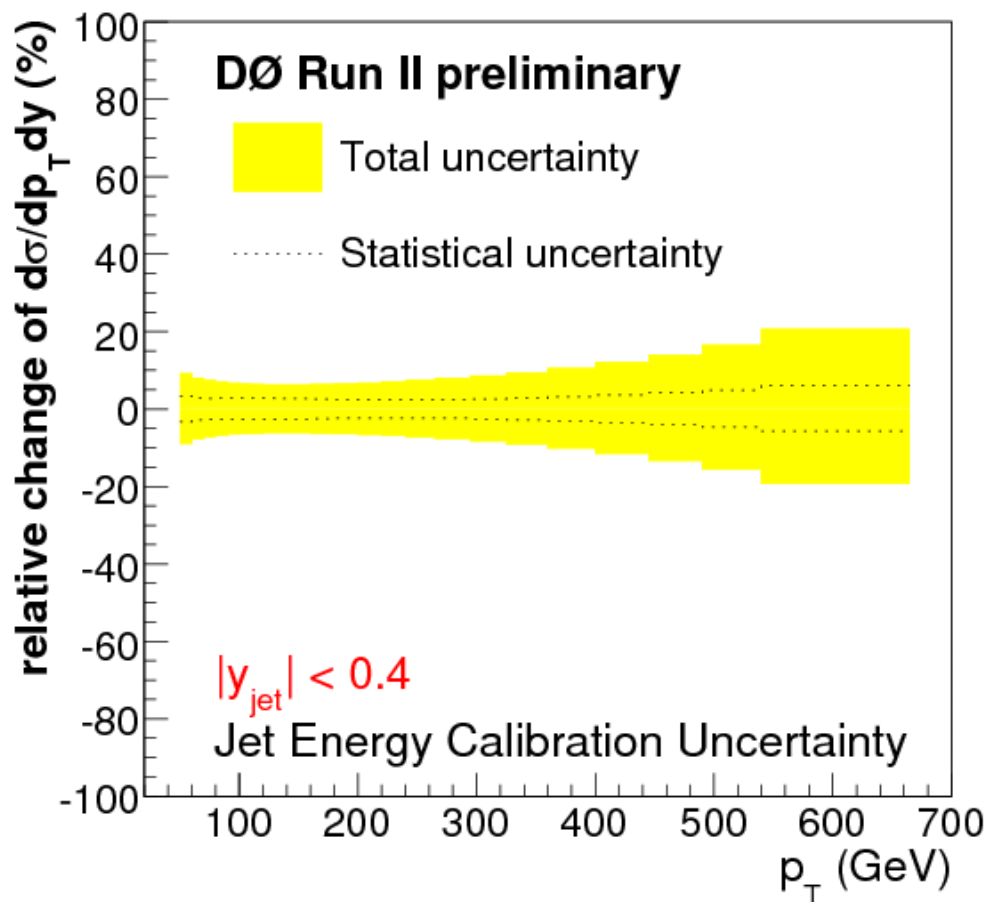


- Small detail: correction to p_T is much more important
- Jets are biased in rapidity on average toward the center of the calorimeter
- At most (in ICR), bias little less than half a cell width



JES uncertainty

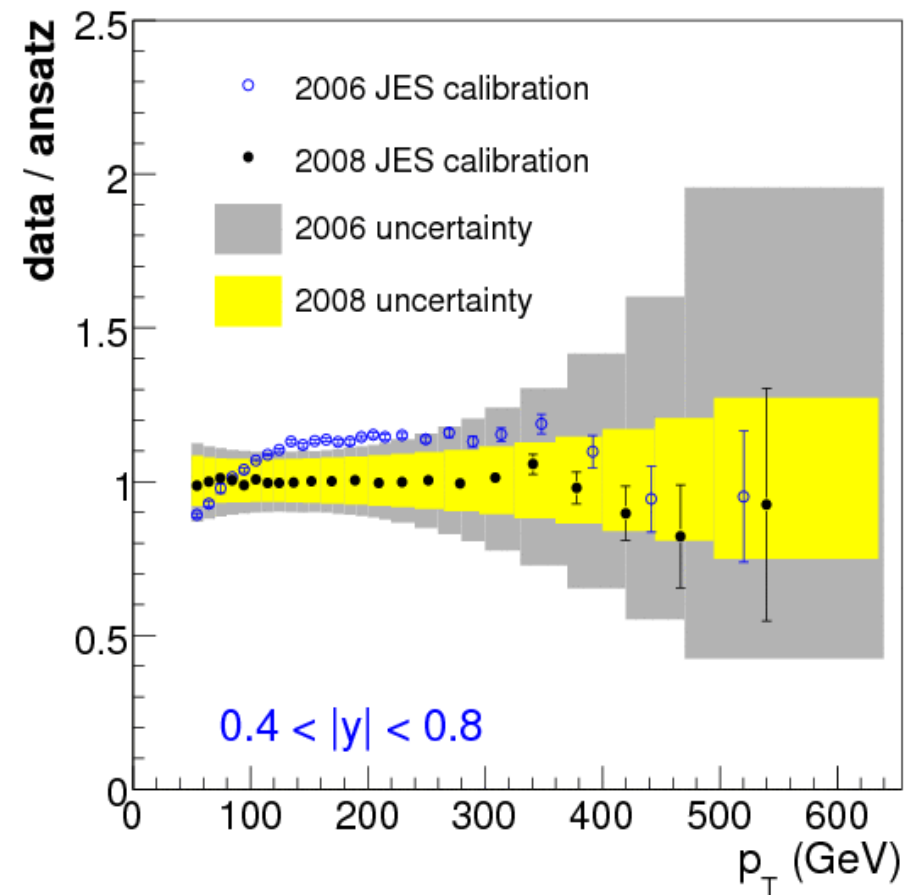
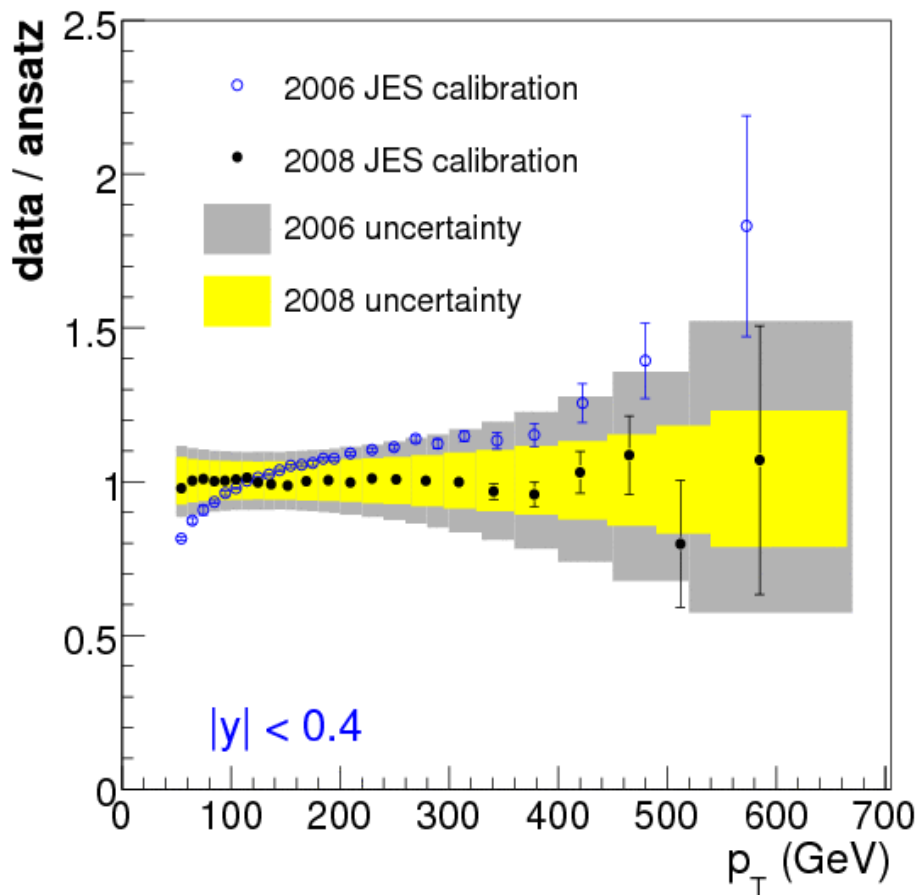
- JES uncertainty is propagated to the cross section using fit to data
- Method cross checked by shifting all jets by JES uncertainty
- 1% JES uncertainty is now 5—10% in CC, 10—25% in EC





Improvement since 2006

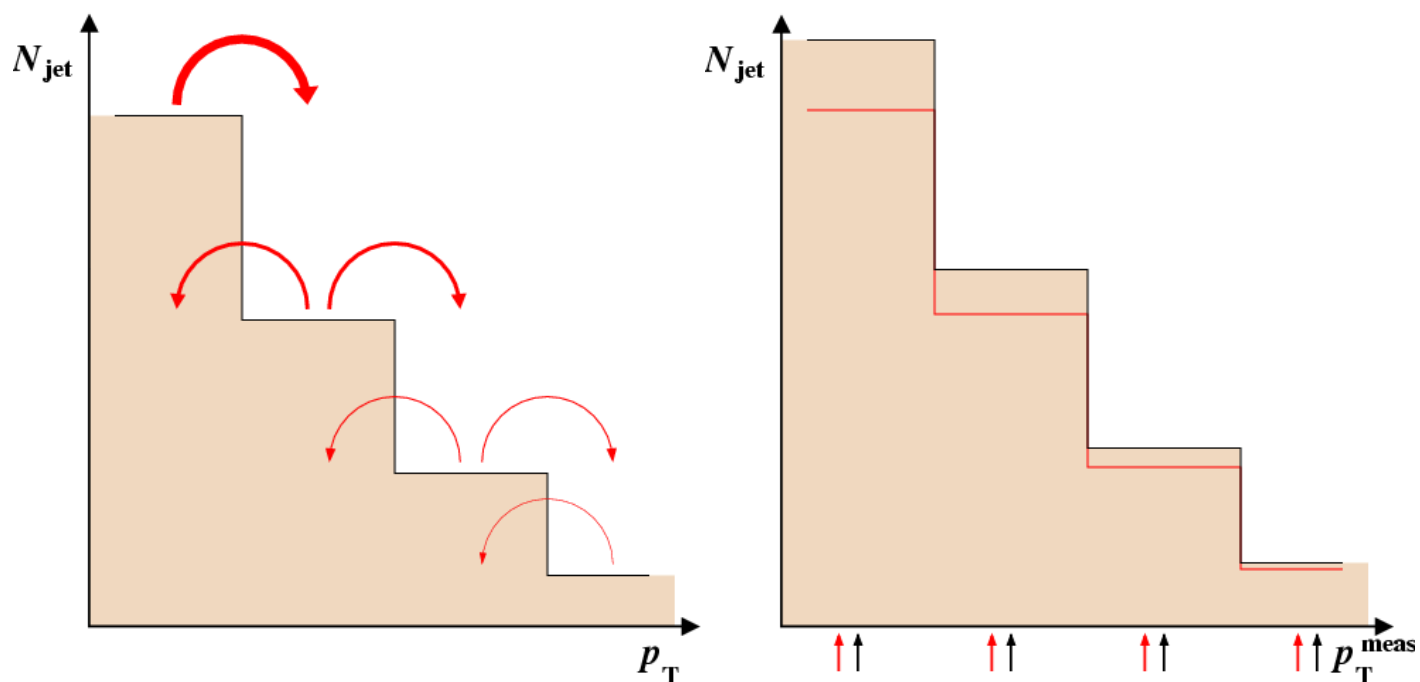
- The uncertainties have improved by up to factor two and more in the central region since preliminary JES (2006)
- Forward regions not published before, but improvement over factor ten





Resolution and unfolding

$$\frac{d^2 \sigma}{dp_T dy} = \frac{N}{\epsilon \cdot L \cdot \Delta p_T \Delta y} \cdot C_{smear} \text{ versus } p_T$$



Events can move in and out of p_T bins due to calorimeter energy resolution



Jet p_T resolution

- True jet p_T resolution is the RMS (or Gaussian σ) of reco p_T versus particle p_T

$$\frac{\sigma_{p_T}}{p_T} = \text{RMS} \left(\frac{p_T^{\text{reco}} - p_T^{\text{ptcl}}}{p_T^{\text{ptcl}}} \right)$$

Jet p_T is well described by a Gaussian at low p_T
 $\Rightarrow \text{RMS} \approx \sigma$

- We can measure the resolution in data using dijet asymmetry A

Raw asymmetry

$$A = \frac{p_{T,1} - p_{T,2}}{p_{T,1} + p_{T,2}}$$

Raw resolution

$$\frac{\sigma_{p_T}}{p_T} = \sqrt{2} \sigma_A$$

- Requires corrections for **soft radiation** (unreconstructed soft jets) and **particle level imbalance** (e.g. fragmentation fluctuations, primordial k_T of partons inside proton)

- soft radiation correction comes from DATA
- particle level imbalance comes from MC

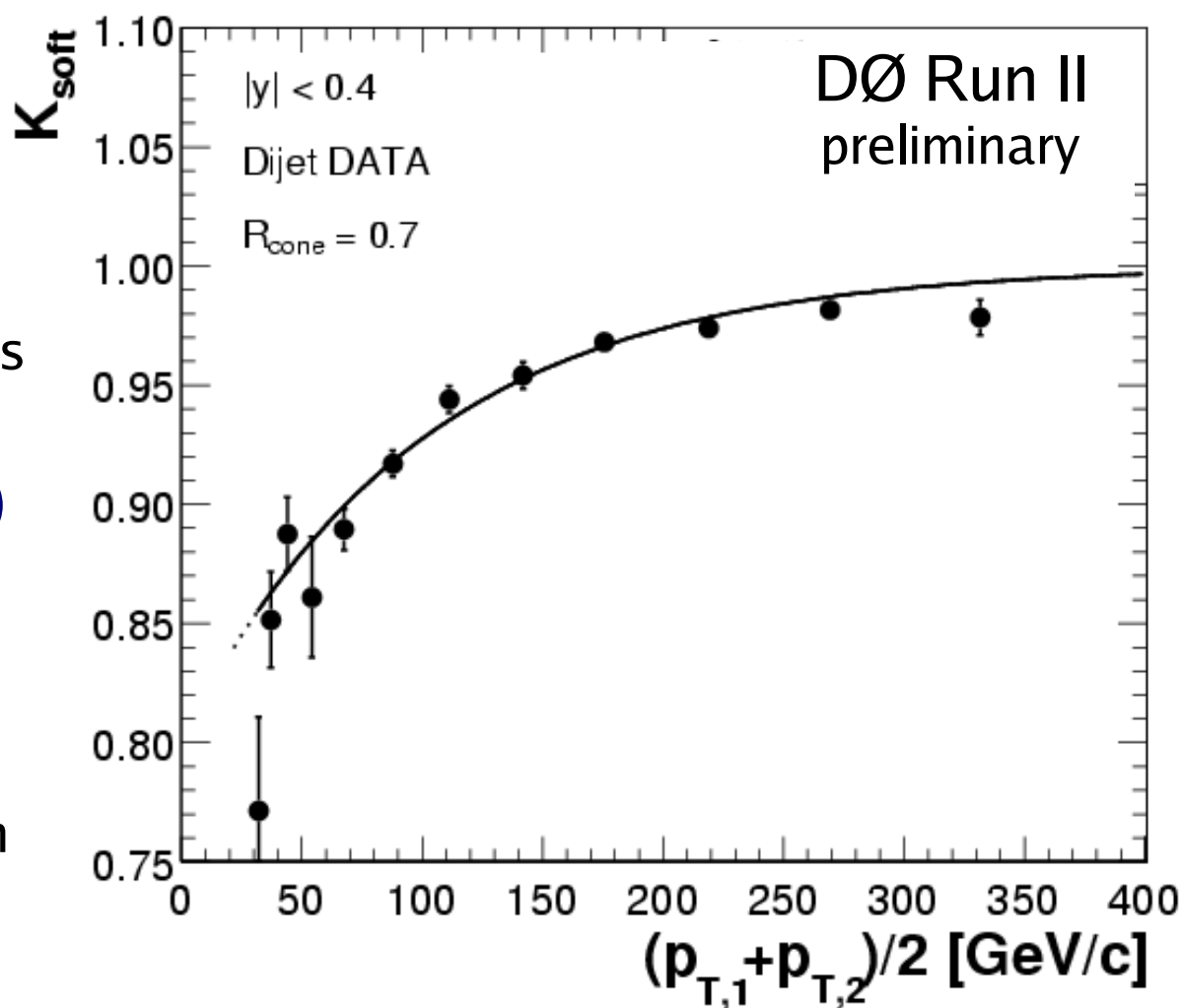


Soft radiation correction

- Soft radiation estimated by increasing reconstruction threshold $p_{T,soft}^{cut}$ and the bias
- Extrapolation to $p_{T,soft}^{cut} \rightarrow 0$ gives the correction
- Soft radiation correction vanishes asymptotically at high p_T :

$$k_{soft}(p_T) = 1 - \exp(-a_0 - a_1 p_T)$$

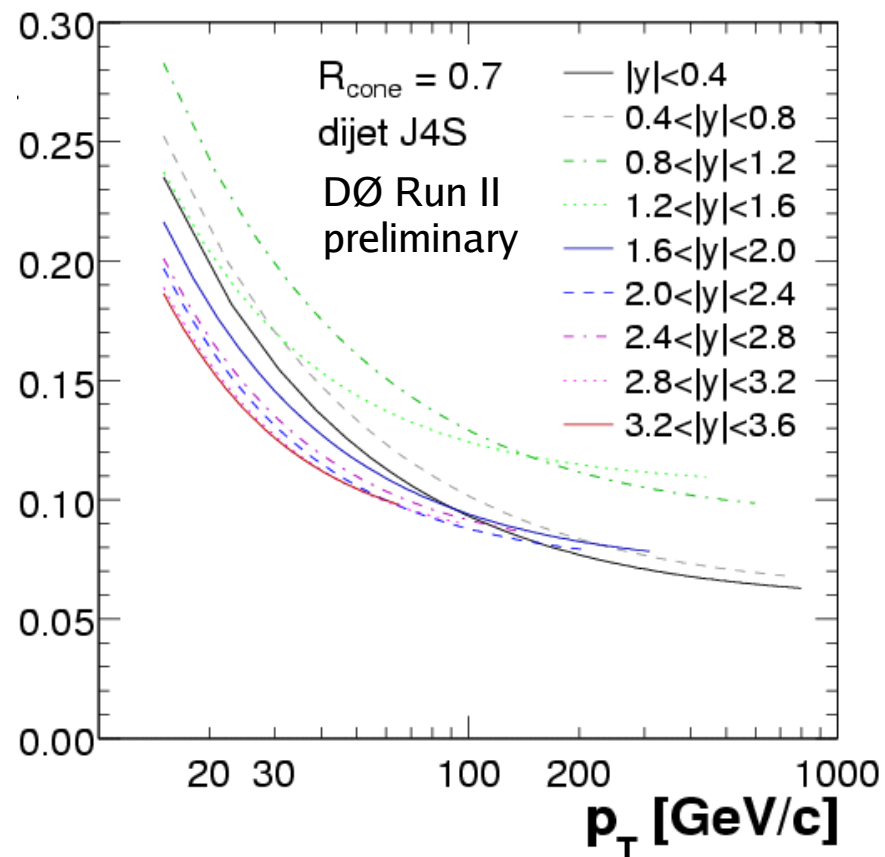
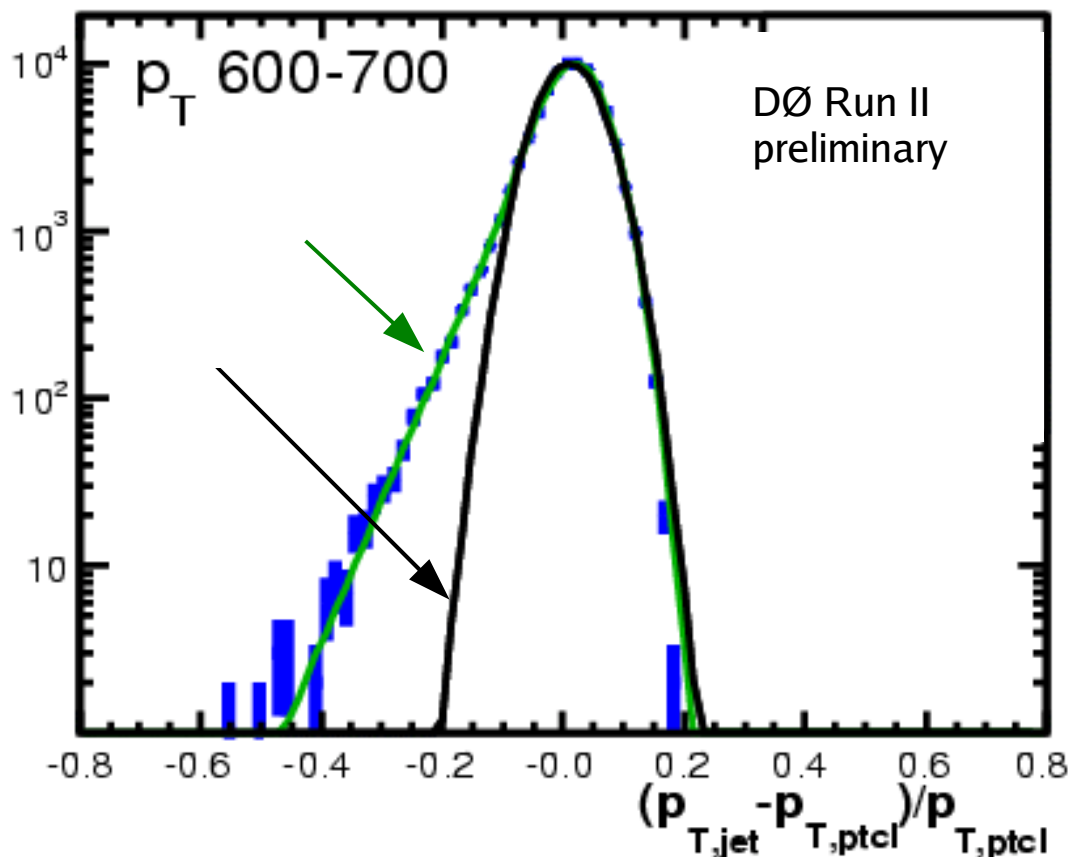
- Particle level imbalance from asymmetry in pure particle level MC after soft radiation correction
- Small correction, <10% everywhere





Jet p_T resolution

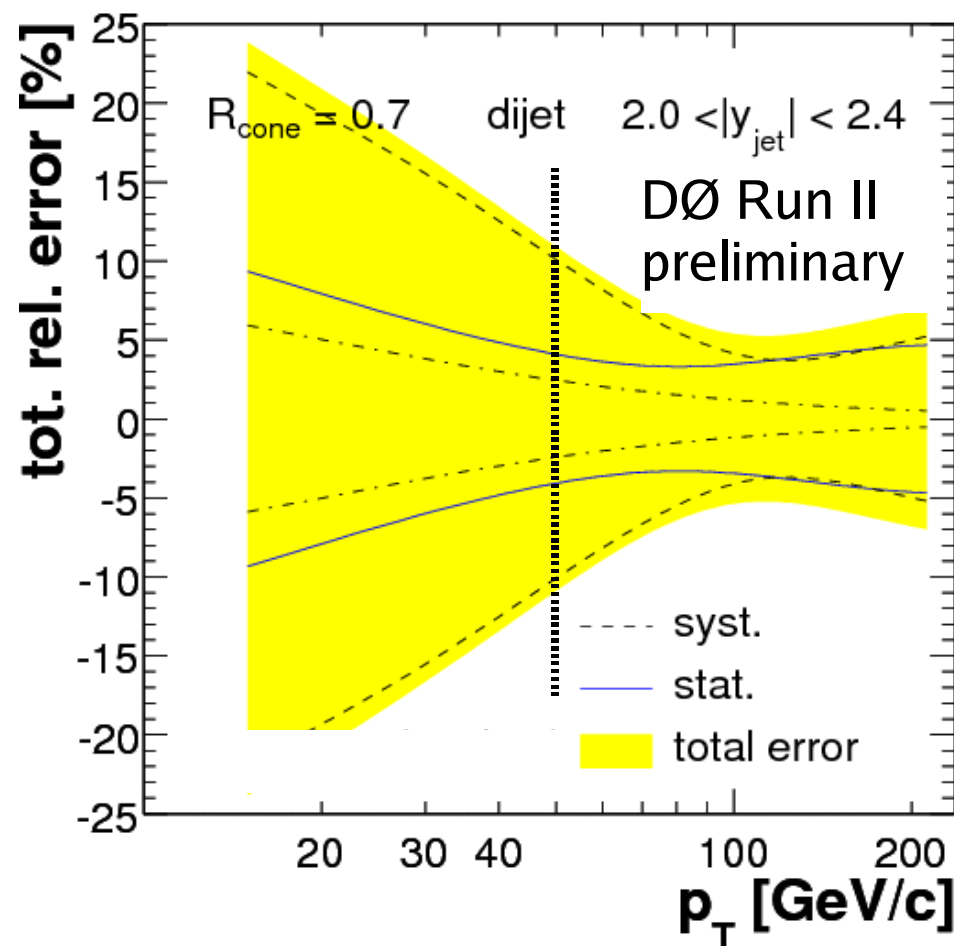
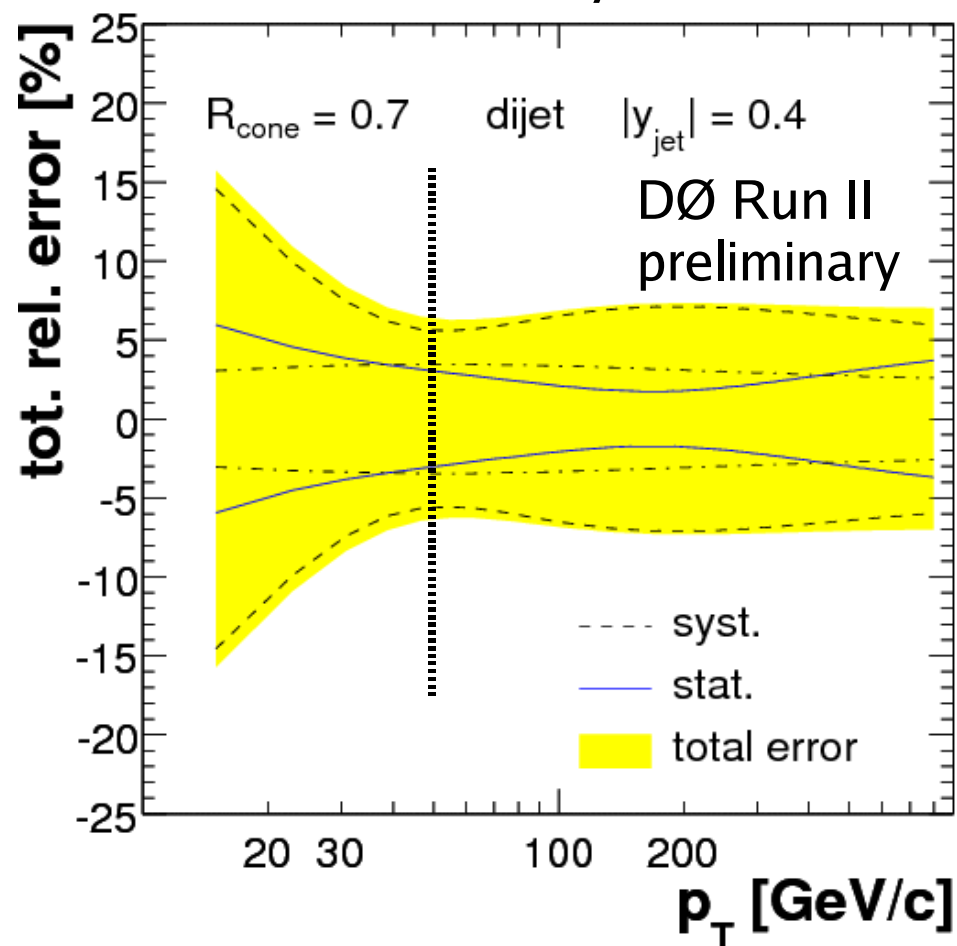
- Jet p_T resolution is measured directly on **dijet data** using p_T asymmetry
- Parametrized by Noise, Stochastic and Constant terms:
$$\frac{\sigma_{p_T}}{p_T} = \sqrt{\frac{N^2}{p_T^2} + \frac{S^2}{p_T} + C^2}$$
- Smearing shape from MC truth: non-Gaussian tails explicitly accounted for
High p_T punch-through





Resolution uncertainty

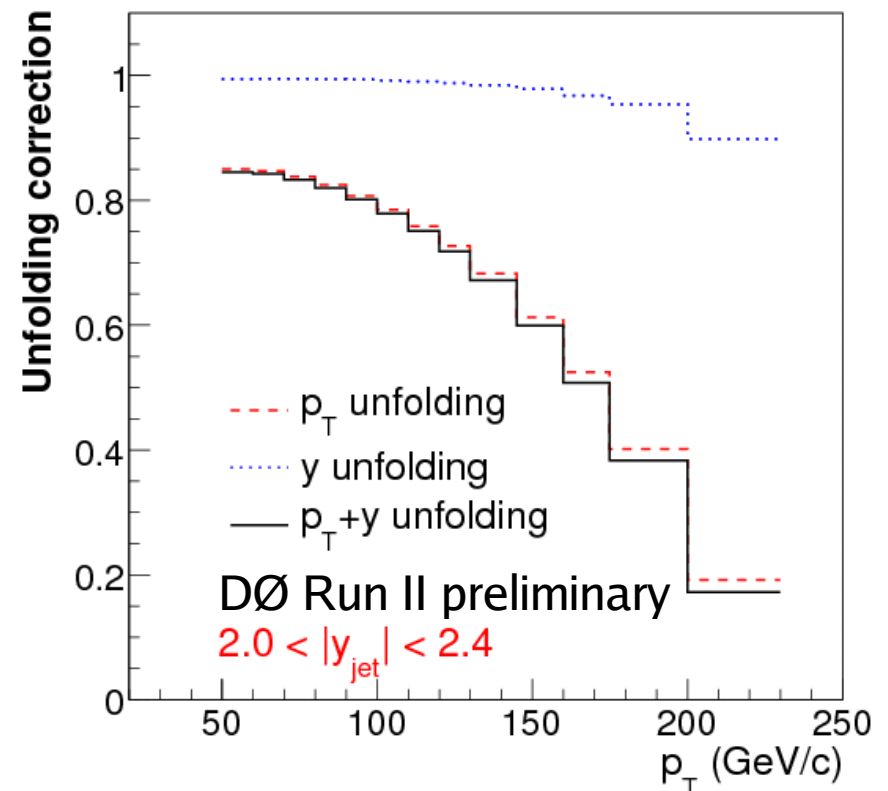
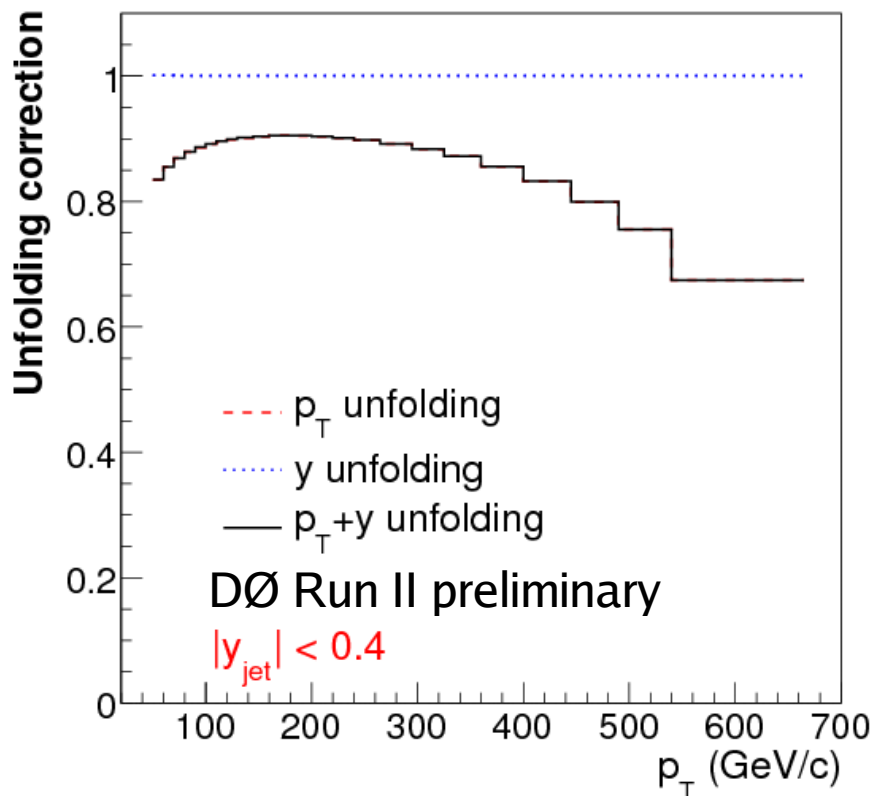
- Resolution uncertainty dominated by particle level imbalance in CC, statistics and method systematics in EC
- Overall uncertainty at 5—7% level





Jet p_T unfolding

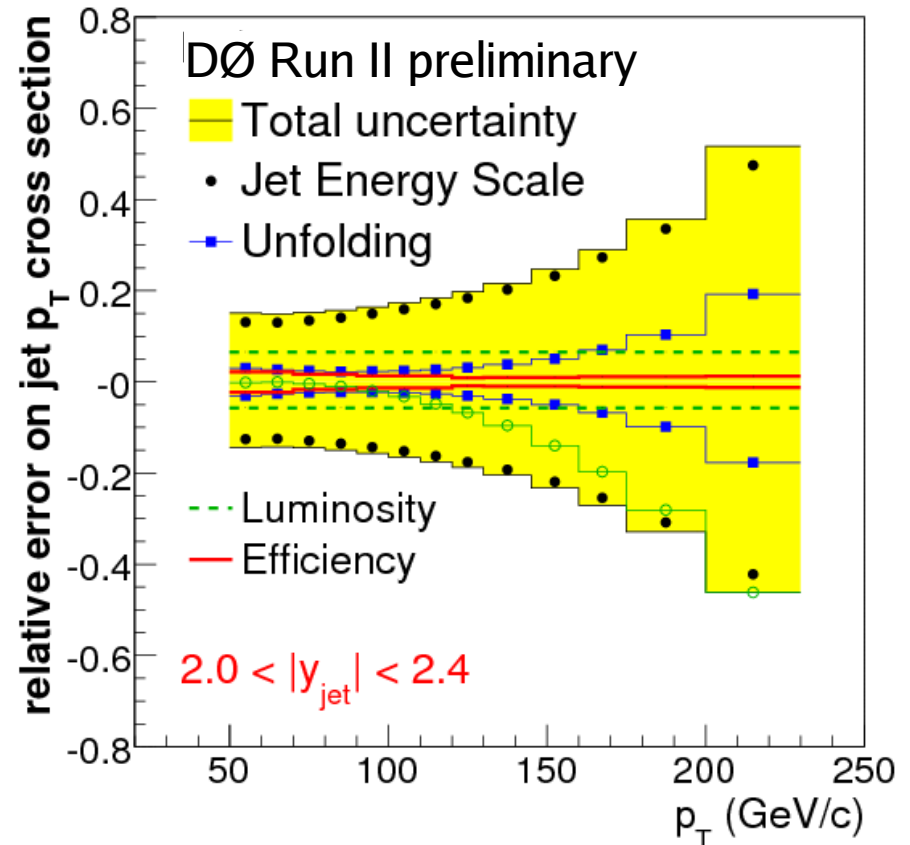
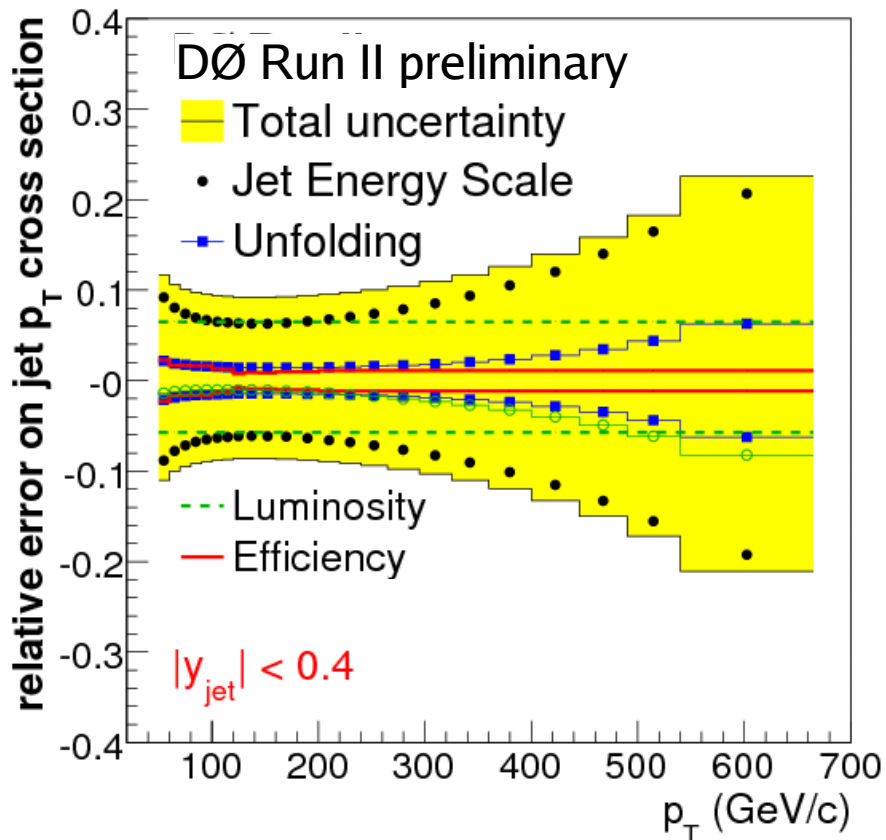
- Observed cross section is higher than true because more events migrate from high (and low) $p_{T,ptcl}$ into a given bin of measured p_T than migrate out of the bin due to jet p_T resolution \Rightarrow net increase
- Model the true cross section (ansatz method) and smear it (\Rightarrow resolution!) to obtain the observed cross section and then iteratively fit this to data





Components of uncertainty

- Total uncertainty is dominated by the (much improved!) JES
- Unfolding ($\approx p_T$ resolution) uncertainty much smaller than JES
- Luminosity is a significant uncertainty at low p_T in CC
- Efficiency uncertainty negligible





Final results

Double differential
cross section

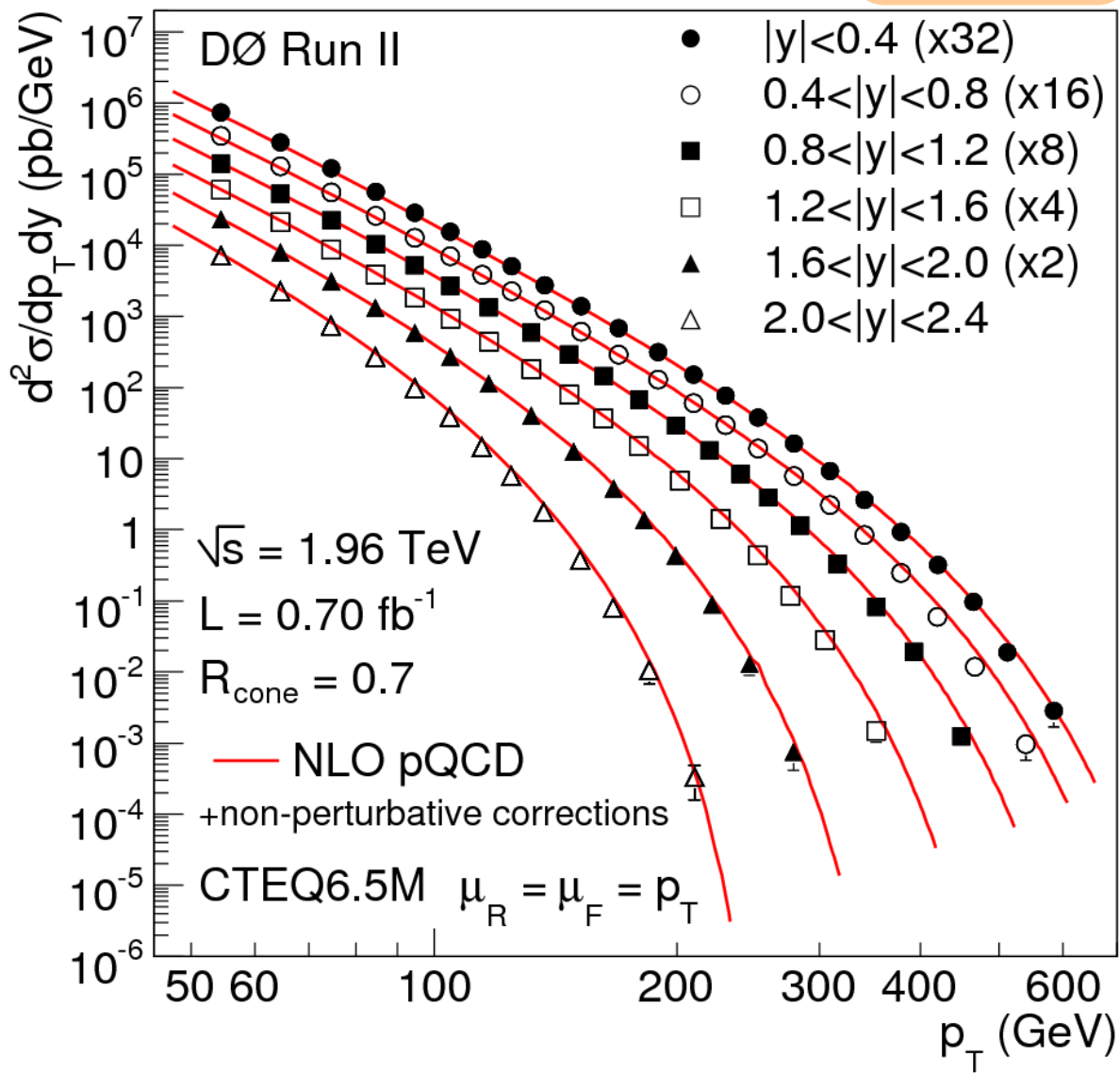
$$\frac{d^2 \sigma}{dp_T dy} = \frac{N}{\epsilon \cdot L \cdot \Delta p_T \Delta y} \cdot C_{smear} \quad \textit{versus } p_T$$



Final results

PRL plot

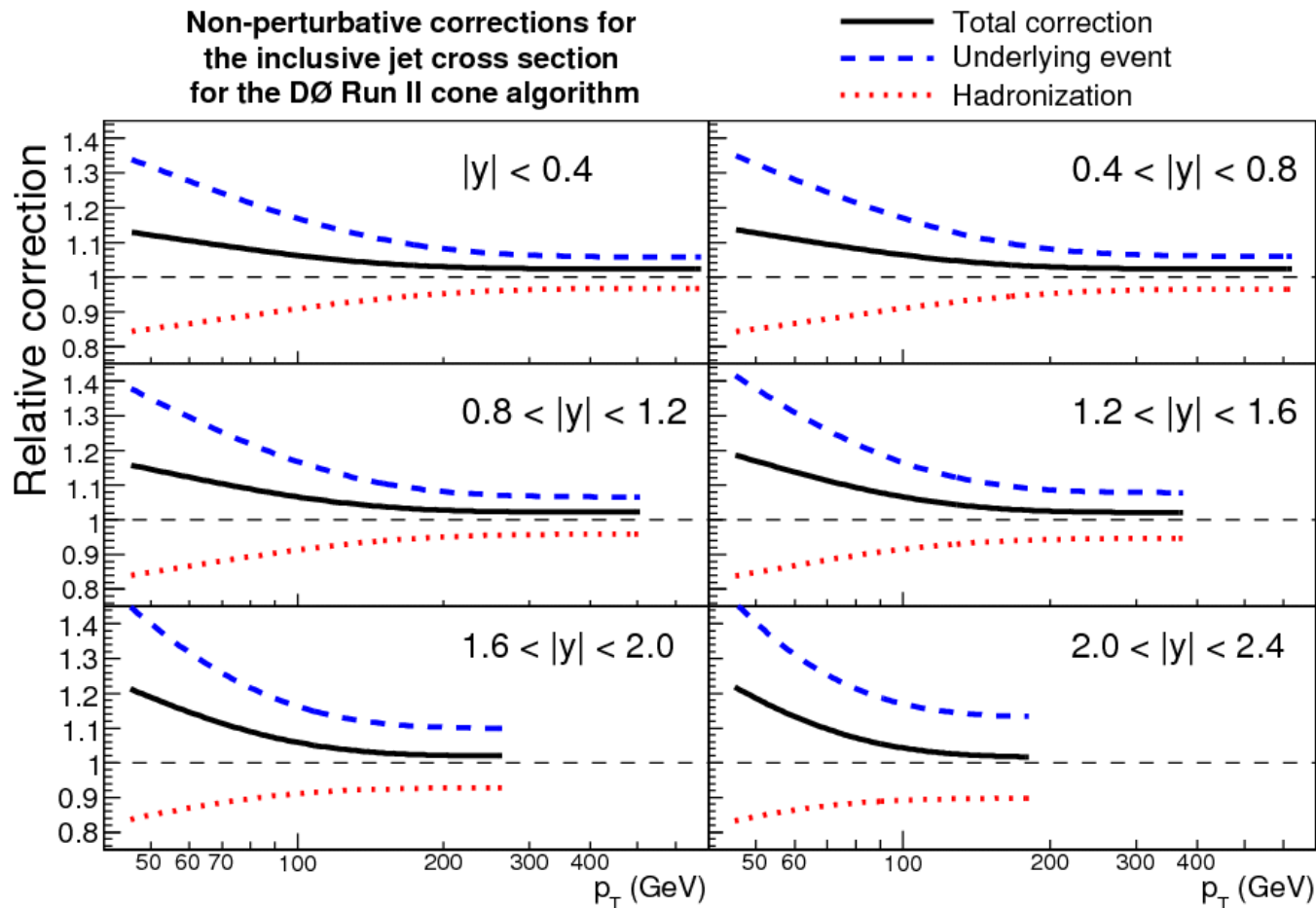
- Largest data set from Run II with the widest rapidity coverage ($|y| < 2.4$) and smallest uncertainties to date
- Uncertainties competitive with (better than) Run I and CDF
- Jet spectrum presented at **particle level** with **midpoint cone** ($R_{\text{cone}} = 0.7$)
- Compared to next-to-leading order (NLO) theory with CTEQ6.5M PDFs and non-perturbative corrections from Pythia





Non-perturbative corrections

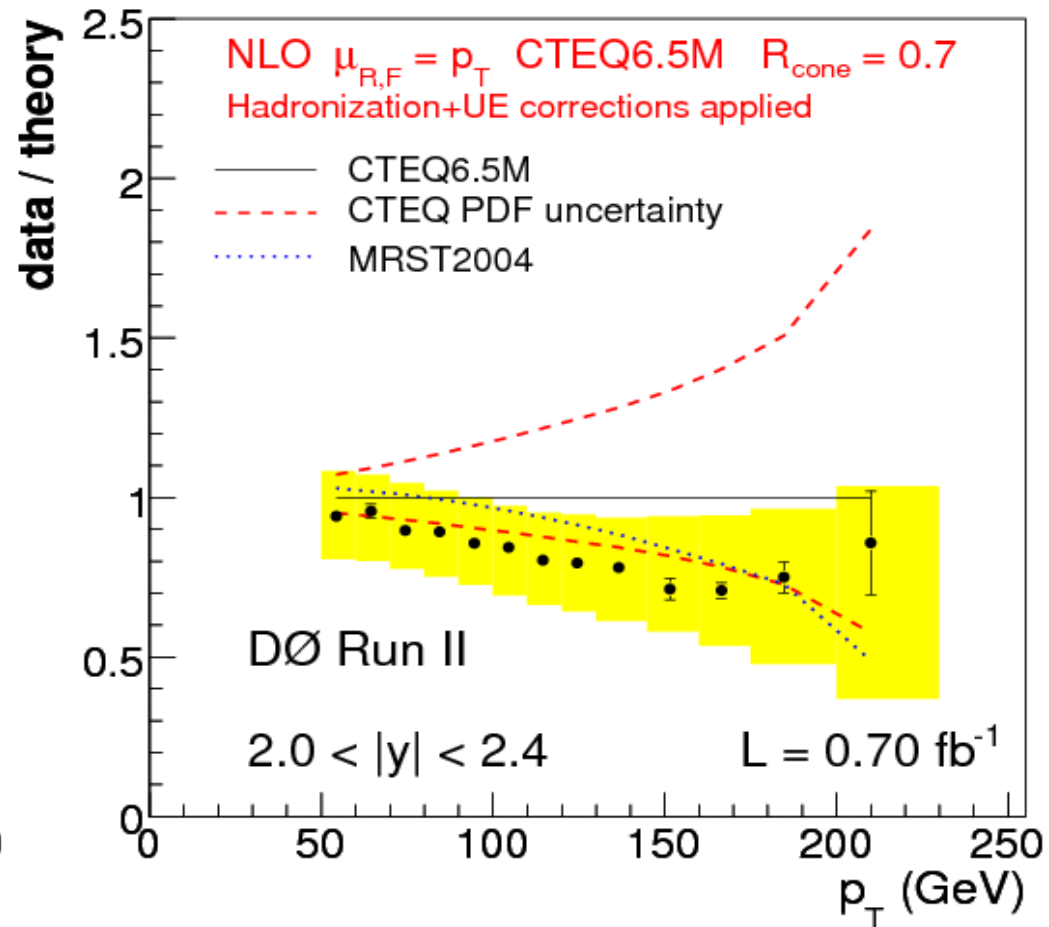
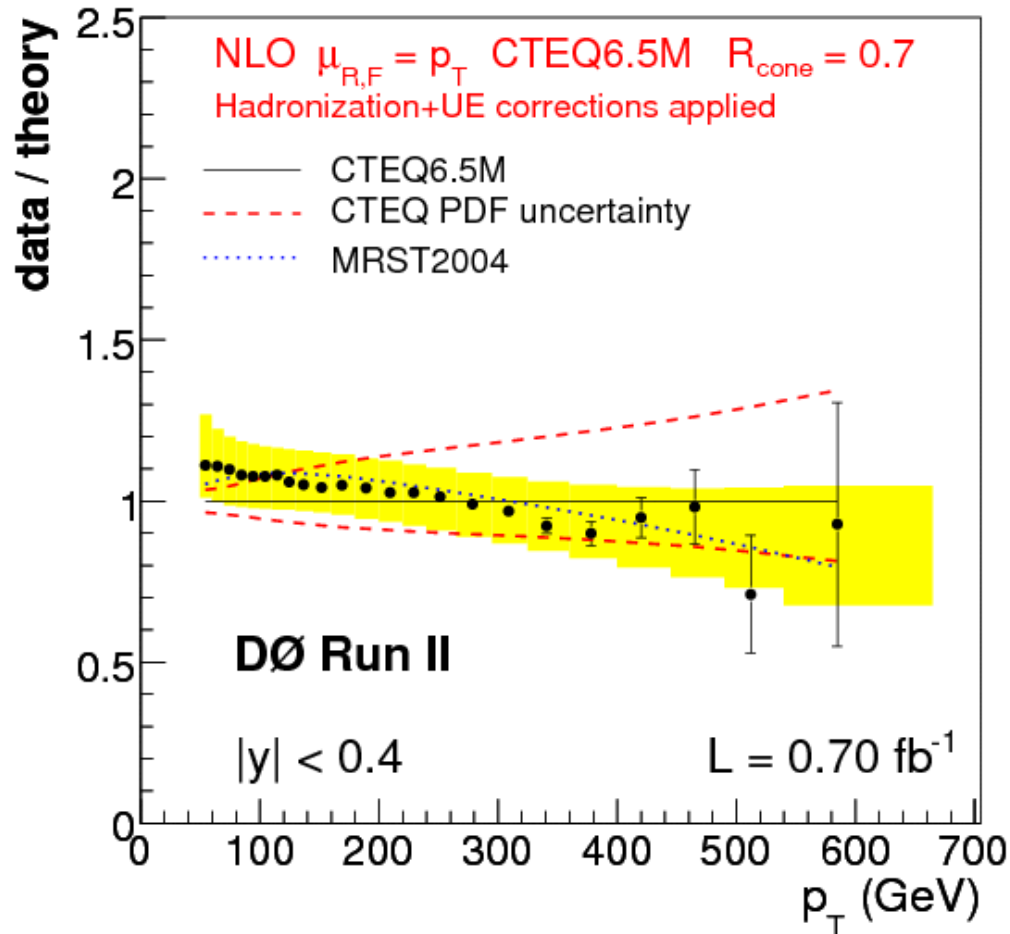
- Hadronization and underlying event soft QCD effects and cannot be calculated with perturbation theory
- Pythia tune A used to calculate the non-perturbative corrections to theory





Comparison to theory

- Comparing data and theory, the general tendency is to favor MRST2004 PDFs or the lower edge of CTEQ6.5 uncertainty \Rightarrow less high-x gluon
- CTEQ6.5 reduced PDF uncertainties by $\approx \times 2$ compared to CTEQ6.1

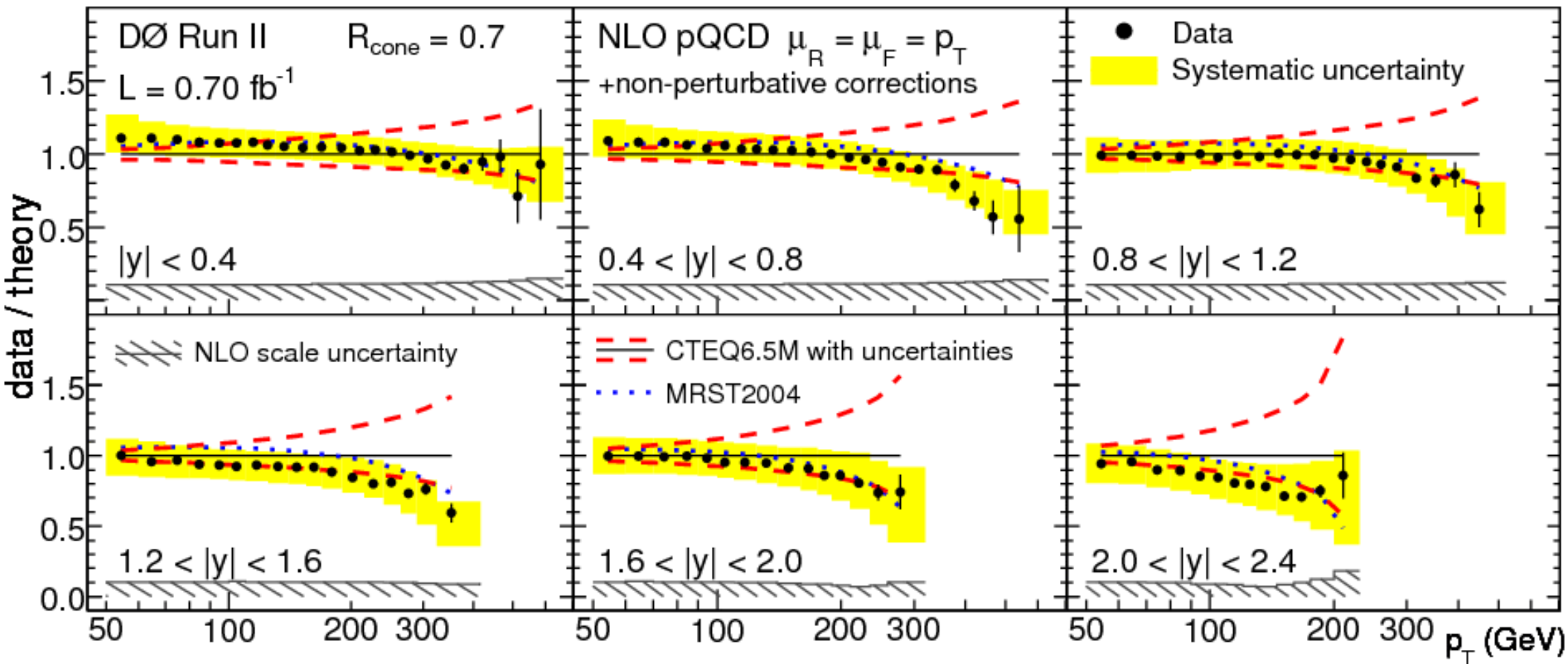




Final results

- Good agreement between data and theory at all rapidities; MRST2004 PDFs and the lower end of CTEQ6.5 PDF uncertainty favored
- Scale uncertainty in next-to-leading order (NLO) theory comparable to experimental uncertainty at low p_T

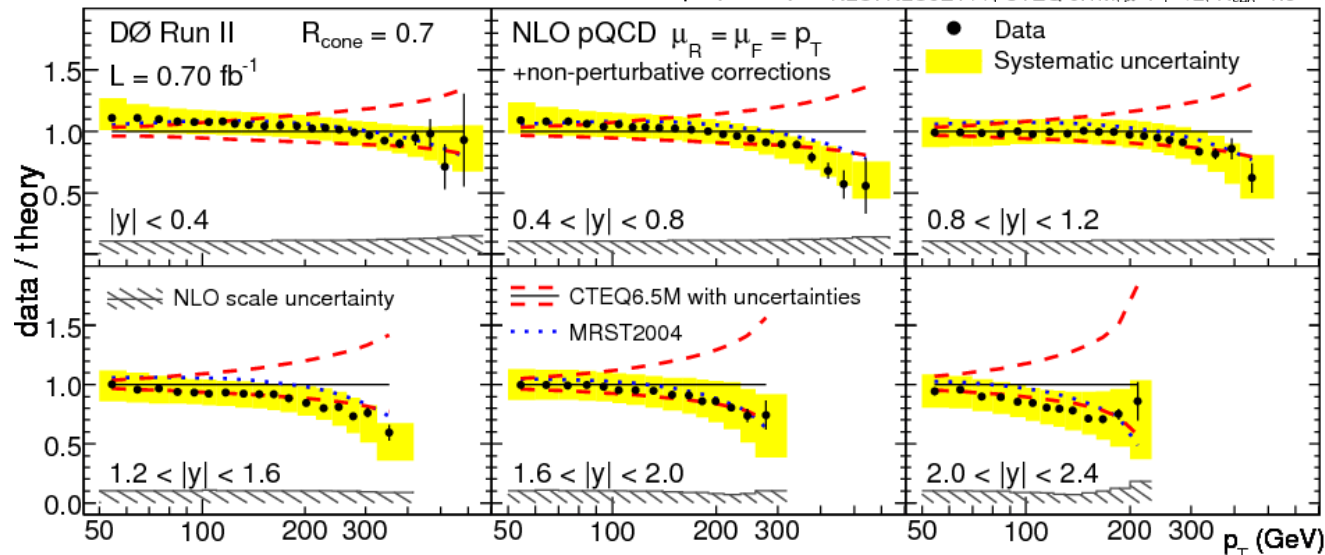
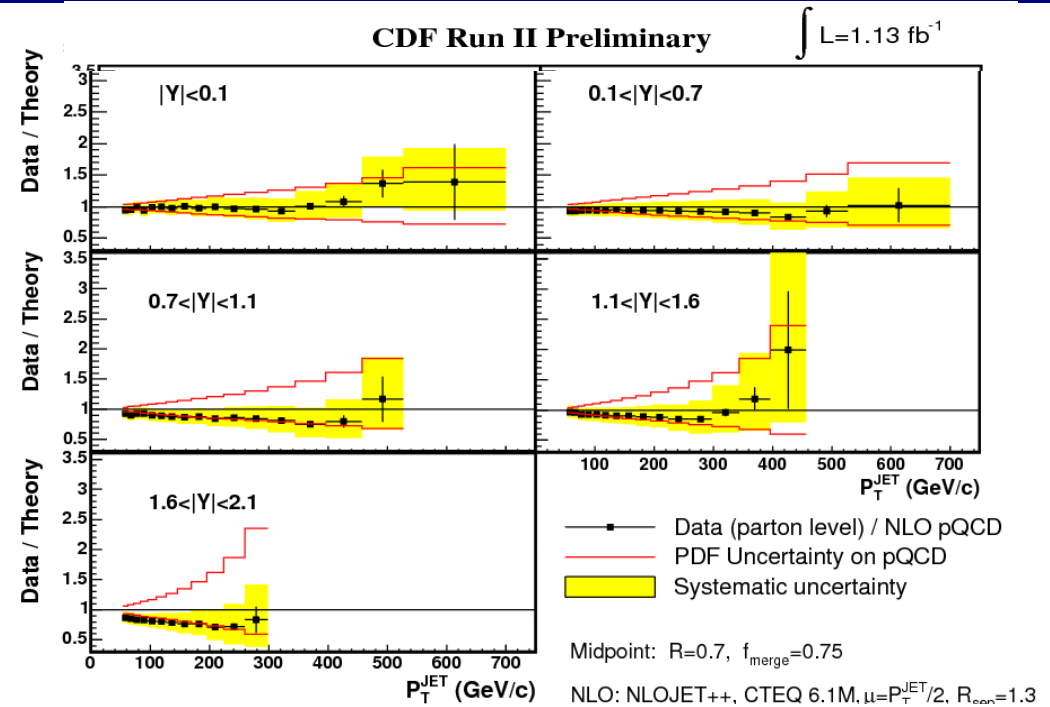
PRL plot





DØ and CDF comparison

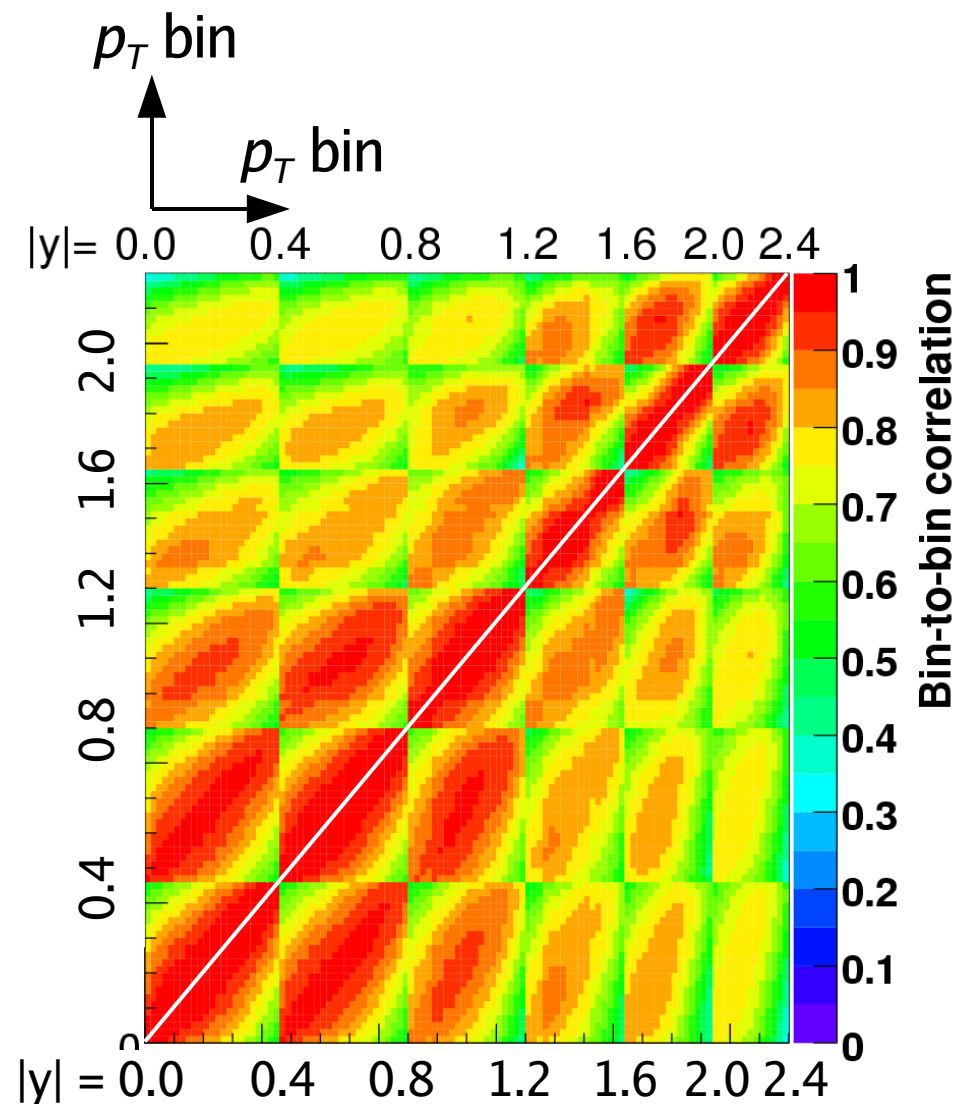
- The DØ and CDF data are compatible within uncertainties
- Note that the CTEQ6.1 PDF band in the CDF plot is twice as wide as the CTEQ6.5 PDF band in the DØ plot
- Central values of the theory slightly different





Uncertainty correlations

- The uncertainty correlations are provided in the format CTEQ uses: set of independent variations (sources) describing how points move together
- Average bin-to-bin correlation of about **80%** with **RMS of 10%**
- Using the correlation information in the global PDF fit should **further reduce the effective uncertainty** in the measurement

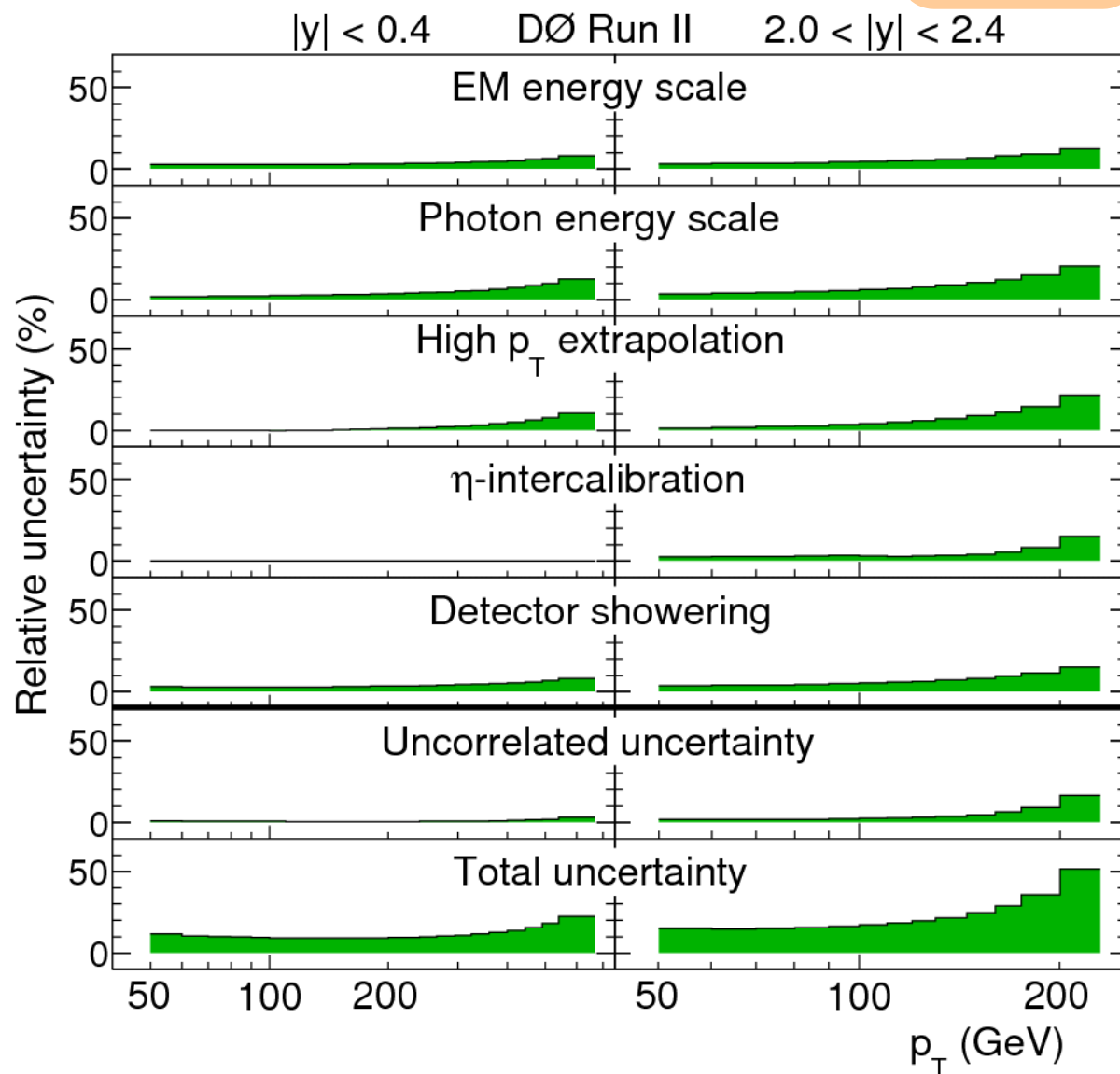




Uncertainty correlations

PRL plot

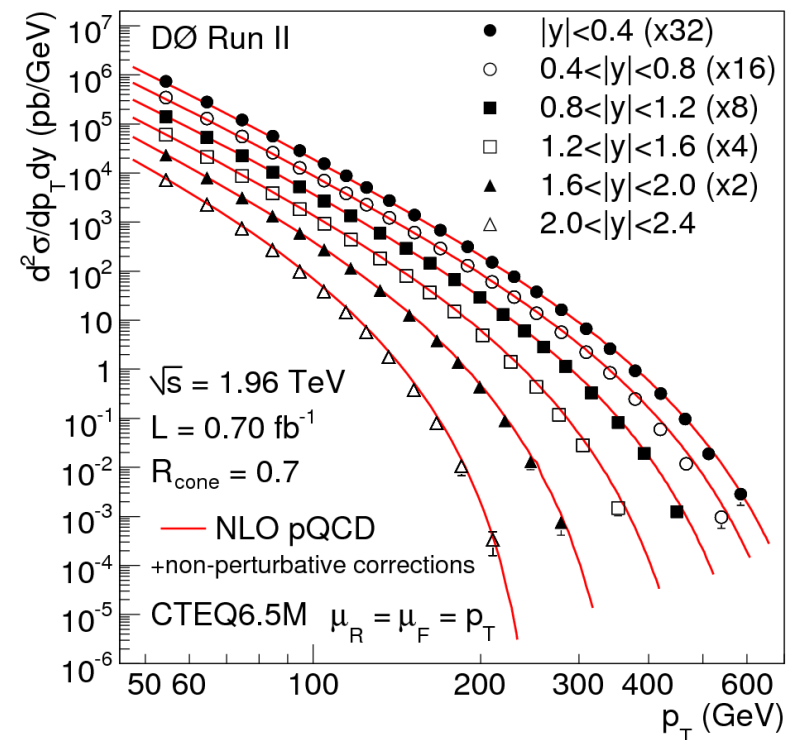
- Leading sources are from JES:
 - **EM energy scale** ($Z \rightarrow e^+e^-$ calibration)
 - **Photon energy scale** (MC description of e/γ response, material budget)
 - **High p_T extrapolation** (fragmentation in Pythia/Herwig, PDFs)
 - **Rapidity decorrelation** (uncertainty in η -dependence)
 - **Detector showering** (goodness of template fits)
- Only five highest out of 23 correlated systematics shown





Conclusions

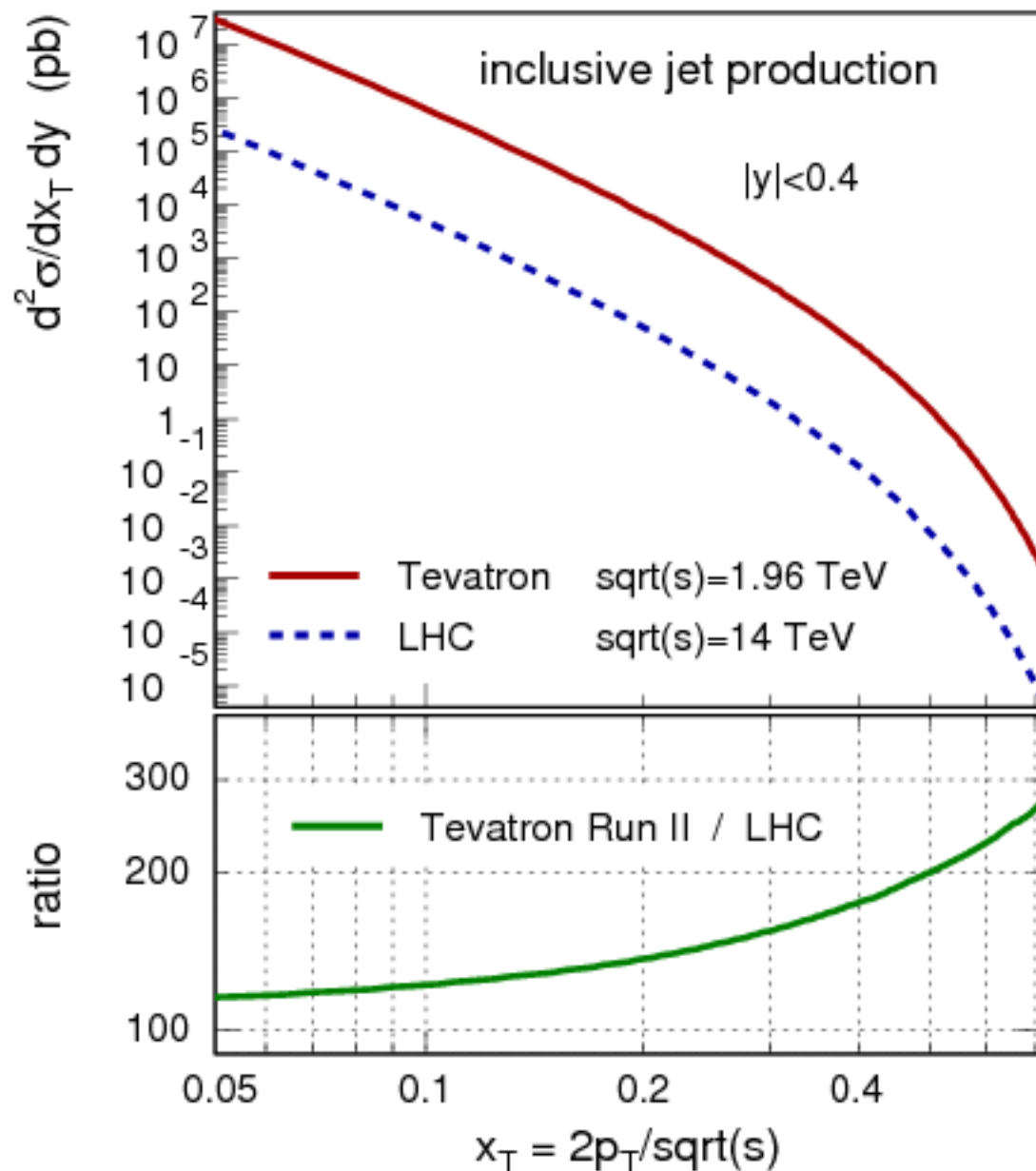
- Detailed inclusive jet cross section measurement over eight orders of magnitude in range $p_T = 50\text{--}600$ GeV with wide rapidity coverage (six bins in $|y| < 2.4$)
- Good agreement with NLO pQCD calculations observed, with reduced high x gluon favored compared to CTEQ6.5M
- Uncertainty correlations studied in detail and correlations found to be high; 23+1 sources provided for global PDF fits
- Request from CTEQ and MRSW groups for data to be incorporated to global PDF fits
- **Submission of PRL and publication of data tables within next couple of days**





Outlook

- Luminosity has increased by $\times 10$ and cross section at 550 GeV by $\times 3$ since Run I
 - $\Rightarrow \times 3$ constraint for high- x gluon PDF
 - $\Rightarrow \times 5$ constraint for quark substructure
- In the future, LHC needs $\sim 200 \text{ fb}^{-1}$ for similar high x PDF sensitivity
 - \Rightarrow leading result for years
- LHC will also need 1% level systematics, which took us 7 years



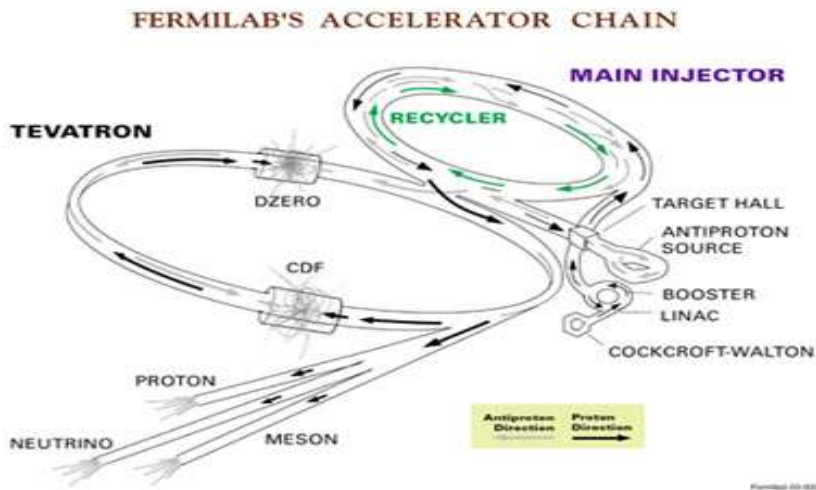
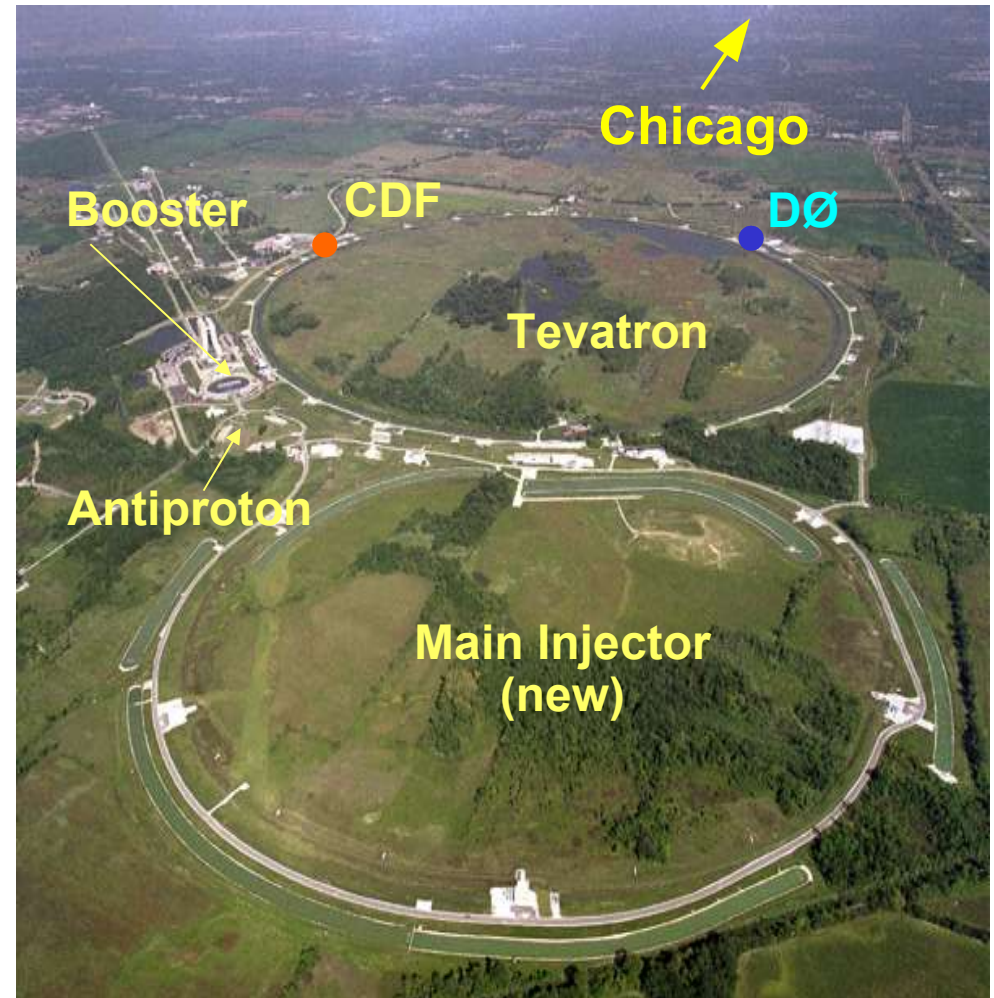


Back-up slides



Fermilab Tevatron Collider

- Proton-antiproton collisions at a center-of-mass energy of 1.96 TeV at the world's premier (still) hadron collider, the Fermilab Tevatron Collider
- Fermilab is located in Batavia, Illinois, about 80 km west of Chicago

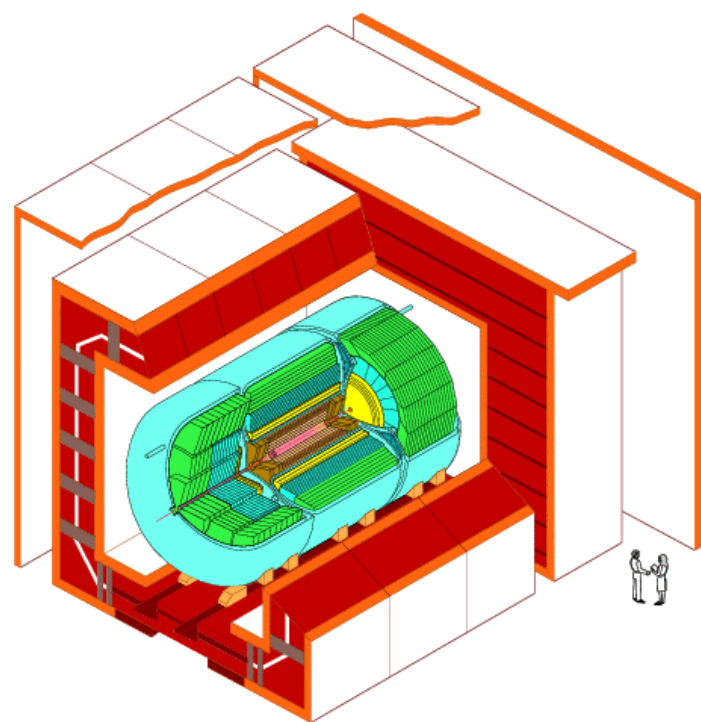


- Tevatron ring is around 6 km (2π) in circumference
- Two big detectors, CDF and D0



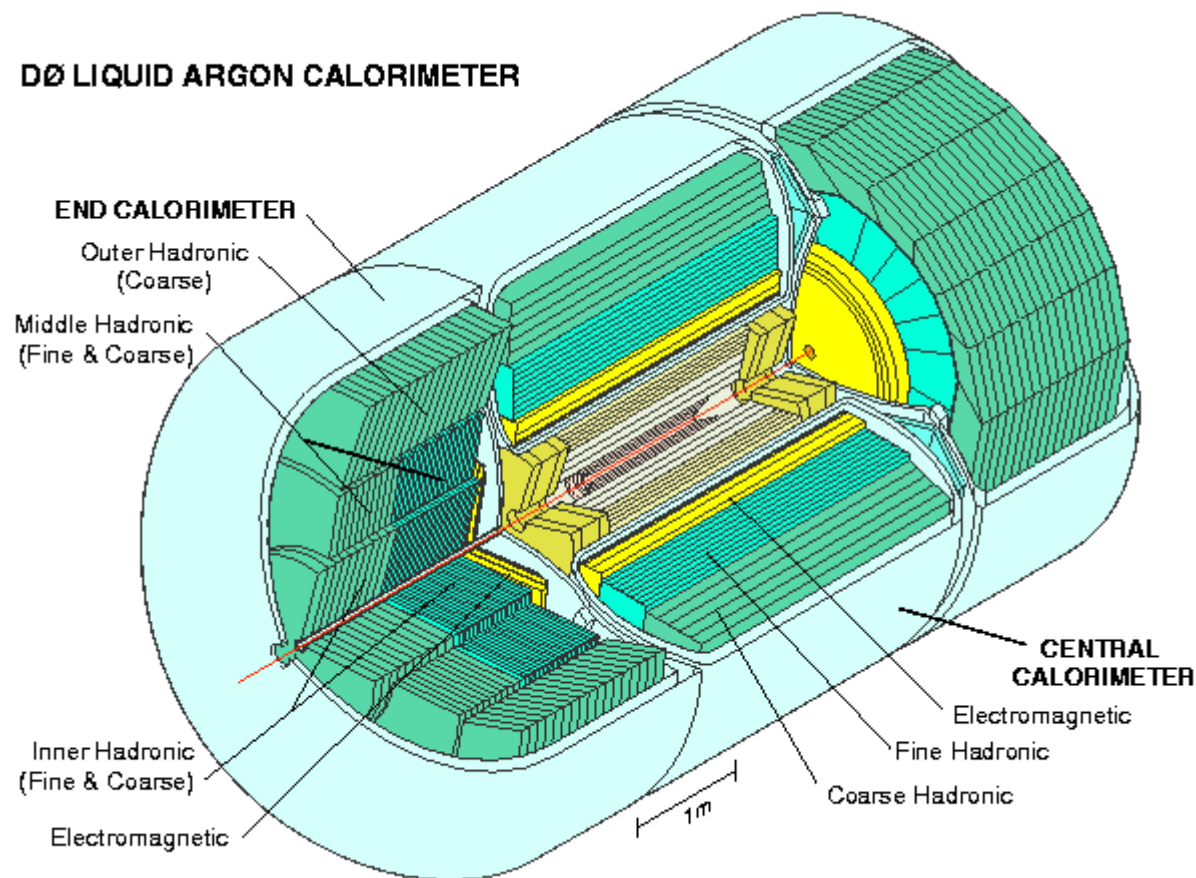
DØ experiment

- Main components: tracker, **electromagnetic calorimeter**, **hadronic calorimeter**, muon detectors
- Upgraded for Run II with new silicon and scintillating fiber trackers, 2 T solenoid magnet (for tracking), preshower detectors, and new electronics, triggers and data acquisition



DØ Detector

DØ LIQUID ARGON CALORIMETER





DØ calorimeter



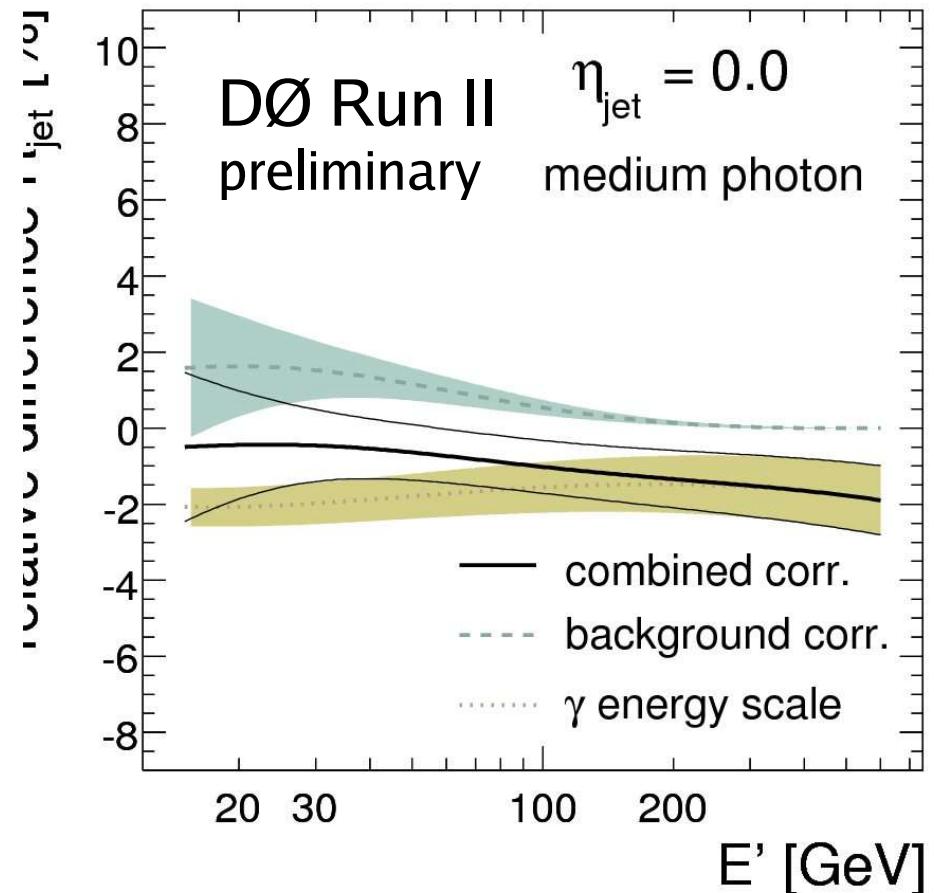
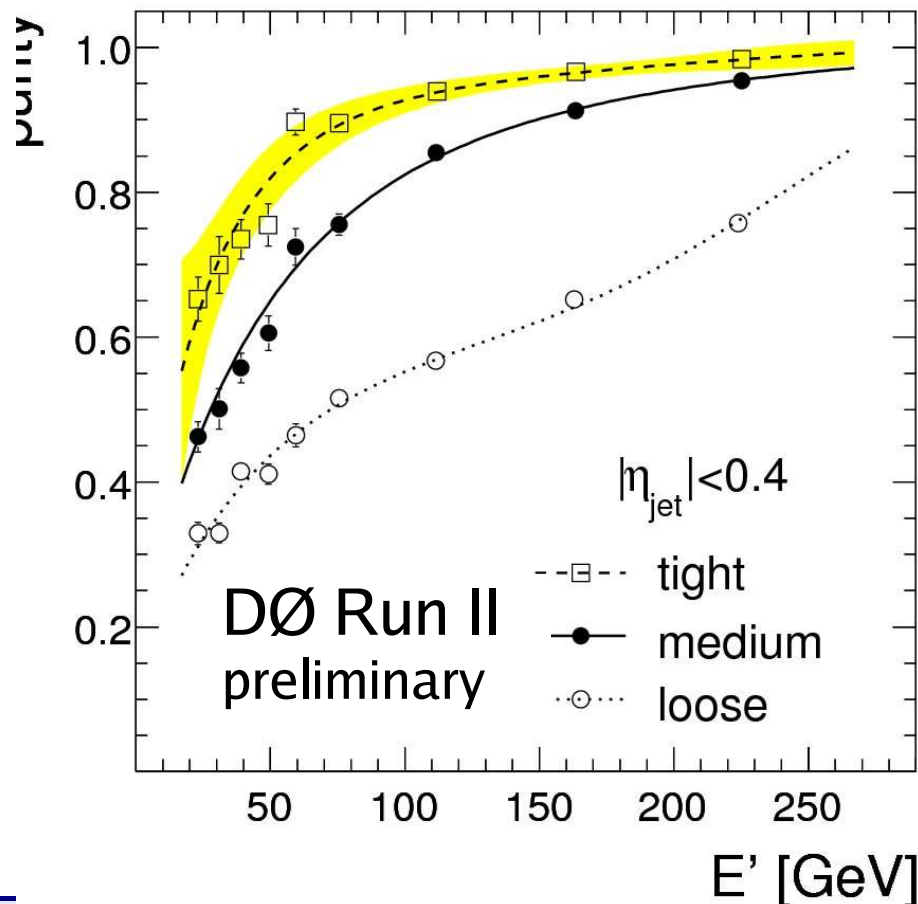
- Uranium-Liquid Argon calorimeter
- Stable, uniform response, radiation hard, fine segmentation
- Compensating ($e / \pi \sim 1$)
- Uniform, hermetic, full coverage in $|\eta| < 4.2$
- Good energy resolution
- New readout electronics to operate in Run II environment

- **Uniform, hermetic with full coverage**
 - $|\eta| < 4.2$ ($\theta \approx 2^\circ$), $\lambda_{\text{int}} \sim 7.2$ (total)
- **Single particle energy resolution**
 - e : $\sigma/E = 15\% / \sqrt{E} \oplus 0.3\%$
 - π : $\sigma/E = 45\% / \sqrt{E} \oplus 4\%$



EM-jet background

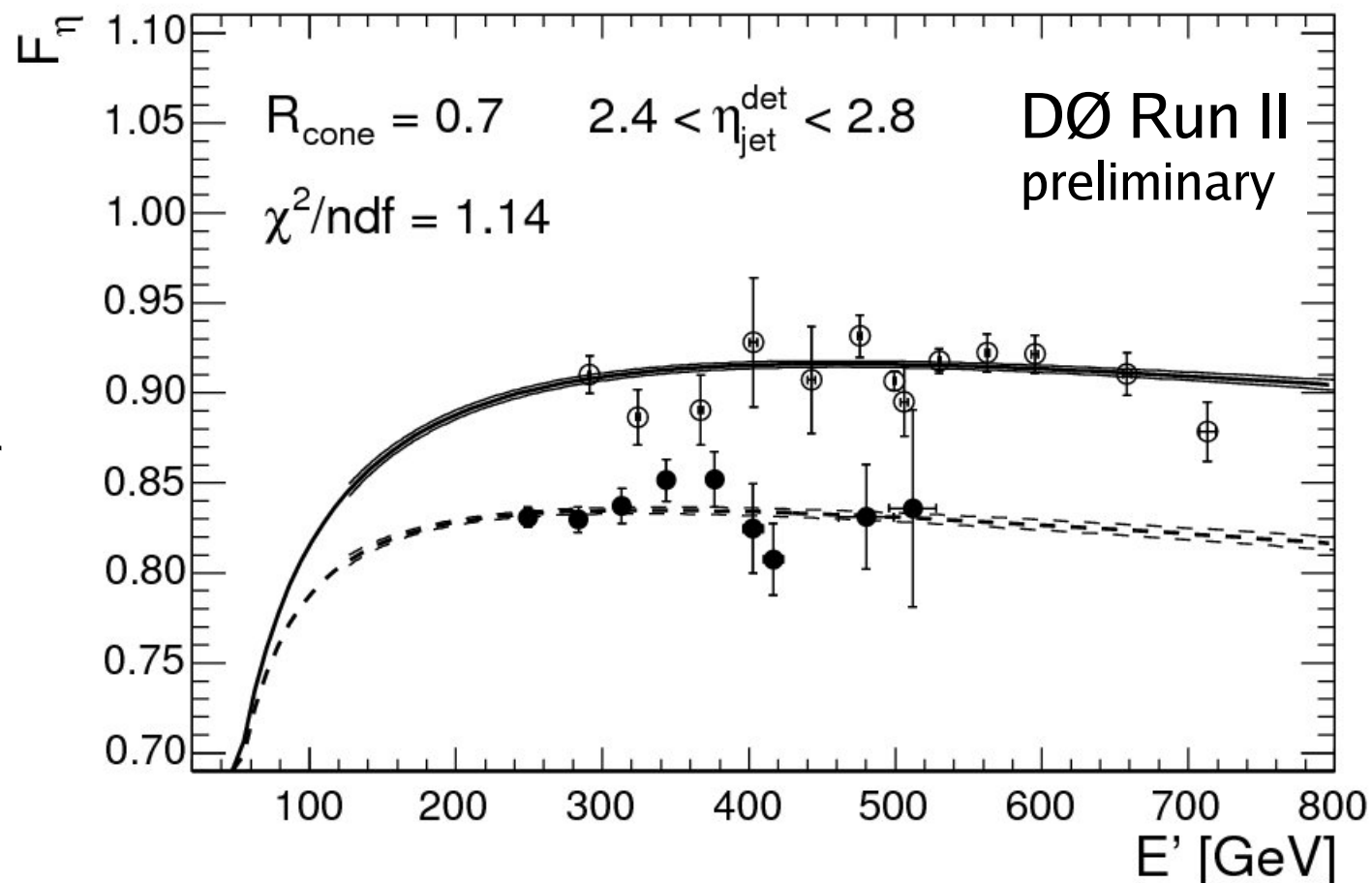
- Even with the tightest photon ID, γ +jet sample has significant EM-jet (leading $\pi^0 \rightarrow \gamma + \gamma$) background (dijet cross section $\times 1000$)
- To reduce systematics, derived purity and energy scale for EM-jets, which are considered as part of the calibration sample $\Rightarrow (\gamma/\text{EM-jet}) + \text{jet}$ sample





Eta-intercalibration

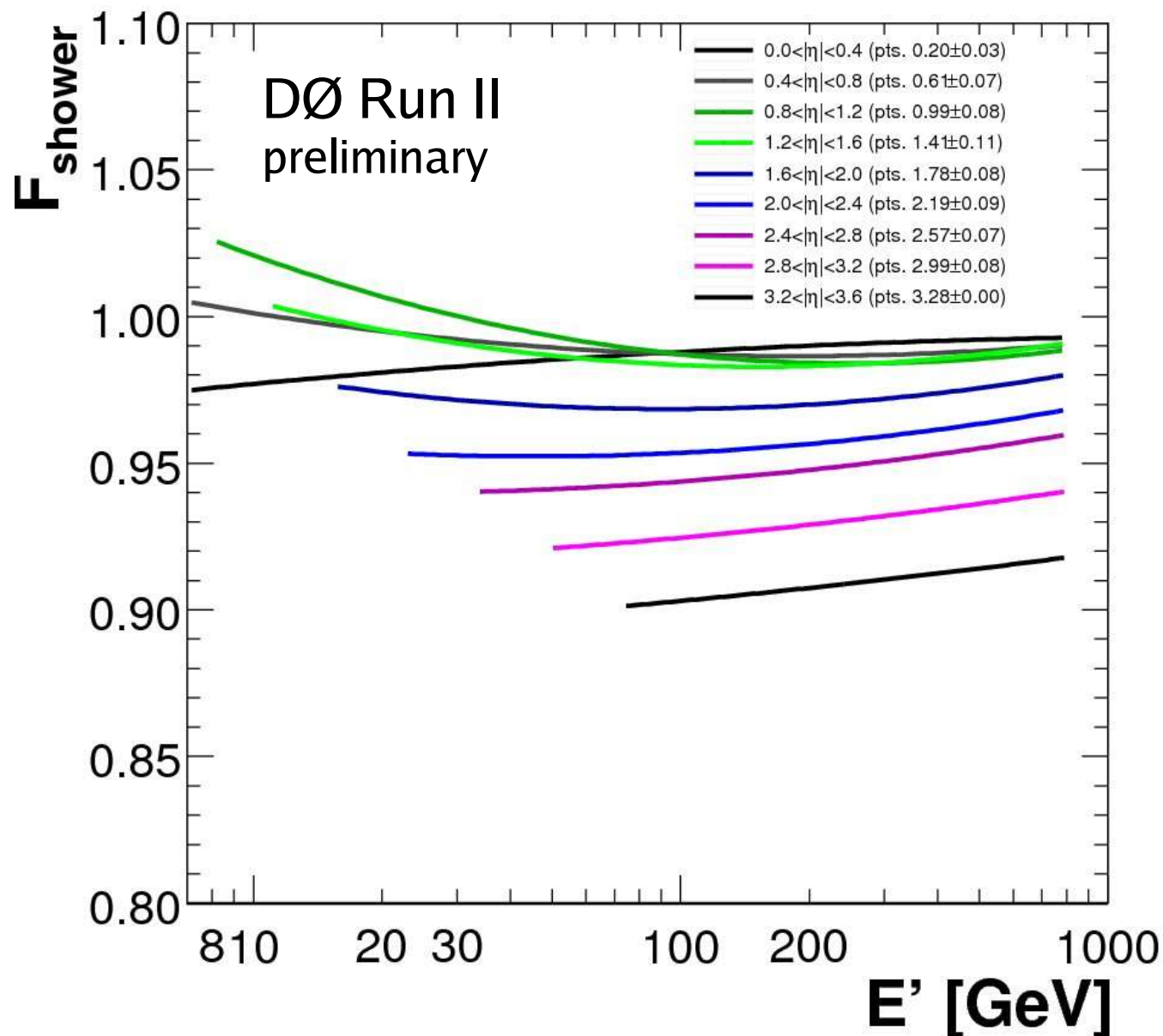
- Response η -dependence calibrated with respect to central jets and photons
- Dijets increase statistics at high p_T in the forward region compared to γ +jets
- Simultaneous fit to dijet and γ +jet samples taking into account sample differences
- Resolution bias for central jet in dijets explicitly corrected for and calibrated using central jet pairs





Showering

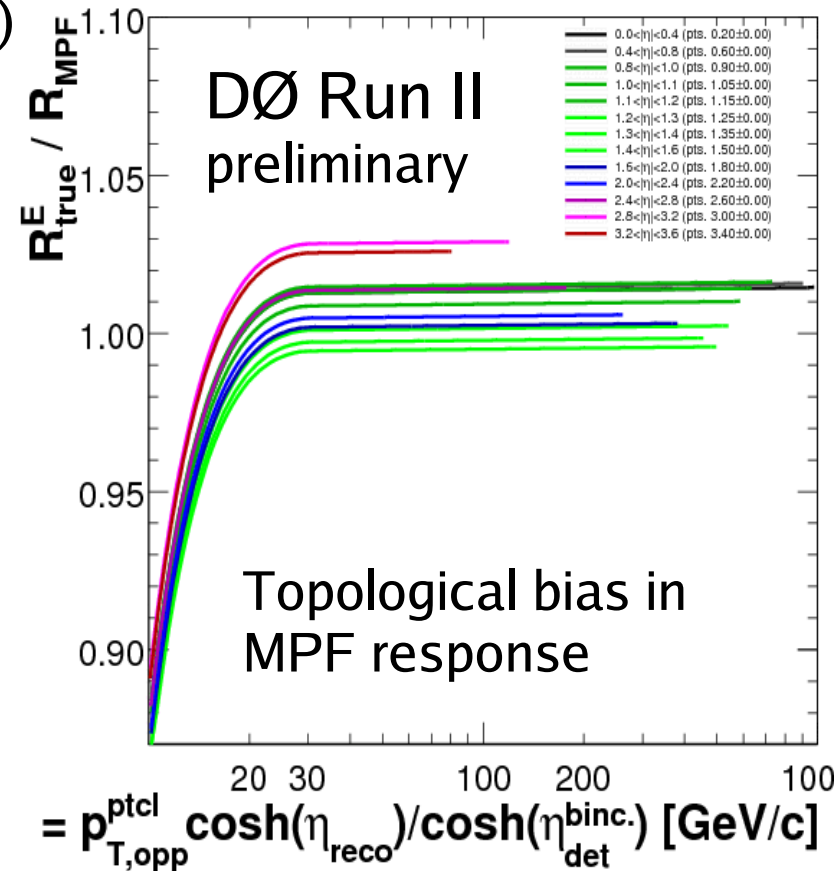
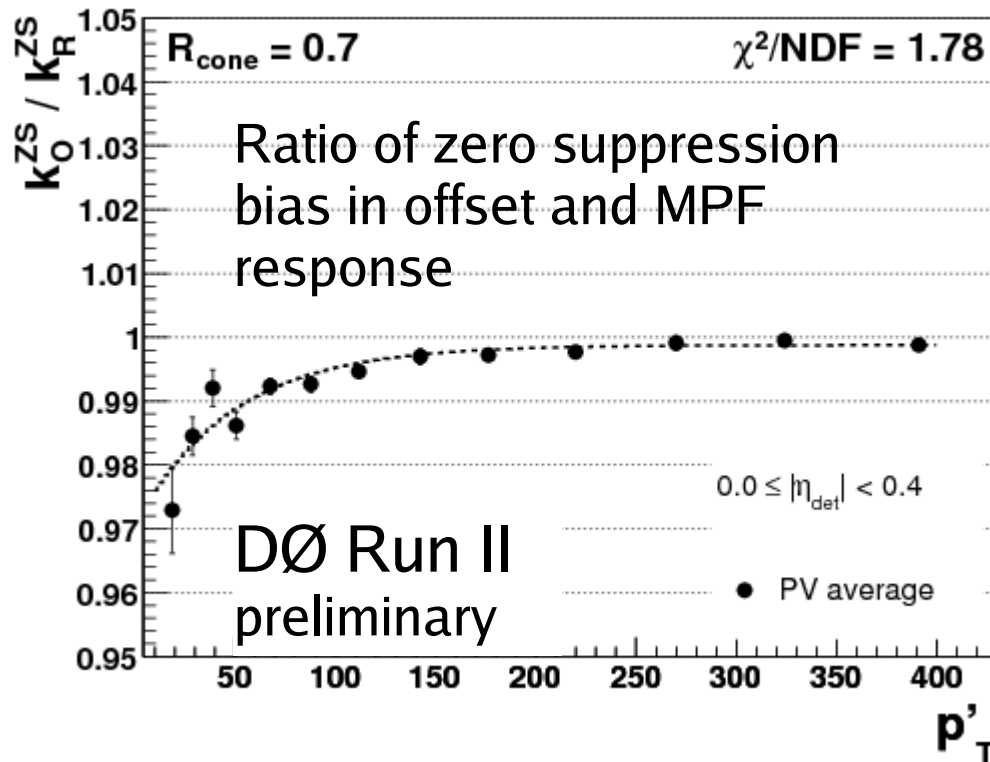
- Custom showering correction derived for the dijet sample using scaled MC
- Small correction in CC, but increases in EC where the real size (in xy -coordinates) of the jet cone decreases in the η -direction





Bias corrections

- Bias corrections corrections for zero suppression and topological effects
 - Zero suppression affects both offset and MPF response (offset larger in high energy environment), but effects almost cancel
 - Topological bias accounts for difference between jet core and full recoil (jet core has higher energy and response)

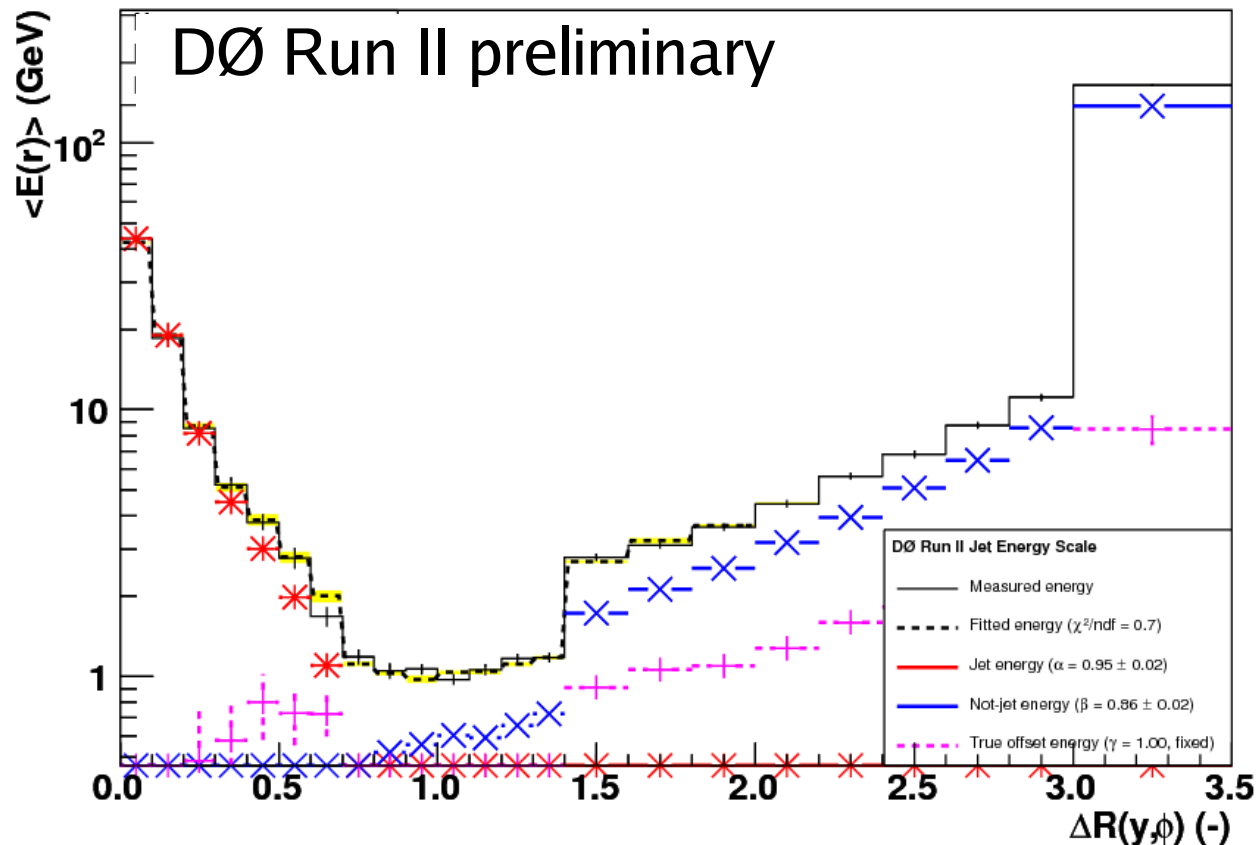




JES: Showering

- Showering energy profiles fitted in γ +jet data
- Good agreement between tuned MC and data-based method
- Typical correction $\sim 1\%$ in CC, up to 5% in EC

Energy profiles ($0.0 < |\eta_d| < 0.4$, $100.0 < p_T' < 130.0\text{GeV}$, $R_{\text{jet}}=0.7$)





Resolution uncertainty

- Leading uncertainty is resolution, ansatz fit contributes only little
- Uncertainty from resolution smaller than from JES, but increases quickly at higher rapidity and with worse resolution (large C_{smear})

